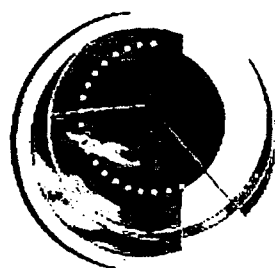


# Reserapport samt VKK föredrag

EWEC'97, i Dublin, oktober 1997

sammanställt av Anders Östman och Sven-Erik Thor



**ewec97**



EUROPEAN WIND ENERGY CONFERENCE



FLYGTEKNISKA  
FÖRSÖKSANSTALTEN

THE AERONAUTICAL RESEARCH INSTITUTE OF SWEDEN

## Reserapport samt VKK föredrag

- EWEC'97, i Dublin, oktober 1997

- sammanställt av Anders Östman och Sven-Erik Thor



**ewec97**



EUROPEAN WIND ENERGY CONFERENCE



FLYGTEKNISKA  
FÖRSÖKSANSTALTEN  
THE AERONAUTICAL RESEARCH INSTITUTE OF SWEDEN



## Sammanfattning

Den Europeiska vindenergiföreningen, EWEA, arrangerar vart tredje år en konferens och utställning, European Wind Energy Conference EWEC. I år, 1997, arrangerades EWEC'97 i Dublin. Vart tredje år arrangerar dessutom Europeiska Unionen EUWEC sin vindenergikonferens. Konferenserna är förskjutna ett och ett halvt år inbördes. Det innebär att det i Europa arrangeras vindkonferenser var 18:e månad.

I föreliggande rapport redovisas erfarenheter från EWEC'97. Tyngdpunkten har lagts på att referera det som hände inom de olika forskningsområdena som VKK är verksamma inom. Erfarenheter från övriga områden kommer att sammanställas av Vattenfall på uppdrag av Elforsk. För en fullständig information från konferensen rekommenderar vi därför läsning av båda rapporterna.

Nästa europeiska vindenergikonferens, EUWEC'99, arrangeras i Nice i mars 1999.

Konferensens olika avsnitt har bevakats av följande personer som även har författat texten under respektive avsnitt.

- |                                     |                  |
|-------------------------------------|------------------|
| 1. Vindunderlag och potentialfrågor | Hans Bergström   |
| 2. Aerodynamik                      | Anders Björck    |
| 3. Dynamik                          | Hans Ganander    |
| 4. Funktion och prestanda           | Jan-Åke Dahlberg |
| 5. Elsystem och reglering           | Ola Carlson      |
| 6. Nätintegration                   | Ola Carlson      |
| 7. Buller                           | Sten Ljunggren   |
| 8. Acceptansfrågor                  | Karin Hammarlund |
| 9. Stora vindturbiner               | Sven-Erik Thor   |



# Innehållsförteckning

<b>1 INLEDNING</b>	<b>7</b>
<b>2 ALLMÄNT OM KONFERENSEN</b>	<b>7</b>
<b>3 INVIGNINGEN</b>	<b>8</b>
<b>4 REFERAT FRÅN TEKNIKOMRÅDEN</b>	<b>9</b>
4.1 Vindunderlag och potentialfrågor	9
4.2 Aerodynamik	12
4.3 Strukturdynamik	16
4.4 Funktion och prestanda	17
4.5 Elsystem och reglerteknik	18
4.6 Nätintegration	21
4.7 Buller	22
4.8 Acceptansfrågor	24
4.9 Stora maskiner	25
4.10 Övrigt	25
<b>5 SAMMANSTÄLLNING AV VKK PRESENTATIONER</b>	<b>27</b>



# 1 Inledning

Den 6 - 9:e oktober 1997 arrangerades EWEC'97 i Dublin. Konferensen samlade cirka 460 deltagare. Som jämförelse kan nämnas att den förra vindkonferensen i Europa, EUWEC'96 i Göteborg, samlade cirka 600 personer.

Erfarenheter som presenterades på konferensen visar att vindkraften ökar kraftigt i de olika europeiska länderna. Under det senaste året har utbyggnaden varit mycket kraftig i ett flertal länder, speciellt i Tyskland. Under 1996 ökade den installerade vindkraften med 1300MW och vid slutet av 1996 fanns det totalt i hela världen ungefär 6100 MW.

Tyskland och USA är de länder som har mest vindkraft i världen. Danmark ligger på tredje plats och Sverige finns på åttonde plats med 103 MW installerad effekt.

## 2 Allmänt om konferensen

Årets konferens hade samlat färre deltagare än EUWEC'96 i Göteborg. Anledningen var enligt uppgift att konferenslokalerna på Dublin Castle inte klarade av mer än cirka 300 deltagare. Arrangören hade därför varit sparsamma med annonsering av arrangemanget.

Det var 26 olika länder representerade. Nedanstående tabell visar deltagarantal från några olika länder.

England	73
Danmark	68
Irland	58
Tyskland	46
Holland	40
Spanien	24
USA	23
Sverige	22
Japan	18
Grekland	17
Finland	16
Frankrike	11

samt ett mindre antal från Belgien, Kanada, Kina, Estland, Italien, Malta, Mexico, Marocko, Norge, Polen, Portugal, Sydafrika, Ryssland och Schweiz. Totalt var 460 personer anmälda till konferensen.



Totalt presenterades 104 muntliga föredrag och 107 "posters". Översiktligt program för konferensen framgår av Figur 1. Vindkraftskonsortiet presenterade 13 olika föredrag och "posters". I anslutning till konferenslokalerna fanns en utställning.

Utställningen av "posters" fick speciell uppmärksamhet vid konferensen genom det "poster award" som delades ut till bästa "poster".

### 3 Invigningen

Konferensen invigdes av Irlands **Energiminister** Joe Jacobs. (det lyckades vi inte med i Göteborg). Han redogjorde för det ambitiösa program som man har i Irland för att introducera CO<sub>2</sub>-fri elproduktion. Vindkraften kommer att vara en viktig del i en sådan politik. Andelen vindkraft är för närvarande liten, men den ökar snabbt. I juni -97 hade man 24.5 MW installerad effekt och den kommer vid årsskiftet 97/98 att vara 50 MW.

Arrangören hade för invigningen engagerat ett flertal "tunga" namn inom energiområdet:

*Joanna Tachmintzis* från EU-kommissionen redogjorde för den strategi som kommissionen har för att introducera förnybar elproduktion i Europa. Målet är att vi skall ha 12% år 2010, i dag är andelen 6%. För att stimulera denna introduktion kommer kommissionen inom en snar framtid att presentera ett "white paper" om energi samt en tillhörande "plan for action". I sitt anförande pekade hon på några frågor som är viktiga vid den framtida utvecklingen av vindkraften:

- frågor kring tillgången till elnätet måste lösas
- rättsliga aspekter vid introduktion av vindkraften i landskapet
- viktigt att se samband mellan vindkraftstillverkning och arbetstillfällen
- minskning av CO<sub>2</sub>-utsläpp med 15% mellan åren 1990 och 2010

Den sista punkten kommer att vara EU:s krav vid FN-konferensen om miljöpåverkan som kommer att arrangeras i december 1997 i Kyoto, Japan.

*M. Jefferson*, Deputy Secretary General, World Energy Council, menade att kemin bakom växthuseffekterna förstås till fullo och att det är av stor vikt att minska CO<sub>2</sub>-utsläppen i världen. Ett citat - Om kineserna fortsätter att öka sin kolanvändning i nuvarande takt kommer man om 15-20 år att få säga "good-bye" till sina risskördar.

*Birger T. Madsen* gav en sammanställning av vindkraftens status och utbyggnad just nu. Han visade att EU:s planer 1990 var att det år 2000 skulle finnas 4000 MW installerad vindkraft. Det målet har vi redan i dag uppnått. Utbyggnaden har således gått betydligt snabbare än vad man förutsåg på EWEC'91 i Amsterdam.

Madsen pekade på de trender som han såg för framtidens vindkraftverk:

- uppskalning kommer att fortsätta
- direktdrivna generatorer kommer att ta marknadsandelar
- "offshore" och stora maskiner kommer i framtiden
- prognos för 2001 är att det finns 9406 MW
- aggregat av storleken 500 - 1000 kW kommer att vara marknadsledande under de kommande fem åren

Sammanfattningsvis kan vi konstatera att de presentationer som gjordes vid invigningen var mycket optimistiska om vindkraftens fördelar och möjligheter i framtiden.

*Kuriosa.* Ett intressant påpekande gjordes av G. van Kuik avseende de engelska orden "windmill" och "wind power". Observera att det finns ett mellanslag i wind power och att så ej är fallet i windmill. Detta beror enligt lexikonet på att windmill betraktas som något vardagligt och inarbetat. G. vanKuik tyckte därför att det nu är dags att skriva ihop wind power till ett ord!

## 4 Referat från teknikområden

VKK var representerade vid konferensen med 13 föredrag och posters. I denna rapport finns en sammanställning av dessa. Dessutom bifogas några föredrag med anknytning till VKK:s verksamhet. Samtliga föredrag kommer senare att presenteras i proceedings från konferensen.

Nedan görs en sammanställning av olika "teknikområden". Erfarenheter från övriga områden kommer att sammanställas av Vattenfall Utveckling AB på uppdrag av Elforsk. För fullständig information från konferensen rekommenderar vi därför läsning av båda rapporterna.

### 4.1 Vindunderlag och potentialfrågor

Två sessioner med föredrag tillsammans med en postersession behandlade ämnet vindresurser. Presentationerna, sammanlagt 26 st, kan indelas i följande huvudgrupper:

- vindklimat, potential och modeller
- instrument och kalibrering

Generellt kan sägas att många presentationer behandlade förhållandena i komplex och heterogen terräng, medan off shore endast berördes i ett par fall. Kanske beror detta delvis på den felaktiga föreställningen att vindförhållandena till havs är 'snälla' och okomplicerade. Förhållandervis mycket arbete verkade också ha lagts ned på s.k. 'site calibration', d.v.s. hur man ska kunna verifiera energiproduktion mot en referens då man har heterogen terräng. Däremot sades tyvärr inget om bättre metoder och modeller för att kunna optimera valet av platser för vindturbiner i en heterogen omgivning med mycket variabla vindförhållanden, syftande till att turbinerna skall kunna placeras så att de producerar så mycket energi som möjligt.

### **Vindklimat, potential och modeller**

Resultat från studier av vindpotential rapporterades från tre områden, Östersjön, Irland, samt Kolahalvön. I det senare fallet har enbart den danska WA<sup>S</sup>P modellen använts tillsammans med mer eller mindre bristfälliga data från 12 meteorologiska stationer, medan i fallet Irland en intressant metod använts där man kombinerar WA<sup>S</sup>P körningar för den småskaliga och detaljerade vindkarteringen, med körningar med en mycket mer fullständig mesoskalemodell för det atmosfäriska gränsskiktet, den s.k. KAMM-modellen från Karlsruhe i Tyskland. Denna modell kan på ett mera realistiskt sätt än WA<sup>S</sup>P modellera vindfältet med en rumsupplösning av 5 km. Detta mesoskaliga vindfält kan sedan användas som underlag för en mer detaljerad kartläggning med WA<sup>S</sup>P. Metoden att utnyttja en numerisk mesoskalemodell bör ge en betydligt bättre vindpotentialkartering än vad som är möjligt om enbart WA<sup>S</sup>P används. Vindkarteringen över Östersjön har gjorts enbart med hjälp av en mesoskalig gränsskiktsmodell, MIUU-modellen från Meteorologiska institutionen i Uppsala, och syftade till att få en första uppfattning om vindpotentialen över öppet hav. MIUU-modellen kan, till skillnad från den betydligt enklare WA<sup>S</sup>P, generera de klimatologiskt betydelsefulla vindmaxima på relativt låg höjd som frekvent observerats i Östersjöområdet. I en poster redogjordes för observationer av dessa vindmaxima (low level jets) samt visades ett par exempel på vindfält med MIUU-modellen från fall med sådana vindmaxima.

En presentation redogjorde för en sensitivitetsstudie av hur väl vindklimatet bestämt med WA<sup>S</sup>P stämmer överens med mätningar i mycket komplex terräng i Portugal, samt vad upplösningen i det tillgängliga digitala kartmaterialet betyder för resultatet. Det visade sig att om man helt oförbehållslöst använder mätningar från en plats i ett bergsområde för att bestämma vindklimatet på en annan plats kunde felet uppgå till  $\pm 40$ -50%. Om man däremot valde sin referensstation så att dess komplexitetsgrad avseende terrängens utseende stämde överens med vad man hade på den plats man skall uppskatta vindklimatet på, så kunde felet nedbringas

till storleksordningen  $\pm 5-10\%$ . Detta är ju dock fortfarande stora fel, och med tanke på att man i de flesta praktiska fall har mycket få mätstationer att tillgå och därför egentligen i praktiken inte alls har några möjligheter att ställa krav på platserna, så är fel av storleksordningen flera tiotals procent nog att befara i många fall. Slutsatsen får nog bli att bättre modeller måste till för att man ska kunna bedöma vindpotentialen i heterogen terräng. Att utnyttja modeller som inte är gjorda för att användas i bergsområden är inte att rekommendera.

Generellt avseende vindar i komplex och heterogen terräng kan nämnas tre studier. Från mätningar på Shetlandsöarna rapporterades om analyser av hur de statistiska egenskaperna hos det turbulenta vindfältet modifieras i komplex terräng jämfört med mer homogena förhållanden, speciellt då i termer av spektra och koherens. I en annan presentation redogjordes för vissa resultat vad avser medelvind och turbulensstatistik i komplex terräng på Marmari i Grekland. En analys från en fjälldal vid Suorva i Lappland visade att det inte enbart är på högfjället som en god vindpotential kan förekomma.

Flera presentationer handlade om vindförhållandena och vindenergi generellt i arktisk miljö där problem med nedisning kan förekomma. Speciellt har Finland här varit aktivt. I en studie redogjordes för ett första försök att kartera var i Europa nedisning kan befaras.

### **Instrument och kalibrering**

Inom detta område gavs 5 presentationer. I två arbeten redovisades studier rörande kalibreringar av skålkorsanemometrar. I det första behandlades erfarenheter av rekommendationer av MEASNET, ett nätverk av mätinstitut. I det andra arbetet redogjordes för en jämförelse mellan kalibreringar av en anemometer som skickats runt i världen till olika vindtunnlar. Båda studierna visar att en kalibreringsnoggrannhet på bättre än 1% inte alltid är så lätt att få. En presentation berörde också problemställningar vad gäller att jämföra prestanda för olika typer av skålkorsanemometrar och föreslog en möjlighet att klassificera anemometrarna.

En typ av anemometrar som under senare år blivit allt vanligare är de s.k. ultraljudsanemometrarna. Dessa mäter vindens tre komponenter genom att mäta tiden det tar för en ultraljudspuls att färdas mellan tre par av sändare-mottagare. Två presentationer handlade om denna typ av anemometrar. Problemet med dem är att de ger en omfattande aerodynamisk störning av vindfältet runt instrumentet, vilket får till följd att mätningarna måste korrigeras med så mycket som upp till 10% på vindhastigheten i vissa vindriktningssektorer för att bli korrekta. Sådana korrekationer är dock möjliga att göra efter kalibrering i vindtunnel, vilket också redovisas i ett arbete där sådana kalibreringar genomförts. En fördel med ultraljudsanemometrar jämfört med skålkorsanemometrar är, fränsett att de

inte har några rörliga delar som slits, att de efter korrektionen inte enbart ger vinden i horisontalplanet utan alla tre komponenterna, dessutom med en frekvensupplösning av hela 20 Hz.

## 4.2 Aerodynamik

Aerodynamik presenterades under två muntliga sessioner samt med 12 posters.

Presentationerna kan indelas i följande ämnesområden.

- Profildesign
- Navier-Stokes metoder och potentialströmningsmodeller.
- Buller
- "Dubbel-stall"
- Dynamisk stall
- Is-problematik

Nedan följer kommentarer kring några av presentationerna.

### Profil och bladdesign

Risö visade på en testrigg för profilprov som de använder i den danska VELUX-tunneln samt på exempel på utveckling av profiler. Peter Fuglesang visade hur han använt en generell numerisk optimeringsmetod i kombination med profilberäkningsprogrammet XFOIL för att designa profiler. Han visade ett exempel med en 24 % t/c "koncept-profil". Denna hade optimerats för att erhålla maximal strukturell styvhet med bivillkor för stallkaraktistik, design-CI och glidtal. Optimeringsförfarandet visar på stora möjligheter att ta fram bra profiler skräddarsydda för vindkraftverk. Det är uppenbart att Danmark (Risö) satsar på att ta fram skräddarsydda profiler för framtida danska bladprojekt.

City University i London har sedan flera år ett EU-projekt på gång tillsammans med Ecotecnica i Spanien och numera i en andra fas även med LM Glasfiber. Projektet handlar om "Air-jet vortex generators". Virvelgeneratorer (Vortex generators, VG) har redan förut använts för att få en profil som utan VG's skulle få avlöst gränsskikt att vidmakthålla anliggande strömning. (avlöst strömning ger högre motstånd och förlust av lyftkraft). Normalt används små deltagningar som ställs upp vinkelrätt mot ytan (höjden på vingarna är av samma storlek som gränsskiktet, typiskt ca 20 mm för en 20-metersvinge). Problemet med dessa VG's är att de orsakar ett "paracitmotstånd" vid låga vindar då de egentligen inte behövs. För att reglera effekten av VG's skulle man vilja kunna justera deras höjd. Projektet "Air-jet vortex generators" går ut på att man blåser ut luft genom små hål i vingen. Luftströmmen som blåses ut orsakar en virvel som blandar ner energirik strömning från utanför gränsskiktet ner till ström-

ningen vid bladytan på samma sätt som mer konventionella VG's. Vid låga vindar blåses ingen luft ut och vingen blir som en vinge utan VG's. När man närmar sig stall kan man börja blåsa ut luft och fördröja stallen. Vid stall är förhoppningen att man skall kunna reglera stallförloppet och på så sätt effekten. Tanken är att man skall få en stall-reglerad turbin med samma gynnsamma effektkurva som en pitch-reglerad. Man har utfört 2-D vindtunnelprov som visar att "Air-jet vortex generators" fungerar. Inledande fullskaleprov har gjorts. Man hade hål vid radiella stationer mellan 55-75%  $r/R$ . Fullskaleproven visade att man kunde höja max effekt från ca 140-160 kW för den specifika turbinen med hjälp av blåsning. Vid dessa försök hade man en fläkt i navet för att erhålla tillräckligt högt tryck till utblåset. För att driva denna fläkt åtgick emellertid en relativt stor effekt och mycket av effektvinsten försvann. Förhoppningar finns dock att man skall kunna designa tilluftkanlen i vingen bättre och att det fungerar bättre med utblås på större radier. Man kommer dock även att se hur långt man kan nå genom att använda enbart "ramtrycket". Sammanfattningsvis så kan man säga att man ännu inte lyckats uppnå hela målet att ge en stall-reglerad turbin lika stor energifångning som en pitch-reglerad turbin med samma radie. Projektet visar ändå på goda möjligheter till både god reglering och förhöjning av verkningsgraden med hjälp av "Air-jet vortex generators".

### **Navier-Stokes metoder och potentialströmningsmodeller**

Nio presentationer handlade om beräkningar med Navier-Stokes tidsmedelvärdesbildade ekvationer och beräkningar med potentialmetoder. Jämfört med konferenser tidigare år kan man se att framsteg görs på området för Navier-Stokes metoder och att presentationer med Navier-Stokes lösningar är fler än presentationer med potentialströmningsmetoder. Man redovisar nu N-S beräkningar på hela turbinblad. Utifrån jämförelse med 2D beräkningar och 3D beräkningar på blad hoppas man t.ex. att kunna ta fram semi-empiriska korrektionsmetoder att användas i BEM-beräkningar (Hansen, Sörensen, m.fl.). Samtliga deltagare påtalade dock att utveckling av turbulensmodeller fortfarande behövs för att kunna prediktera  $C_l$  och  $C_d$  i "post-stall"-området" med större säkerhet.

### **Buller**

Tre presentationer hade anknytning till buller. Resultat från EU JOULE III projekten DRAW och STENO presenterades. I projektet DRAW skall man förbättra/utveckla existerande beräkningsmetoder för bullerberäkningar. Man utför mätningar av buller från 2D profiler i en ekofri vindtunnel. Man mäter gränsskiktsp parametrar (t.ex. instationära trycknivåer på profilytan) samtidigt som man mäter buller med sofistikerade "antennar". Utifrån mätningarna skall man ta fram samband mellan buller och gränsskiktsp parametrar. Man har även studerat buller p.g.a. turbulens i den an-

strömmande luften (inflow turbulens noise). Dessa senare mätningar verifierar till stor del de teoretiska modeller som man utvecklar. T.ex. har man visat och verifierat hur man kan konstruera profiler som har en utformning (främst runt framkanten) så att "inflow turbulence noise" kan minskas.

I STENO har man gjort fullskaleprov med "serrated trailing edges" Detta innebär att bakkanten är sågtandad. Enligt teorin skall en sådan bakkant kunna ge en reduktion av bullret genererat av det turbulenta gränsskiktet (trailing edge noise) med flera dB. Dessa teorier har också bekräftats vid 2D vindtunnelprov. De fullskaleprov man utfört visar att man, relativt ett blad utan sågtands-bakkant, erhåller en reduktion av bullret för vissa frekvenser men för andra frekvenser så ökar istället bullret. Proven är dock ännu inte slutförda och resultaten än så länge preliminära.

Kristian S. Dahl hade en poster som visar att man börjat med "Computational Aero-Acoustics" på Risö. Detta innebär att man beräknar ljudet direkt från lösningen av en instationär CFD beräkning. Man har beräknat ljudsignaturen från en profil vid hög anfallsvinkel då periodiska avlösningssfenomen uppträder. Man har dock problem med att uppnå stabilitet i ljudberäkningarna.

### **Dubbel-stall**

Många stall-reglerade turbiner (de med NACA 63-200 profiler) uppvisar multipla nivåer på effekten i stallområdet. Detta är inte önskvärt då man helst vill ha en entydig vind-effekt kurva. Det är t.ex. annars svårt att uppskatta energiproduktionen från vindkraftverken. Man har länge sökt en rimlig förklaring på detta fenomen. Risö har även funnit att flera nivåer på  $C_l$  är möjligt vid genomförda vindtunnelprov, såväl 2D prov som prov med ett icke-roterande hela blad. För konstant anfallsvinkel kan strömningen ändra sig och resultera i olika  $C_l$ -nivåer. (Detta är inte repetitivt på samma sett som statisk stall-hysteres). Genom analys med CFD kod har man funnit att fenomenet troligen har att göra med gränsskiktomslag. NACA 63-215 profilen är mycket känslig för ifall omslag till turbulent gränsskikt sker (eller inte sker) innan laminär-separation och en laminär gränsskikts-bubbla utbildar sig. Ifall laminär-separation sker så är strömningen sedan mycket beroende på hur snabbt omslag till turbulent strömning sker i bubblan. Det är troligt att små störningar i omslagsprocessen (t.ex. små radiella flöden i gränsskiktet) kan påverka ifall man får en kort bubbla och anliggande strömning efter bubblan eller ifall omslag sker så sent att bubblan inte återanligger vilket orsakar kraftig avlösning och ett lägre  $C_l$ .

Vad är det då för vits med att man kommit på en trolig anledning till "dubbel-stall"? Jo, man kan i framtiden se till att inte använda denna typ

av profiler med en funktion av anfallsvinkeln så att lyftkraften blir så extremt känslig för störningar i omslagsprocessen.

### **Dynamisk stall**

Herman Snel visade hur man matematiskt kan simulera det fenomen att lyftkraften får en oscillerande del vid kraftigt avlöst strömning. Genom att bestämma konstanter i den (icke-linjära) matematiska modellen fick han god överensstämmelse med resultat från vindtunnelprov med dynamisk stall där "oscillerande överslängar" av lyftkraften uppmätts. Det är ännu osäkert huruvida dessa "oscillerande överslängar" har någon betydelse för lasterna på bladet. Detta skall utredas. En stor finess är att den modell som Snel redovisade kan läggas till existerande semi-empiriska modeller för dynamisk stall av den typ som bl.a. använts i VIDYN.

FFA och Teknikgruppen visade i en presentation (Computations of Aerodynamic Damping for Blade Vibrations in Stall) på hur den beräknade aerodynamiska dämpningen av bladsvängningar är beroende av hur man modellerar effekten av dynamisk stall. Man visade även hur viktigt bladets utböjningsformer är. Den aerodynamiska dämpningen är beroende av hur anfallsvinkeln för ett bladelement ser ut som funktion av tiden under det att bladet svänger. Relativt små ändringar i orienteringen av bladets huvudtröghetsaxel har en stor inverkan på dämpningen av svängningar. Detta visar hur viktigt det är att ha turbinens strukturella beteende väl beskrivet, men visar även på möjligheterna att medelst kopplingar mellan olika typer av rörelser skapa bättre aerodynamisk dämpning.

### **Is-problematik**

Henry Seifert visade prov på nedisning av blad. Man har gjutit av ett flertal blad som varit nedisade och gjort modeller som man kört 2D-prov i vindtunnel med. Detta har lett till en omfattande databas med  $C_l$ ,  $C_d$  och  $C_m$  för nedisade profiler.

Per Völund från Risö redovisade resultaten från ett JOULE projekt med syftet att studera is-inducerade laster. Man visade hur man ofta får en kraftig minskning av den elektriska effekten. Det finns dock fall då den kan öka i stall-området. Detta beror på att bladytan ökar utan att  $C_l$  och  $C_d$  "förstörs" i samma omfattning. Man har ägnat stor tid att studera de dynamiska lasterna. Man har studerat frekvensspektra av bladrotmoment för fall då blad varit fria från is respektive nedisade. Man hävdade att egenviktsinflytandet av isen var försumbart. Vid frekvensen för den första "edge-moden" kan man se en stor förhöjning av lastnivåerna för nedisade blad. Vid 13 m/s har en turbin visat på kraftiga vibrationsnivåer trots att bladens uppvärmningssystem var igång.



### 4.3 Strukturdynamik

Vad muntliga presentationer och posters beträffar var mitt intresse särskilt inriktat på att följa upp strukturdynamik och verifieringar av beräkningsprogram. I det följande ges en personlig bild av vad konferensen gav på dessa områden. Man konstaterade emellertid snabbt att konferensprogrammet inte innehåller någon explicit rubrik som berör detta. Sett över några år innebär detta en märkbar förändring. Beräkningsprogram och strukturdynamik ingår emellertid som en basresurs för studier på många andra områden inom vindkrafttekniken. Utveckling av aerodynamik som beaktar effekter av strukturdynamik, m.a.o. aeroelasticitet är ett sådant område som i dag är mycket aktuellt. Studier av laster på vindkraftaggregat och hur de påverkas av vaksituationer förutsätter också strukturmodeller. Frågor kring extremaster och utmattning likaså. VKK är redan involverade i de flesta av de projekt med sådan inriktning, som presenterades.

Två presentationer förtjänar ändå att nämnas explicit. Den första är Tomas Kruegers "Reduction of fatigue loads on wind energy converters by advanced control methods". Förutom att han presenterade möjligheterna med reglering för att behärska aggregatdynamiken, är det värt att notera det behov som uppstår i samband med att man i Tyskland i ökande grad lokaliserar aggregat inomlands. Detta kräver högre torn och då blir torn-dynamiken en viktig fråga.

Den andra presentationen, som jag vill nämna, gjordes av Spyros Voutsinas, i vilken han mycket proffsigt presenterade det nyutvecklade beräkningsprogrammet GAST. På sikt är målet att detta skall inkludera både komplett struktur och moderna modeller av aerodynamik. Strukturmodellen utgörs av en FE-beskrivning, som normalt leder till några hundra frihetsgrader. Det finns planer på att programmet framöver skall finnas allmänt tillgängligt på nätet ("public domain"). Vid intervju framkom att finansiering av detta återstår, och att planerna är inom storleksordningen ett år. I dag sker uttestning av programmet på kraftfulla arbetsstationer.

Utvecklingen av vindkraftteknologin i framtiden togs upp av Peter Hjuler Jensen vid konferensens sista presentation "Wind turbine technology in the 21:st century". Förutom att han blickade bakåt och konstaterade hur svårt det var att för 10-15 år sedan kunna förutsäga situationen i dag och att det sannolikt är lika svårt med förutsägelser i dag, konstaterade han att utvecklingen mot konkurrenskraftigare aggregat leder till lättare och flexiblare aggregat. Detta ställer ökade krav på verifierade och tillförlitliga "Design Codes". Andra ingredienser i utvecklingen, som han betonade, var variabelt varvtal, normer och säkerhetsmarginaler för design.

## 4.4 Funktion och prestanda

### FO.1 Windfarms in hostile terrain

Ett EU projekt som började 1/1 96 med Garrad & Hassan som koordinator. Syftet är att kartlägga belastning i farmerna samt registrera extremförhållanden. Problem med väderförhållanden blixtnedslag m.m. har gjort att man ej fått igång mätningar. Man hoppas kunna mäta under vintern 97/98. Projektet avslutas 1988. Under projekteringen konstaterade man att olika standarder stämde dåligt överens samt att lite hjälp erbjöds.

### FO.2 How complex can a power curve measurement be, Helmut Klug

#### Extrapolation av vindhastighet

Redovisar en metod att extrapolera vindhastigheten till navhöjd som kan användas för stora turbiner för att hålla kostnaden för masten nere. Genom att kombinera information från vindhastighet och temperatur från flera höjder kunde en noggrannare extrapolation göras. Metoden fungerar ej nära kust samt under vissa väderförhållanden. Då anpassningen ej blir så bra förkastas data.

#### Alternativ kalibrering av mätplats

Metoden går ut på att kalibrera en mätplats genom att använda vindhastighetsgivaren på maskinhustaket vid stillastående turbin. Platsfelet på maskinhustaket kartläggs m.h.a lasermätning på modell i vindtunnel (utan blad!?) Vissa experimentella jämförelser med fullskala visar att man kan få hygglig överensstämmelse.

### FO.3 Comparing the Power Performance Results by Using the Nacelle and the Mast Anemometer, Ionassis Antonio

Man har undersökt hur sambandet mellan vindhastighet på maskinhustaket och fri vindhastighet påverkas av ändringar på turbinen, bladvinkel virvelgeneratorer girfel m.m.

Grundsambandet bestäms med vindar från en fri sektor. Detta samband används sedan för att bestämma vind-effektkurvan med vindar från en sektor med stora hinder (kolupplag, kolkraftverk). Man konstaterar att sambandet ändras då man gör smärre ingrepp med turbinen samt att metoden med att använda vindhastighet på masinhustaket endast kan användas för att verifiera vindeffektkurvan för en turbin då man får ett identiskt samband som för referensturbinen. Om sambandet avviker vet man inget.

**FO.4 Vestas Experience with Offshore Installation**

Vestas har installerat 10 (19?) turbiner V39-500 kW på Tunø Knob.

Man konstaterar att intresset för havslokalisering bland kraftföretag och andra intressenter svängt helt om i Danmark det senaste halvåret och att intresset nu är mycket stort.

Modifieringar på själva turbinen, föranlett av havslokalisering, ökade kostnaderna med ca 5%. Man kompletterade turbinen med en extra kran på maskinhustaket. Varvtalet kunde ökas från 30 till 33 rpm eftersom bullerkraven är lägre till havs.

Tillgängligheten är hittills något lägre än för motsvarande landbaserade aggregat p.g.a. att man ej kan komma åt turbinerna då våghöjden är >1m samt p.g.a. vissa fågelstudier då turbinerna stoppats. Övriga erfarenheter är att turbulensen är lägre, produktionen ca 25 % högre och kostnaderna högre men ändå 25 % lägre än förväntat.

Kostnaderna för nätanslutning och fundament uppvisar de största skillnaderna gentemot landbaserade aggregat. Man konstaterar att kostnaderna för fundamentet är stora, men att de ej är så markant beroende av storleken, vilket gynnar stora aggregat till havs.

**FO.5 Condition monitoring of wind farms using 10 minute average**

Syftet är att förbättra produktionen i vindfarmer genom att använda SCADA (Supervisory Control and Data Acquisition). Förbättringen åstadkoms genom att försöka sortera bort yttre faktorer, smalare sektorer samt använda vindhastigheten som skalfaktor. Metoden används för att detektera olika fel i bladvinkel, växellåda, girfel etc. Verkar fungera bra.

**FO.6 Assessment of power performance measurement and evaluation in complex terrain.**

Undersökning av inverkan på prestanda från olika parametrar som är förknippade med komplex terräng. Analysen som huvudsakligen utförs genom "mångvariabelanalys" visar hur olika parametrar inverkar. Arbetet ingår som en del i EWTS-II och syftar till att ta fram en teknisk bas för fortsatt standardiseringsarbete.

## 4.5 Elsystem och reglerteknik

Konferensen hade avdelningarna Dynamics & Control, Electrical Components och Grid Integration som behandlade el- och reglerteknik.

Det allmänna intrycket är att variabelt varvtal kommer att dominera på sikt, p.g.a. att nätkvalitén och bullret måste tas i beaktning. Vidare så verkar merparten av deltagarna vara överens om att självkommuterade om-

riktare, vilka använder sig av IGBT-ventiler, kommer att användas och att de nätkommuterade omriktarna kommer att fasas ut på sikt.

Inom området elektriska komponenter presenterades fyra artiklar som behandlade direktdrivna generatorer, två som berörde aktiva filter, en om vindkraftverkets jordning, två som visade på bromsning av en asynkron-generator vid nätbortfall, en på skydd mot blixtnedslag och en behandlade optimal storlek av transformatorer.

T. Hartkopf, M. Hofmann och S. Jöckel med artikeln "Direct-drive generators for megawatt wind turbines" hade undersökt olika typer av magnetisering i kombination med olika typer av likriktare för direktdrivna generatorer. Resultaten visade att permanentmagnetiserade generatorer är lättare, effektivare och billigare än elektriskt magnetiserade. Vidare visades att likriktning med IGBT-omriktare har en fördel över likriktning med dioder. Den senare fördelen är inte lika övertygande som den med PM magnetisering.

I artikeln "Direct drive, geared drive, intermediate solution-comparison of design features and operating economics" av G. Boehmeke och R. Bolt visades på klara fördelar för den konventionella växlade drivlinan med asynkron-generator. Ekonomiska fördelar kan bara visas för den direktdrivna generatorm om mycket höga felfall är antagna för det växlade alternativet. En kommentar till resultaten är att de höga kostnaderna för det direktdrivna alternativet har sin grund i att den direktdrivna generatorm var en traditionellt elektriskt magnetiserad synkron-generator.

Från VKK:s sida presenterades två artiklar, A. Grauers, O. Carlson, E. Högberg, P. Lundmark, M. Johnsson och S. Svenning "Tests and design evaluation of a 20 kW direct-driven permanent magnet generator with a frequency converter" och J. Svensson "The rating of the voltage source inverter in a hybrid wind park with high power quality". Den först nämnda beskrev provmetoder, provresultat och beräkningar av förluster för en 20 kW PM direktdriven generator. Provresultaten visade på goda elektriska prestanda, men då den provade generatorm är en prototyp rekommenderades några mindre justeringar för att uppnå märkeffekten 20 kW.

J. Svensson visade i sin artikel på möjligheterna att med en IGBT-växelriktare aktivt filtrera de övertoner som finns på nätet samtidigt som växelriktaren överför vindkraftverkets effekt ut på nätet.

Å. Larson visade på sina resultat från arbetet inom Elforsk med artikeln "Optimal size of transformers" att den optimala skenbara effekten på en transformator är detsamma som generatorms märkeffekt eller något lägre.

En intressant artikel, J. H. Carstens, "Active filters for power-smoothing and compensation of reactive power and harmonics", behandlades aktiv

effekt utjämning och aktiv filtrering av ström övertoner från en vindpark. Effektpulsationer uppstår mellan asynkrongeneratorn och nätet för ett vindkraftverk med ett konstantvarvtal. Dessa effektpulsationer kan uppgå till 20% av märkeffekten. Genom att använda sig av ett energilager kan omriktaren leverera eller konsumera aktiv effekt och på så sätt jämna ut effektfuktuationerna på nätet. Den mest intressanta energilagringssprincipen som artikeln beskriver är supraledande spolar.

Under rubriken Dynamics & Control kunde man finna 5 muntliga presentationer och 9 posters. Ytterligare några reglertekniskt inriktade bidrag återfanns under övriga rubriker.

Flera presentationer berörde reglering av aggregat med variabelt varvtal, som ju är den inriktning som studerats inom svensk vindenergiforskning.

I ett bidrag från Darmstadt, Tyskland, använde man sig av den gamla välkända  $w^2$  metoden som för länge sedan prövats på Hönö. I simuleringar har man studerat effekttransienter vid övergången till märkeffekt, utan att egentligen komma med några slutsatser som inte var kända sedan tidigare.

Sessionens ordförande Bill Leithead presenterade en artikel, "A robust two-level control design approach to variable speed stall regulated wind turbines" om en designmetod för aktiv stall reglering som ökar stabilitetsmarginalerna jämfört med en traditionell regulator. Metoden påminner mycket om den kaskadreglering som presenterades i Thommy Ekelunds avhandling. Man har en inre snabb reglering av varvtalet och en långsammare yttre för att ta hand om effekten. Priset för ökad robusthet är försämrade prestanda, det vill säga större effektvariation.

Från Risö kom intressanta praktiska resultat där man utrustat ett standardaggregat ifrån Vestas med variabelt varvtal med hjälp av en Sami Star ifrån ABB i artikel "Experimental investigation of combined variable speed/variable pitch controlled wind turbines" av H. Bindner, A.V. Rebsdorf och W. Byberg. Tyvärr visade det sig att effekten under märkvind försämrades vid variabelt varvtal. Detta antogs bero på att den verkliga effekt/varvtals karakteristiken avvek ifrån den som antagits vid reglerdesignen. En personlig reflektion är att Samin drar en hel del effekt, vilket konstaterats tidigare för NWP 400.

I övrigt så handlade det bland annat om bladvinkelreglering. Vid Aalborgs universitet hade man med robust  $H_\infty$  reglering lyckats reducera pitch variationen med 20 % utan att försämma effektregeringen.

En grupp från Kassel visade i artikeln "Reduction of fatigue loads on wind energy converters by advanced control methods" att det var möjligt att reducera flapmomentet genom att utgå ifrån en alternativ (stationär) strategi som innebar minskad effekt. Dessutom presenterades idéer om

aktiv dämpning av tornrörelsen med hjälp av pitchreglering, samt yaw- och tiltkompensering med individuell pitchreglering.

Från VKK presenterade T. Ekelund artiklen "Continuous yaw-control for load reduction" som behandlade möjligheten att minska dynamiska laster genom styrning av sidvridsservot. Teoretiska studier visade att lasterna i tornet minskade.

## 4.6 Nätintegration

Avdelningen Grid Integration hade indelats i två sessioner, Grid Integration A och Grid Integration B. Ordförande i den första sessionen, Grid Integration A, var den mycket kunniga David Milborrow. Denna mycket intressanta session inleddes av Gerhard Gerdes som gav en överblick av elkvalitetsmätningar med artikeln "Overview and development of procedures on power quality measurements of wind turbines". Artikeln var författad av G. Gerdes, F. Santjer och R. Klosse, samtliga från DEWI i Tyskland. I Tyskland klassificeras vindkraftverkens elektriska egenskaper. Syftet med denna klassificering är att bestämma vilken påverkan vindkraftverken kommer att ha vid en nätanslutning. DEWI har hittills mätt elkvaliteten på ett 40-tal olika vindkraftverk. Tyvärr "äger" inte DEWI mätningarna, så all publicering av elkvaliteten från ett visst fabrikat eller en viss typ av vindkraftverk omöjliggörs. I denna presentation hade vindkraftverken indelats i olika grupper med avseende på effekttorlek, ex 400-600 kW.

John Olav Tande tidigare anställd på Risø (numera verksam vid EFD) presenterade artikeln "Power quality requirements for grid connected wind turbines". Artikeln som var skriven tillsammans med Paul Gardner från Garrad Hassan and Partners Limited behandlade resultaten från IEC:s arbete i TC 88 med samma titel som artikeln. IEC:s arbete behandlar vindkraftverk anslutna till trefasnät och med en märkeffekt över 50 kVA. Kortfattat kan sägas att arbetet innefattar fyra delar; karaktäristiska elkvalitetsparametrar för vindkraftverk, mätprocedurer, elkvalitetskrav samt metoder för att fastställa vindkraftverkens inverkan på elkvaliteten.

I ett EU-projekt har en datormodell för beräkning av flicker från vindkraftverk utvecklats. Detta arbete presenterades i två artiklar, dels artikeln "An electrical system model for predicting flicker from wind turbines", dels artikeln "Design tools for the prediction of flicker". I den senare presenterades av E. A. Bossanyi från Garrad Hassan and Partners Limited och den tidigare presenterade av N. Jenkins från UMIST. Resultaten visar att såväl X/R-förhållandet som kortslutningskvoten på nätet påverkar flickernivån.

Ordförande i den andra mindre intressanta sessionen, Grid Integration B, var Rich Watson från University College i Dublin. Sessionen innehöll sju presentationer varav tre artiklar behandlade prognostiseringen av vind och därmed förutsägelsen av vilken uteffekt vindkraftverken kan tänkas ge i ett kortare och längre tidsperspektiv. Dessa tre var L. Landberg, Risø, med artikeln "Predicting the power output from wind farms", G. Kariotakis et al med artikeln "Advanced short-term forecasting of wind power production" och T. S. Nielsen et al med artikeln "Statistical methods for predicting wind power".

I två artiklar behandlades långsiktig planering av vindkraft i elsystemet. Artiklarna hette "Long term planning of wind energy in conventional power systems" skriven av P. Skjerk Christensen, L. H. Nielsen och K. Skytte samt "Electrical power from widely-dispersed wind turbines" författad av M. Durstewitz et al.

De sista två artiklarna "Power control for wind turbines in weak grids" av John Olav Tande och Henrik Bindner samt "Control requirements for optimal operation of large isolated systems with increased wind power penetration" av M. Papadopoulos et al behandlade hur modern kraftelektro-nik kan användas för att minimera påverkan från vindkraften i svaga eller autonoma nät.

Ola Carlson från Elkraftteknik på Chalmers deltog i en studieresa till nordvästra Irland där besöktes tre vindfarmer. Två med Vestas turbiner och en med USA tillverkade Zond vindkraftverk. Den vindparken med sex Vestasmaskiner hade en medelvind på 10 m/s och var utrustad med en "Voltage control unit". Denna enhet fungerade så att om nätspänningen blev för hög på grund av låg konsumtion på nätet och hög vindkraftsproduktion, minskades effekten från ett vindkraftverk tills att nätspänningen inte blev för hög. Vad som var gemensamt för samtliga uppställningsplatser var de stora väganläggningarna i något fall 5 km och 20 % av anläggningskostnaden. Vägarna var byggda så att de "flöt" ovanpå torven som täckte marken i dessa trakter.

Vidare berättade personalen från Zond att deras nästa vindkraftverk var ett 700 kW aggregat med variabelt varvtal. Elsystemet för detta aggregat bestod av en släpringad asynkrongenerator med en rotorkaskad av IGBT-omriktare för en mindre del av effekten.

## 4.7 Buller

I det följande ges en sammanfattning av de fyra föredrag och fem posters som presenterades vid konferensen och där innehållet huvudsakligen berörde bullerfrågor. I vissa fall presenterades i flera posters eller ett föredrag plus ett poster vilket förklarar varför sammanfattning inte upptar nio rubriker.

**H. Klug et al (DEWI): Noise from wind turbines or: how many Megawatts can you get for a 100 dB(A)?**

Klug visade i sitt föredrag att ett typiskt aggregat på 150 kW för fem år sedan hade en ljudeffektnivå på 100 dB(A). Samma värde gällde för tre år sedan för ett aggregat på 500 kW och nu talar man om aggregat i megawattklass med samma ljudemission. Klug påpekade att detta har åstadkommits tack vare kundernas tryck och med ganska enkla tekniska åtgärder (dvs huvudsakligen reducerad bladspets hastighet). Mekaniskt buller har också minskat påtagligt, men har fortfarande avgörande betydelse för kringboendes acceptans av aggregatet.

**S. Ljunggren (KTH): A new IEA document for the measurement of noise immission from wind turbines at receptor locations.**

Ett nytt IEA-dokument har just blivit färdigt, se bilagd kopia av föredraget.

**T. Dassan et al (dvs prof Wagner, Stuttgarts tekniska högskola, och olika medarbetare vid NLR, TNO och VUB): Comparison of measured and predicted airfoil self-noise with application to wind turbine noise reduction.**

Vid prof Wagners institution pågår ett större arbete beträffande prediktering av aerodynamiskt buller. Målet är att få en modell där hänsyn tas till samtliga relevanta indata. I det här aktuella projektet utförs mätningar och predikteringar av bakkantsbuller samt buller orsakat av inströmmande turbulens.

13 olika modeller har testats i två av NLRs vindtunnlar. Om resultaten sågs att de till en del bekräftar de teoretiska predikteringarna men också att de ger anledning till en kritisk granskning av de teoretiska modellerna.

**K.A. Braun et al: Noise reduction by using serrated trailing edges.**

Ämnet har ju diskuterats livligt de senaste åren. I det här aktuella projektet har man gjort mätningar på en turbin (1 MW) där yttre delen av ett blad gjorts sågtandformad i bakkanten. Med hjälp av kraftiga riktmikrofon kunde minskningen i bulleralstring bestämmas. Författarna värderade mätresultatet till ca två dB. Det kunde dock konstateras att minskningen var större vid låga frekvenser än vid höga, vilket i praktiken medför att minskningen är något större än så.

K.A. Braun poängterade att den sågformade bakkanten nog gav ungefär den bullerminskning som förväntades; problemet var bara att bakkanten gav upphov till buller av ett nytt, tidigare obeaktat slag (när luften passerar mellan sågtänderna).



**Voutsinas et al (T.U. Athen): Numerical modelling of noise emission and propagation.**

Emissionsmodellen bygger i hög grad på en tidigare semi-empirisk modell publicerad av Brook m fl 1989. Resultaten kan därför inte bli särskilt exakta men kan vara användbara för uppskattningar i tidiga planeringssteden.

Utbredningsmodellen är förmodligen intressantare. Vid höga frekvenser används en strålgångsmodell, som på något sätt modifierats med hänsyn till refraktionen. Vid lägre frekvenser används en direktbestämning med hjälp av vågekvationen. Hänsyn tas enligt uppgift till markytans inverkan, det framgår dock inte vilken impedansmodell som används.

**O. Fégeant (KTH): Measurement of noise immission at receptor locations: use of a vertical measurement board to improve signal-to-noise ratios.**

Med hjälp av en vertikal mätskiva som underlag för mikrofonen kan man framhäva signalen från turbinen bland allt vindbrus. Resultatet har tagits upp i det nya IEA-dokument för immissionsmätningar. En kopia på föredraget bifogas.

**K.S. Dahl et al (Risø): Prediction of noise generated by low speed, separated, unsteady flow over an airfoil.**

Naver-Stokes ekvationer löses numeriskt i tre steg. Först bestäms de aerodynamiska lasterna med hjälp av ett förenklat förfarande (fluiden förutsätts vara inkompressibel). Därefter gör man en korrektion så att man får fram en lösning för kompressibel fluid. I tredje steget beräknas slutligen det aerodynamiska bullret med de tidigare bestämda lasterna som drivande termer.

## 4.8 Acceptansfrågor

Acceptansfrågor diskuterades i allmänna termer av flera föredragshållare. Man menade att dessa frågor har en hög prioritet men man gav inga direkta råd för hur man skall behandla detta i ett bredare perspektiv kopplat till lokalisering. Karin Hammarlund presenterade ett föredrag om vindkraft och acceptansfrågor, se Appendix 13.

En designstudie redovisades av Rob van Beek. Långa slanka torn var rekommendationen, inte speciellt revolutionerande, men ett av alternativen var en fackverksmast. Motivet för att använda ett sådant var att det går att göra dessa slanka i den bemärkelsen att strukturen är genomsläpplig och inte utgör ett solitt visuellt hinder i naturen.

Endast en muntlig framställning och en poster behandlade människors uppfattningar om vindkraft ur en social synvinkel. Vindkraftens påverkan på omgivningen hanteras alltså fortfarande framförallt som naturvetenskapliga och tekniska effekter. Designfrågorna börjar färgas av landskapsarkitekternas nyfikenhet på människors upplevelser men även detta område domineras av uppskattade preferenser. Upplevelseprocessen hanteras alltså som renodlat visuell och förövrigt handlar det om bättre teknik för att mäta buller. Från publiken höjdes röster angående hur man skall hantera människors uppfattningar och protester. I detta fallet efterlyses en anpassad etablering av vindkraft som tillvaratar den berörda befolkningens intressen. Det krävs mer integrerad forskning som kan hantera bl.a. den subjektiva upplevelsen av ljudet från vindkraftverk.

## 4.9 Stora maskiner

Torsdagen ägnades åt stora maskiner/WEGA II och framtidens maskiner.

Havslokalisering och framtida möjligheter med detta presenterades på ett mycket övertygande och professionellt sätt av P. Morthorst. Denna studie är väl värd att läsa som en introduktion till ekonomi och förutsättningar för etablering av vindkraft till havs, se proceedings när dom kommer.

## 4.10 Övrigt

### Något från avslutningen

Till sist några punkter som P. J. Jensen från Risö framlade i sitt slutanförande på konferensen.

Om vindkraftverken:

- högre flexibilitet i strukturen - beräkningstungt
- högre drivline flexibilitet - variabelt varvtal, omriktare
- högre flexibilitet i regleringen - anpassning av kontrollsystem för uppställningsplats
- adaptiv nätanslutning

Vad behövs för en stabil utveckling av vindkraften:

- ambitiösa mål - 25 % av EU elenergi
- marknads incitament - gröna skatter
- ökad R & D program



## 5 Sammanställning av VKK presentationer

VKK var representerade vid konferensen med 12 föredrag och posters. I denna rapport finns en sammanställning av dessa. Dessutom bifogas några föredrag med anknytning till VKK:s verksamhet. Samtliga föredrag kommer senare att presenteras i proceedings från konferensen.

- [1] Hans Bergström, 'Wind Resources in an Arctic Mountain Valley'
- [2] Birgitta Källstrand, 'Low Level Jets in The Baltic Sea Area'
- [3] Stefan Sandström, 'Simulations of The Climatological Wind Field in The Baltic Sea Area Using a Meso-Scale Higher Order Closure Model'
- [4] Anders Björck, Jan-Åke Dahlberg, Anders Östman, Hans Ganander, 'Computations of Aerodynamic Damping for Blade Vibrations in Stall'
- [5] Hans Ganander, Hjalmar Johansson, Christian Hinsch, Henry Seifert, 'Comparison of Load Measurements Between the Large Wind Turbines Aeolus II and Näsudden II'
- [6] Holger Söker, Evangelos Morfiadakis, Theodore Kossivas, Anders Östman, 'Footprinting Wind Turbine Fatigue Loads'
- [7] Anders Grauers, Ola Carlson, Erik Högberg, Per Lundmark, Magnus Johnsson, Sven Svenning, 'Tests and Design Evaluation of a 20 kW Direct-Driven Permanent Magnet Generator With a Frequency Converter'
- [8] Jan Svensson, 'The Rating of the Voltage Source Inverter in a Hybrid Wind Park With High Power Quality'
- [9] Åke Larsson, 'Optimal Size of Wind Turbine Transformer'
- [10] Tommy Ekelund, 'Continuous Yaw-Control for Load Reduction'
- [11] Sten Ljunggren, 'A New IEA Document for the Measurement of Noise Immission from Wind Turbines at Receptor Locations'
- [12] Olivier Fégeant, 'Measurements of Noise Immission from Wind Turbines at Receptor Locations: Use of a Vertical Microphone Board to Improve the Signal-to-Noise Ratio'
- [13] Karin Hammarlund, 'The Social Impacts of Wind Power'
- [14] Staffan Engström, Göran Dalén, Jan Norling, (Föredrag utanför VKK, men av allmänt intresse) 'Evaluation of the Nordic 1000 Prototype'

ewec97



EUROPEAN WIND ENERGY CONFERENCE

Monday 6th October	Tuesday 7th October	Wednesday 8th October		Thursday 9th October	times of sessions
Arrival & Registration	Session IV: European and International Programmes	Session IX: Resource Assessment A	Session X: Electrical Components	Session XVII: Large Wind Turbines & Offshore Session XVIII: Autonomous Systems	[08:30 - 10:15]
	Break	Break		Break	
Session I: Opening [10:15-12:30]	Session V: Financial, Business & Market Issues Session VI: Operation & Performance	Session XI: Grid Integration A	Session XII: Resource Assessment B	Session XIX: Special Session on Large Wind Turbines & Closing	[10:45 - 13:00]
Lunch	Lunch	Lunch		Farewell Reception Conference Ends	[13:00 - 14:00]
Session II: Wind Energy Issues & Achievements	Session VII: Planning & Environmental Issues Session VIII: Dynamics & Control	Session XIII: Aerodynamics A	Session XIV: Grid Integration B		[14:00 - 16:00]
Break	Break	Break			[16:00 - 16:30]
Session III: National Programmes & Policies	Poster Session & Reception	Session XV: Loading & Fatigue/Standards & Certification	Session XVI: Aerodynamics B		[16:30 - 18:30]
AGM of EWEA [18.30] in Bedford Hall Conference Reception in St Patricks Hall [18.30 - 20.00]	Informal music session in evening using wind industry talent in Mother Redcaps a nearby pub [21.00]	Conference Banquet in Trinity College [20.00]		Post conference tour of windfarms Thursday-Saturday in evening	

Figur 1. Översiktligt konferensprogram

# Appendix 1

## Wind Resources in an Arctic Mountain Valley

Hans Bergström



# WIND RESOURCES IN AN ARCTIC MOUNTAIN VALLEY

*Hans Bergström*

*Department of Meteorology, Uppsala University, Box 516, S-751 20 Uppsala, Sweden*

## ABSTRACT

Wind measurements during one year on a 36 m high tower located in an Arctic mountain valley in Lapland, Sweden, have been analysed. The results indicate that high mean wind speed climates may be found also in low elevation terrain of the Scandinavian mountain range. The annual mean wind speed at the height 35 m was estimated to be 7.5 m/s. Strong evidence of channelling was found in the wind direction distribution at, which showed two distinct peaks in the direction of the valley.

## 1 INTRODUCTION

It is often assumed that due to sheltering effects upon the lower elevation terrain, mean wind speed will be higher on mountains and ridges than in valleys. Earlier investigations in the Torneträsk area in northern Sweden show, however, that also valleys may have quite a high mean wind speed. During several experiments on the ice of Lake Torneträsk it has been shown that due to channelling effects, winds are often very high over the lake itself and at least also over the land areas close to its western shores, see [1] and [2]. At Abisko south of the lake, on the other hand, the mean wind speed is usually much lower. Estimates indicate that at 10 m height the mean wind speed over the lake may be as high as around 6 m/s, which is also true at the western shore of Lake Torneträsk, whereas the mean wind speed at Abisko is only about 3 m/s.

The reason for this somewhat unexpected high mean wind speed over the central parts of the Torneträsk valley is due to channelling effects of two physical origins. The first one is forced channelling and is of most importance when the wind direction is more or less along the dominant valleys. When an air flow meets a mountain range with tops and valleys, the air is accelerated when it is forced to pass between the mountain tops. The second one may be called pressure driven channelling or 'gap winds', and is of most importance with wind directions more or less perpendicular to the valley axis. With such a wind direction, the air pressure gradient will be along the valley axis, and this pressure gradient will accelerate the air in the direction towards the low pressure, up to some hundred metres height over the valley bottom. For this effect to become important, it is needed that the surface roughness is very small, so that the friction between the air flow and the ground will also be small. This is often the case in arctic areas, as the ground during perhaps half of the year is covered with snow or ice. Also lakes and dams in the valleys will be favourable for the gap winds to develop as the surface roughness of water is also very low.

Many valleys of the Scandinavian mountain range are oriented more or less as the Torneträsk valley, with their axes from west-northwest to east-southeast. But there are of

course also lots of differences, for example as regards the valley widths, the occurrence of lakes or dams in the valley bottoms, and the height differences between the valley bottoms and the surrounding mountains. The exact importance of all these factors is presently poorly known, but it may be expected that mean wind conditions at least in some mountain valleys are more favourable than has earlier been assumed. This will also mean that some easier accessed mountain terrain could be suitable for wind energy from a wind resource point of view, not only the higher elevation terrain without roads and often also with a higher frequency of icing conditions.

## 2 MEASUREMENTS

In the mountain valley at Suorva (18°12'E, 67°32'N) in northern Sweden, people have often reported rather severe wind conditions. For this reason wind measurements began to be taken in November 1995 on a 36 m high tower located on a small hill close to the Suorva dam. Wind speed was measured at 4 heights (10 m, 17 m, 25 m and 35 m) using Cassella cup anemometers mounted on booms reaching about 1.2 m from the tower. Wind direction was observed at the 10 m level using a wind vane potentiometer instrument. At the same four heights where the wind speed was observed, the temperature was measured using ventilated and radiation shielded Pt-500 thermometers. The data logging system was connected to the serial port of a PC, and data was stored on the hard disk as 1 min averages.

The Suorva tower site is located on a small peninsula, at a rocky hill with almost no vegetation. Its height is about 20 m above the upstream lake Suorvajaure. Along the lower parts of the valley sides, some mountain birch forests are found. The valley as a whole is here rather narrow, only about 3 km between the rather steep fell sides. The direction of the valley axis is approximately northwest to southeast. On both sides of the valley the mountains typically reach 1200 to 2000 m above sea level. The water surfaces of the lakes and dams on the valley bottom are between 415 and 453 m above sea level. The elevation differences are thus about 1000 m, or even more, between valley bottom and mountain tops, cf. Figure 1.





Fig 1. Map of the area around Suorva, showing the measurement site Suorva.

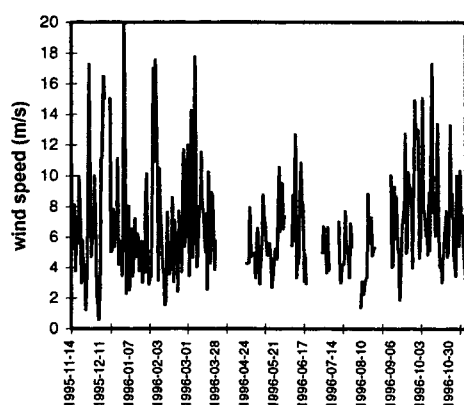


Fig 2. Daily mean wind speed at Suorva, 10 m level.

Table 1. Mean wind speed at Suorva.

	Height (m)			
	10	17	25	35
January	8.4	9.2	9.7	10.0
February	6.0	6.5	6.7	6.9
March	7.3	7.9	8.2	8.5
April	6.4	7.0	7.4	7.6
May	5.8	6.3	6.6	6.9
June	6.5	7.1	7.6	7.9
July	5.2	5.6	6.0	6.2
August	4.5	4.8	5.0	5.2
September	8.0	8.6	8.9	9.1
October	7.5	8.1	8.4	8.6
November	6.2	6.7	6.9	7.1
December	7.0	7.6	7.8	8.1
year	6.57	7.12	7.43	7.67

### 3 RESULTS

Data from one year, 14 November 1995 to 13 November 1996, have been analysed from the Suorva site. Due to problems with the data logging system at Suorva, there are some periods with missing data, but as a whole, data is available for 74% of the time during the one year

measurement period. In Figure 2 the measured daily mean wind speed at the 10 m height is plotted.

#### 3.1 Wind statistics

The monthly values of mean wind speed are presented in Table 1. The observed annual mean wind speed, 7.7 m/s at 35 m height, is indeed very high to be at an inland location. In fact it is even higher than observed at many of the coastal sites in southern Sweden, where for example the four year average wind speed at Alsvik on Gotland is 7.0 m/s at 36 m height, while at Näsudden the 10 year average at 38 m is 6.9 m/s. Usually wind speed should have a minimum during summer and a maximum during autumn and winter. Such an annual variation is however not clearly seen in the observations at Suorva. Although a minimum is found in July and August, June 1996 was a windy month. During the rest of the year the monthly averages vary rather sporadically between the months.

The annual mean wind profile is plotted in Figure 3. The increase in mean wind speed from 10 m to 35 m is about 1.1 m/s on an annual basis, as can also be seen in Table 1. Although the thermal stratification is slightly stable most of the time, the mean profiles show a close to logarithmic variation with height. The curvature of the profile is even slightly of the type that would be expected for unstable stratification. The reason for this behaviour is the small hill where the measurement tower is located. This hill causes a speed up of the wind in a layer close to the ground, leading to some strengthening of the wind up to 10-20 m height and thereby the observed near logarithmic wind profiles as a mean.

Assuming a logarithmic wind profile we have

$$U = \frac{u_*}{k} \ln \frac{z}{z_0} \quad (1)$$

where  $U$  is the mean wind speed,  $u_*$  is the friction velocity,  $k=0.4$  is the von Kármán constant,  $z$  is the height above ground, and  $z_0$  is the roughness parameter. By regression the observed mean wind profiles could be adapted to the logarithmic profiles, and the surface roughness parameter may be determined. As a mean we get  $z_0=0.01$  m with a standard deviation of 0.01m. This value could be expected as an overall average in the type of terrain we have at Suorva, with alternating almost bare rocks, low vegetation, some mountain birch, water surfaces, snow and ice cover.

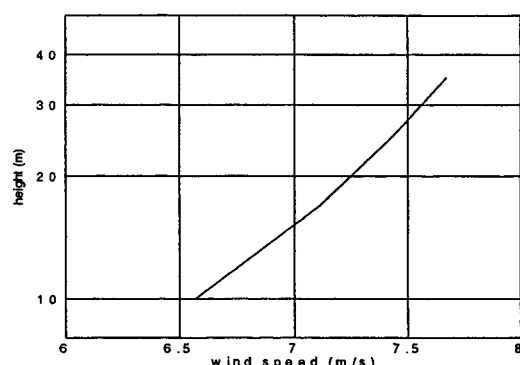


Fig 3. Annual mean wind speed profile at Suorva.

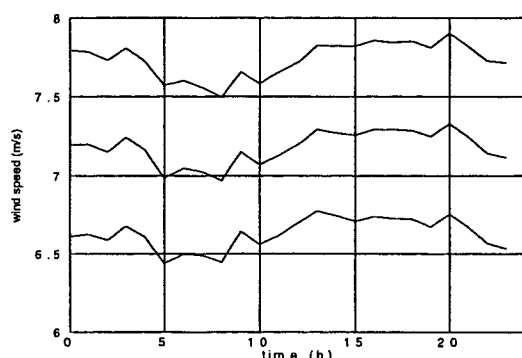


Fig 4. Annual average of the daily variation of wind speed at Suorva. Heights 10 m, 17 m, and 35 m.

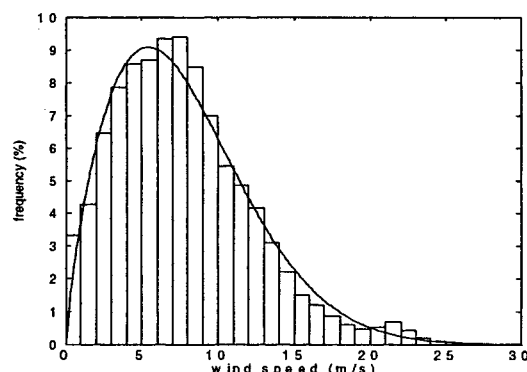


Fig 5. Distribution of mean wind speed at 35 m. The curve gives the corresponding Weibull distribution.

The annual average of the daily variation of mean wind speed is illustrated in Figure 4. Usually the wind climate exhibits maximum wind speed during the day, while a minimum is observed during the night. This is caused by unstable stratification during days and stable stratification during nights. At Suorva a tendency of this could be observed for some months, while other months have very small daily variations or even the opposite tendency. The reason for this is probably that slightly stable stratification often prevail both day and night all year around.

The wind speed distribution, based on 10 min averages, is illustrated in Figure 5. The modal value is about 7 m/s at the 35 m level. The highest wind speed is about 30 m/s. A distribution of wind speed is usually well modelled by the Weibull distribution, which is given by the relation

$$f(U) = \frac{c}{A} \left( \frac{U}{A} \right)^{(c-1)} \cdot e^{-\left( \frac{U}{A} \right)^c} \quad (2)$$

where  $U$  is the mean wind speed and  $f$  is the relative frequency distribution. This distribution is thus completely described by two parameters, the scale factor  $A$  and the form factor  $c$ . These two parameters have been determined from the one year wind observations at Suorva, and the resulting theoretical distribution is given by the full line in Figure 5. The Weibull parameters are also given in Table 2, together with the median wind speed and the maximum 1 min and 10 min average wind speeds.

The highest wind speed observed during the one year of measurements at Suorva is with 1 min averaging time 29.8 m/s and 32.2 m/s at the 10 m and 35 m levels respectively. The corresponding values for 10 min averaging time is 27.0 m/s and 30.3 m/s. This is higher values than has been observed during 4 years of measurements at Alsвик on Gotland in the Baltic Sea, where the maximum 10 min average value at 36 m height is 27.4 m/s. Following the extreme value analysis presented in [3], the values 30.3 m/s and 32.2 m/s for 10 min and 1 min averages respectively, should correspond to an annual 3 s maximum of about 37 m/s and a 30 year 3 s maximum of about 41 m/s with a 95% confidence limit.

Table 2. Weibull parameters together with the median wind speed and the maximum 1 min and 10 min average wind speeds.

height (m)	scale factor (m/s)	form factor	media n (m/s)	max 1 min (m/s)	max 10 min (m/s)
10	7.51	1.72	6.07	29.8	27.0
17	8.14	1.75	6.60	31.2	28.6
35	8.75	1.76	7.11	32.2	30.3

The wind direction distribution is shown in Figure 6. As could be expected the channelling effects of the valley are clearly seen with two dominant peaks in the distribution. Two secondary peaks can also be seen in the wind direction distribution. One at about 30° and the other at about 205°. The first one corresponds to winds down the very steep mountains to the east of the valley, more or less parallel to the eastern Suorva dam. For the second one winds blow more or less from the part of the valley west of the island Jiertsuoloi. But as a whole the wind direction climate is clearly dominated by flow up or down the valley at Suorva. Although the larger scale climate of Scandinavia is within the climate zone with a dominating westerly flow, wind directions from east to southeast seems to be almost as common as winds from a western or northwestern direction. The reason for this is the local channelling effects of the mountains and the valley. Thus e.g. with a southwesterly large scale flow, a low pressure will be found to the west over the North Atlantic, which will give a pressure driven channelling ('gap wind', cf. above) from an easterly or southeasterly direction along the valley. As a mean the strength of the wind for the two dominating wind directions are, however, slightly different with a higher mean wind speed for winds from the western sector. The average wind speed with winds from the eastern sector are 5.8 m/s and 6.7 m/s at 10 m and 35 m heights respectively, while the corresponding figures for winds from the western sector

are 7.3 m/s and 8.6 m/s. The reason for this is probably to be found in the distribution of the geostrophic wind speed and direction, that is the free atmosphere wind that is in balance with the surface air pressure field in the area.

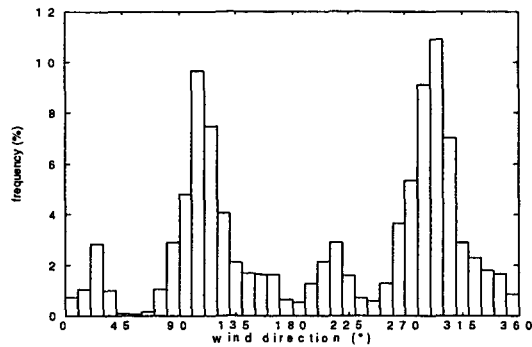


Fig 6. Distribution of wind direction at Suorva.

### 3.2 Temperature statistics

The temperature climate at Suorva is presented in Table 3 as monthly averages and extreme values. At least this very year, the temperature conditions do not seem to be very extreme, the lowest temperature at 10 m height being -31.0°C and the highest 22.4°C.

Table 3: Monthly and annual temperature statistics at Suorva Nov. 1995 to Nov. 1996, 10 m height.

Month	mean	minimum	maximum
January	-6.3	-21.5	4.0
February	-13.3	-31.0	0.4
March	-5.3	-15.9	3.0
April	-2.9	-5.9	0.6
May	0.4	-12.6	10.3
June	6.5	1.3	15.6
July	11.6	6.6	19.3
August	14.5	7.7	22.4
September	5.6	-0.5	11.4
October	2.3	-6.6	10.4
November	-5.9	-20.0	2.3
December	-10.8	-24.0	8.9
year	-0.3	-31.0	22.4

### 3.3 Icing conditions

Ice on the rotor blades of a wind turbine may be a serious problem in arctic mountainous areas, as for example have been reported from northern Finland. No measurements of humidity have been made at Suorva during the year of observations analysed here, but at two weather stations in the area, Ritsem and Vietas, humidity is measured. The frequency distribution of relative humidity at Ritsem 1981-1996 show a peak around 80% to 90% relative humidity. Only about 9% of the time the relative humidity exceeds 95%. The corresponding distribution for Vietas, using the limited amount of data available from February 1996 to January 1997, show a relative humidity above 95% just 2-3% of the time. The part of time with a relative humidity that is high enough for rime, ice, or dew to be formed, is thus relatively small. But for icing conditions to occur, the temperature must be below 0°C. Investigating the probability distribution of relative humidity after having applied the condition that the temperature is below 0°C, show that on an annual basis the part of time when icing conditions may occur is only 4.4% at Ritsem and 1.4% at Vietas. For individual months icing may as a maximum

occur 8-12% of the time during the winter period November to February.

### 3.4 Energy production estimates.

The estimated wind climatology at Suorva has been used to determine the potential energy production using the relation

$$E_p = 8760 \cdot \frac{1}{2} \rho \sum_{i=3}^{25} U_i^2 f_i(U_i) \quad (3)$$

where  $f(U_i)$  is the frequency of wind speed  $U_i$ ,  $\rho=1.225$  kg/m<sup>3</sup> is the air density, and 8760 is the number of hours during one year. The results are presented in Table 4, where we can see that the potential energy production increases from 4640 kWh m<sup>-2</sup> year<sup>-1</sup> at the 30 m level to 5010 kWh m<sup>-2</sup> year<sup>-1</sup> at the 40 m height.

Table 4. Potential energy production estimates.

Height (m)	$E_p$ (kWh m <sup>-2</sup> year <sup>-1</sup> )
30	4640
35	4840
40	5010

## 4 CONCLUSIONS

One year of measurements at Suorva show that the wind power potential may be good also in low elevation terrain in an Arctic mountain range. The resulting annual mean wind speed was as high as 7.5 m/s at 35 m height, which is comparable to the wind conditions at the most favourable coastal sites of southern Sweden. The reason for these high winds is channelling in the valley, which together with low surface roughness result in a high frequency of high wind speed. A low surface roughness is often found in Arctic valleys because of snow cover, ice, and lakes or dams. Previous indications of high winds also in the valley of Lake Torneträsk, together with the present results from Suorva, suggest that high wind conditions may occur frequent in some valleys of the Scandinavian mountain range.

## 5 REFERENCES

- [1] Smedman, A.-S. and Bergström, H., 1995: An experimental study of stably stratified flow in the lee of high mountains. *Monthly Weather Rev.*, Vol. 123, No. 8, 2319-2333.
- [2] Smedman, A.-S., Bergström, H., and Högström, U., 1996: Measured and modelled local wind fields over a frozen lake in a mountainous area. *Contr. Atm. Phys.*, Vol. 69, No. 4, 501-516.
- [3] Bergström, H., 1992: Distribution of extreme wind speed. *Wind Energy Report WE92:2*, Department of Meteorology, Uppsala University. 31 pp.

## ACKNOWLEDGEMENT

The measurements at Suorva and the data analysis have been sponsored by Suorvavind HB, Mikael Segerström, Jokkmokk, with funding from the regional authorities in Luleå.

## Appendix 2

Low Level Jets in The Baltic Sea Area

Birgitta Källstrand



# LOW LEVEL JETS IN THE BALTIC SEA AREA

Birgitta Källstrand

Department of Meteorology, Uppsala University, Box 516, S-751 20 Uppsala, Sweden  
e-mail: birgitta.kallstrand@met.uu.se

## ABSTRACT

Both measurements and simulations with a higher order closure model indicate that low level jet is a common phenomenon in the Baltic Sea area. LLJ is an important factor for the wind climate, giving a higher mean wind speed. A large amount of the LLJs are supposed to be caused by an inertial oscillation in space when relatively warm air flows out over colder water. A part of the LLJ are caused by a sea breeze circulation. To conclude, it is important to take the effect of the LLJs into consideration calculating the wind energy potential offshore.

## 1 INTRODUCTION

The interest in siting wind turbines offshore is increasing. In general a higher mean wind speed and lower turbulence intensity can be expected off shore. But, the wind climate in coastal areas and also further out over sea may show quite large local variations. When the wind blows from sea towards land, the wind speed generally decreases, a decrease that often start a shorter or larger distance upstream the coastline. But, measurements shows that this is not always the case. During certain conditions, the wind speed may be equally high or even higher close to the coast than further offshore. Two examples when this may happen are when we get a low level jet caused by an inertial oscillation in space and when sea breeze evolves.

Low level jets (LLJ), i.e. wind maxima at relatively low levels, have been observed during several experiments at different sites along the Swedish east coast and over the Baltic Sea. For example airborne measurements over the sea during May 29 to June 15 1989, in the vicinity of Ut-längen (A in Figure 1), showed some kind of low level wind speed maximum in 12 of the 25 profiles [1]. During April 30 to 14 June, 1991 pilot balloon trackings were performed at Utlängen, once a day at stochastic hours. The pibal measurements resulted in 52 profiles, corresponding to 62% of the days. 38 (73%) of the pibal profiles showed a more or less distinct LLJ. Figure 2 shows two examples of profiles from these measurements, one profile with and one without a LLJ. Also in measurements from Nässkär [2] (D in Figure 1) and Näsudden (B in Figure 1), LLJ have been studied. In fact, during an experiment at Näsudden in 1988, a LLJ was observed in every profile with onshore winds. The low level jets observed in this area, or at least a large amount of them, are supposed to be caused by an inertial oscillation in space when relatively warm air flows out over colder water.

A low level wind maximum caused by an inertial oscillation, a sea breeze circulation or a thermal wind can not be simulated by simple models that often are used to calculate the wind energy potential. Simulation with a meso-scale higher order closure model, the MIUU model (see e.g. [3]), have been performed for situations with LLJ ([2], [4], [5], [6]). The results is in good agreement with the measurements. [6] also simulated two situations with LLJ over the Baltic Sea with the KAMM model, which is a three-dimen-

sional, non-hydrostatic model with first order closure. In the comparison by [6], both models gave satisfactory results, producing LLJ caused by an inertial oscillation. However, differences in details, both between model results and measurements and between the results of the

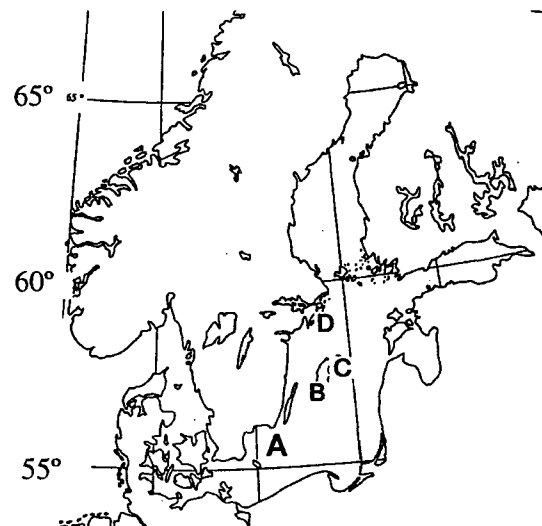


Fig. 1 Map over Scandinavia, with sites mentioned in the text marked. A: Ut-längen, B: Näsudden, C: Östergarnsholm, D: Nässkär.

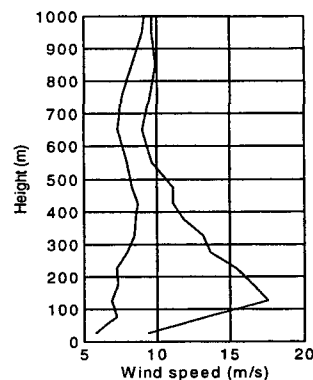


Fig. 2 Two examples of wind speed profiles, with (full line) and without (dashed line) a LLJ. From the pibal trackings at Ut-längen, 1991.

two models, may still be subject to further investigations. Simulations with the MIUU model for a large part of the Baltic Sea gave a wind speed maximum at 150 meters height on an climatological basis [7], [8]. These simulations also show that low level jets give an increase in wind speed of the order of 10% in the Baltic Sea area.

## 2 MEASUREMENTS AT ÖSTERGARNSHOLM

The most recent measurements are performed at a very small, flat island with sea fetch for a large wind direction sector. The island, Östergarnsholm (D in Figure 1), are situated about 5 km east of the larger island Gotland. Three measurement campaigns have been performed, the first in spring 1995, the second in autumn 1996, and the third campaign in spring 1997. Continuous measurements of wind, temperature and turbulence were performed on a 30 m high tower at the southernmost tip of the island. During all three measurement campaigns, pibal trackings and radiosonde measurements were performed. The pibal trackings gives profiles of wind speed and wind direction and the radiosonde measurements gives profiles of temperature and humidity. In 1995 and 1997 also aircraft measurements were performed in the area, giving wind, temperature and humidity. Tether sonde measurements were performed during the measurement campaigns in 1996 and 1997, giving profiles of wind, temperature and humidity. In pilot balloon measurements performed during May 29 to June 15 1995 at Östergarnsholm, a low level jet is seen in 43 of 51 profiles [9]. During the pibal measurements from the period April 30 to June 14, 1997, LLJ occurred in about 2/3 of the 36 profiles. In September 1996, a low level wind speed maximum occurred for a longer or shorter period on four of the eight days with pibal measurements.

## 3 LOW LEVEL JET

Low level jets is a feature that has been observed in many parts of the world and there are several physical processes which may cause a LLJ. The Baltic Sea jet often develops when air is flowing out over the coast. Frictional decoupling occurs over the sea when the sea surface is colder than the land, and an inertial oscillation evolves in space during the subsequent transport over the water. The measurements from Utlängan 1991 have been used to investigate the probability for inertial oscillations to be the cause of these LLJs [10]. About 2/3 of the profiles with low level jets fulfilled the examined criteria for an inertial oscillation in space. Probable reasons for the remaining cases with LLJ are mainly sea breeze circulations and the thermal wind.

### 3.1 LLJ caused by an inertial oscillation

In the case of a LLJ caused by an inertial oscillation in space, the wind maximum appears at a certain distance from the coast, because the air is advected out over the sea. If the air is advected with a mean wind speed  $V_{adv}$ , the wind maximum appears at a distance  $t_{max} \cdot V_{adv}$  from the coast, where  $t_{max}$  is the time it takes for the inertial oscillation to cause a LLJ, i.e. 5-7 hours (at 55°-60° latitude). With an initial wind speed of, for example,  $10 \text{ ms}^{-1}$  and assuming straight trajectories, the wind maximum appears at a distance of 200 km from the coastline.

A schematic illustration (assuming a wind direction about south-west) is shown in Figure 2: Air from a warm land area is transported out over a cold sea. Frictional decoupling occurs and an inertial oscillation evolves (I in Figure 2). The wind accelerates during the transport over the water (II). After about 5-7 hours a wind speed maximum has developed (III). If the air reaches a coast, the inertial oscillation is disturbed and the LLJ disappears (IV). For the case of advection over the Baltic Sea, the development of the inertial oscillation is in most cases disturbed by changing conditions before a full period of the oscillation is completed. A full period of an inertial oscillation is about 14 hours (at these latitudes) - i.e. after 14 hours transport over water the wind speed profile is 'normal' again.

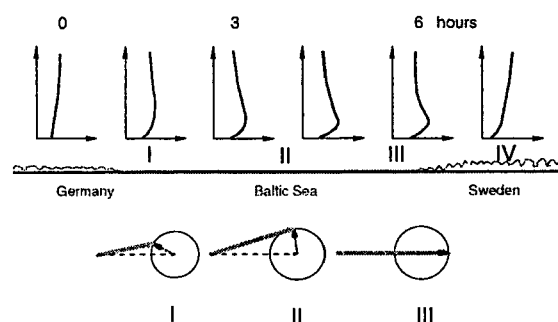


Fig. 3 Schematic illustration of a LLJ caused by an inertial oscillation (see text). The vector sum of the geostrophic wind (dashed line) and the deviation from the geostrophic wind (dotted line) gives the resulting wind (gray full line).

As already mentioned, the wind speed profiles from the measurements at Östergarnsholm in spring 1995 shows a LLJ during large part of the time. As for the experiment at Utlängan in 1991, the land temperature is higher than the water temperature and most of the LLJ are supposed to be caused by an inertial oscillation in space. An example is shown in Figure 4. A time series of (a) wind speed and (b) wind direction for June, 6 are shown, based on profiles from the pibal trackings performed during this day. A LLJ, with its maximum at about 150 meters height is seen, increasing in strength from the morning. As clearly seen in the Figure, a large part of the wind speed profile is affected by the LLJ, giving a wind speed increase in a height interval, not only at the height of the maximum.

In Figure 5, an example of a simulation, with the MIUU model, are shown for a situation with a LLJ caused by an inertial oscillation. The geostrophic wind is in this case from south-east, so the upwind coast is the Baltic States. The wind speed increases with distance from coast, reaching a maximum of about 11 m/s. When the air reaches land (here the island Gotland), the inertial oscillation is disturbed and the LLJ disappears, giving an abrupt wind speed decrease along the coast.

speed. The LLJs may give a larger wind shear than may be expected over sea in general. But, this shear is still smaller than the wind shear that in general can be expected over land, so the net effects of the LLJs over sea is positive for the wind energy potential.

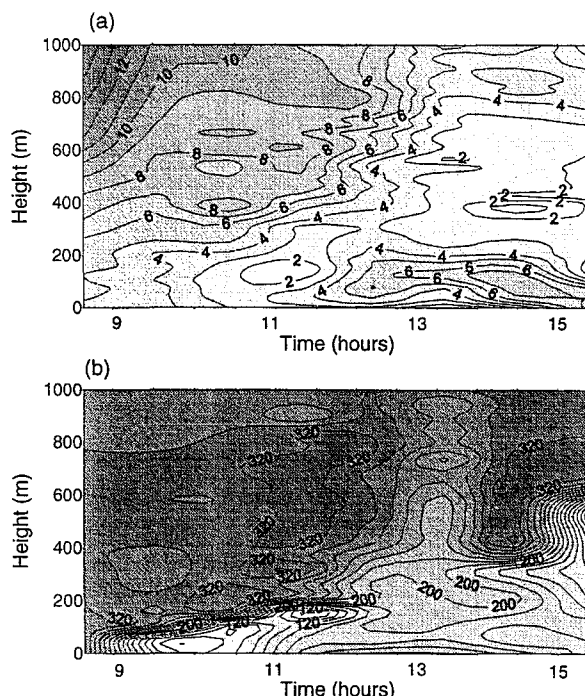


Fig. 6 Time series of (a) wind speed and (b) wind direction during an evolution of a sea breeze. Based on pibal and tether sonde measurements performed at Östergarnsholm 4 May, 1997.

A large amount of the LLJs are supposed to be caused by an inertial oscillation in space when relatively warm air flows out over colder water. In addition, the criteria for LLJ caused by an inertial oscillation to develop are probably fulfilled also in other areas around the world. As an example, [11] conclude that LLJ seen in measurements performed in Canada, may be caused by an inertial oscillation in space. A part of the LLJ in the Baltic Sea area are caused by a sea breeze circulation. That sea breeze circulations occur at many sites around the world is well known. But, it is important to be aware of the variability in the wind that may be caused by irregularities in the coastline, the topography and other factors.

To conclude, it is important to take the effect of the LLJs into consideration calculating the wind energy potential offshore. Since LLJ is not simulated by simple wind models that often are used to calculate the wind energy potential, this is unfortunately not always the case today.

**Acknowledgements:** The author wants to acknowledge Hans Bergström, who has performed the numerical simulations and all persons involved in the measurement campaigns.

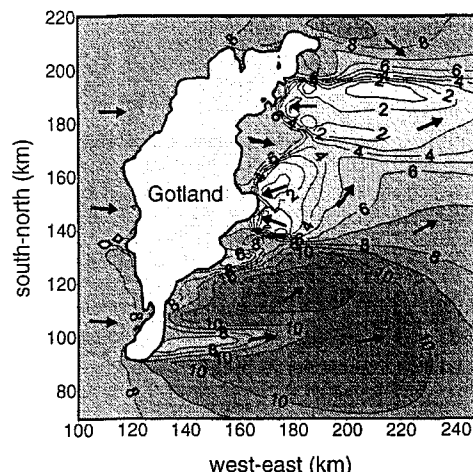


Fig. 7 Numerical simulation of a situation with a sea breeze circulation. Geostrophic wind: 10 m/s, 290°.

## 6 REFERENCES

- [1] Tjernström, M. and Smedman, A., 1993: The vertical turbulence structure of the coastal marine atmospheric boundary layer. *J. Geophys. Res.*, 98, C3, 4809-4826.
- [2] Smedman, A., Bergström, H. and Högström, U., 1995: Spectra, variances and length scales in a marine stable boundary layer dominated by a low level jet. *Boundary-Layer Meteorol.*, 76, 211-232.
- [3] Enger, L., 1990: Simulation of dispersion in a moderately complex terrain. Part A. The fluid dynamic model, *Atmos Environ.*, 24A, 2431-2446.
- [4] Högström, U. and Smedman, A., 1984: The wind regime in coastal areas with special reference to results obtained from the Swedish wind energy program, *Boundary-Layer Meteorol.*, 33, 351-373.
- [5] Bergström, H., 1992: A climatological study of wind power potential in the Blekinge area using a meso-  $\gamma$ -scale higher order closure model. *Wind Energy Report WE 92:01*, Dept. of Meteorol., Uppsala Univ., Sweden, 74 pp.
- [6] Mohr, M., 1997: Comparisons of Simulations with Two Meso-scale Models, the MIUU Model and the KAMM Model, Using Two Low-Level Jet Cases over the Baltic Sea, *Wind Energy Report WE 97:2*, Dept. of Meteorol., Uppsala Univ., Sweden, 107 pp.
- [7] Sandström, S., 1997: Simulations of the Climatological Wind Field in the Baltic Sea Area Using a Meso-scale Higher Order Closure Model. *J. Appl. Meteorol.* In press.
- [8] Sandström, S., 1997: Simulations of the climatological wind field in the Baltic Sea area using a meso-scale higher order closure model. *Proc. of EWEC'97*, Dublin, 1997.
- [9] Smedman, A., Bergström, H. and Högström, U., 1996: The Turbulence Regime of a Very Stable Marine Airflow with Quasi-frictional Decoupling, *J. Geophys. Res.* In press
- [10] Källstrand, B., 1997: Low Level Jets in a Coastal Area During Spring, to be submitted to *Contr. Atmos. Phys*
- [11] Angevine, W. M., Trainer, M., McKeen, S. T., Berkowitz, C. M., 1996b: Local meteorological features affecting chemical measurements at a North Atlantic coastal site, *J. Geophys. Res.*, 101, D22, 28 935-28 946.



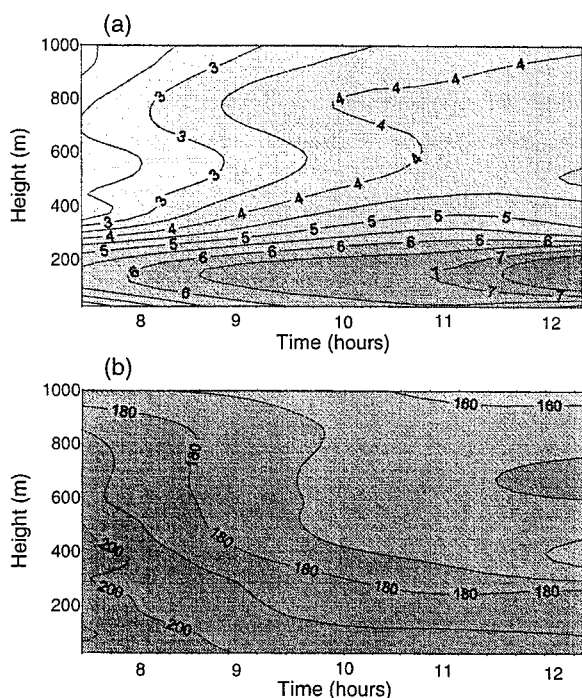


Fig. 4 Time series of (a) wind speed and (b) wind direction during a day with a LLJ caused by an inertial oscillation. Based on pibal measurements performed at Östergarnsholm 6 June, 1995.

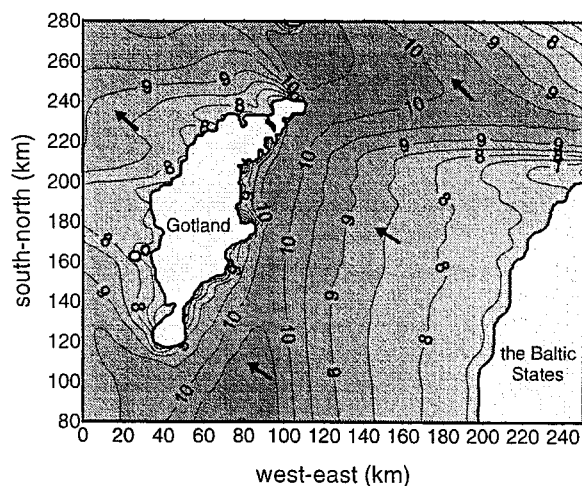


Fig. 5 Numerical simulation of a situation with an inertial oscillation. Geostrophic wind: 8 m/s, 150°.

### 3.2 LLJ caused by a sea breeze circulation

A part of the LLJs in the Baltic Sea are caused by a sea breeze circulation. The temperature difference, between a heated land area and a colder sea do that a sea breeze may evolve, giving onshore winds. This is a common phenomenon mainly during spring and summer. A low geostrophic wind speed is favourable for a sea breeze to develop. A sea breeze may also evolve during higher wind speeds, at least on the 'leeward' coast according to measurements and simulations. A sea breeze circulation in an area with an offshore geostrophic wind direction may thus cause a wind direction change of 180° in the height interval affected by the sea breeze.

Looking at a weather map, a sea breeze situation is characterized by onshore winds all along the coast of the Baltic Sea and at the same time a uniform wind direction at inland weather stations. Also the wind direction taken from a pibal profile, performed during a sea breeze, changed distinctly at a certain height. Above this height, the wind direction agreed well with the observations from the inland stations. The change could be as much as 180°. The conclusion is that the LLJ seen in the pibal profiles are caused by the sea breeze circulation.

In the measurement campaign during May 1997, a high frequency of LLJ was seen in the profiles. During this campaign, wind profiles from both pibal and tether sonde measurements are available. In Figure 6, an example of a LLJ caused by a sea breeze situation is shown. The time series of (a) wind speed and (b) wind direction are based on the pilot balloon and tether sonde measurements performed during May, 4. It is clearly seen that the wind direction changes abruptly, when the sea breeze starts. The wind speed is almost zero at the height where the wind direction changes. The height interval affected by the sea breeze circulation grows during the day, up to about 600 meter. A wind speed maximum appears close to the ground, with a maximum of 7 m/s at about 100 m/s height.

A simulation, with the MIUU model, of a case with a sea breeze situation is shown in Figure 7. In this example, with a quite strong (10 m/s) geostrophic wind from north-east, two sea breeze circulation have evolved at the east coast of Gotland. Thus, the wind direction in the sea breeze is almost opposite to the geostrophic wind direction, giving low wind speeds. In this example, there are large local irregularities in the wind pattern. Such irregularities may be quite common and are caused by numerous factors, for example the shape of the coastline and the topography.

### 3.3 LLJ caused by other mechanisms

A LLJ may also be caused by other mechanisms than an inertial oscillation or a sea breeze circulation. One of these factors is the thermal wind, i.e. the vertical shear of the geostrophic wind. For some of the cases from the investigation of the data from Utö 1991, according to weather maps and other information, a thermal wind in connection with a front passage was the most probable cause of the LLJ. In contrast to the sea breeze and the inertial oscillation in space, a thermal wind may occur at any time of the year.

During the measurement campaign at Östergarnsholm in September 1996, LLJ occurred in a number of wind profiles, even if the frequency seems to be lower than during the measurements performed in spring. A lower frequency of LLJ could be expected, since LLJ caused by inertial oscillations and sea breeze circulations are less probable to appear. However, it is possible to conclude that LLJ of different origin thus affect the wind conditions in the Baltic Sea area not only in spring and early summer, but for most of the year.

## 5 DISCUSSION AND CONCLUSIONS

Both measurements and simulations with a higher order closure model indicate that low level jet is a common phenomenon in the Baltic Sea area. LLJ is an important factor for the wind climate, giving a higher mean wind

## Appendix 3

Simulations of The Climatological Wind  
Field in The Baltic Sea Area Using a Meso-  
Scale Higher Order Closure Model

Stefan Sandström



# SIMULATIONS OF THE CLIMATOLOGICAL WIND FIELD IN THE BALTIC SEA AREA USING A MESO-SCALE HIGHER ORDER CLOSURE MODEL

Stefan Sandström

Department of Meteorology, Uppsala University  
Box 516 S-751 20, Uppsala, Sweden

## ABSTRACT

A three dimensional meso-scale numerical model is utilised to investigate the climatological wind field over the Baltic Sea. The model results have been compared with measurements from two lighthouses outside the Swedish coast as well as with an interpolation of ship measurements. The comparison shows good agreement between the modelled wind field and measurements, with deviations less than  $0.5 \text{ ms}^{-1}$  in the main part of the Baltic sea. Thus, the small deviations between measurements and simulations suggests that the main flow forcing parameters, the climatological statistics, and assumptions made are correct.

## 1. INTRODUCTION

The major problem concerning wind power is the large number of wind turbines that must be installed in order to obtain an energy production that can substantially contribute to the total energy production and replace other energy sources. Offshore siting of wind turbines will therefore be more attractive in the future, since the availability of good land based sites is limited. However, the information about offshore wind resources are sparse. The few existing observing stations are concentrated to the coastal areas and only a few offshore. There are measurements at a few lighthouses outside the Swedish coast. The measurements at the coastal stations are made at only one level, usually between 10 and 30 m above sea level, while for practical wind energy applications the main interest is focused at higher levels. Consequently, as the data from climatological stations are limited, models are necessary to obtain a more detailed information regarding the horizontal and vertical variation of the wind field over the sea. The purpose of the simulations presented is to estimate the climatological wind field over the Baltic Sea with a horizontal resolution of about 5 - 10 km and at levels of interest for wind energy.

## 2. THE MODEL

A three-dimensional meso-scale model, the MIUU model, which is used for the simulations has been developed at the Department of Meteorology, Uppsala University, Sweden [1]. The MIUU model, The model is three-dimensional and hydrostatic with a terrain following coordinate system. The turbulence is parameterized with a 2.5 level scheme. The MIUU model has been proved in earlier studies to simulate this kind of situations very well when compared with data from several field experiments.

## 3. MODELLING THE CLIMATOLOGICAL WIND FIELD

In the ideal case climatological study all synoptic and boundary conditions should be covered, but this would require an unrealistic large number of simulations. Since the MIUU model is rather computer time consuming to run, some compromises have to be made. First, the most important flow forcing parameters have to be identified. These parameters must then be varied in order to cover a wide range of atmospheric conditions. Parameters important to the wind field are:

- geostrophic wind - strength and direction
- thermal stratification - the daily temperature variation
- surface roughness
- topography
- land-sea temperature differences
- thermal wind

One simple way to proceed would be to make simulations using the mean geostrophic wind speed for a few wind directions; the mean temperature for some months to include the annual differences and a daily variation of the temperature. This approach would however diminish the effect of thermal stratification and also the land-sea temperature differences, and would result in an erroneous climatological wind field compared with observations. Therefore, to include the most important parameters affecting the wind field, simulations have been performed for the four seasons represented by the climatological temperatures and daily variations for the months January, April, July and October; 3 geostrophic wind speeds 5, 10,  $15 \text{ ms}^{-1}$  and with eight directions North, Northeast, East, Southeast, South, Southwest, West and Northwest. Thus we end up with 96 model runs to cover the most important parameters determining the boundary layer wind field. All these simulations are then be weighted together using climatological data of the geostrophic wind. The statistics of the geostrophic wind have been evaluated by using a simplified boundary layer wind model described in [2]. With the model it is possible to estimate the geostrophic

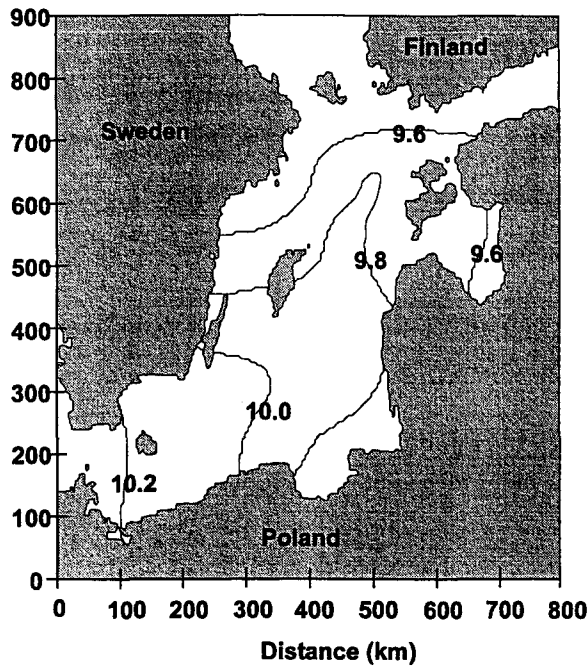


Fig 1. Annual mean geostrophic wind speed obtained from a combination of 1-D simulations and pressure data.

wind from measurements at low height, using the temperature gradient and the wind speed at one height. The geostrophic mean wind speed was found to vary between  $9.6 \text{ ms}^{-1}$  and  $10.2 \text{ ms}^{-1}$  over the Baltic Sea with a standard deviation of  $5.7 \text{ ms}^{-1}$ . The variation of the geostrophic wind is shown in Figure 1.

#### 4. RESULTS

The model results cover the Baltic Sea area and the surrounding countries, an area of  $800 \text{ km} \times 900 \text{ km}$ . The results are shown in Figures 2 and 3. The modelled wind speed over land is not shown in the Figures since the simulations have been focused on the wind field over the Baltic Sea area.

In Figures 2 and 3, the modelled annual mean wind speed at two heights, 66 m and 153 m are presented. The wind speed gradient at the coasts decreases with height. The transition from lower wind speed over land to higher wind speed over sea is rather sharp at lower heights while at higher levels it becomes more of a smooth transition zone. As expected, the highest wind speed is found in the central parts of the Baltic sea, with values around  $9.5 \text{ ms}^{-1}$  at 66 m and up to  $11 \text{ ms}^{-1}$  at 153 m. High wind speeds are also found in the Gulf of Riga, with values about the same as in middle of the Baltic Sea. The annual mean geostrophic wind speed varies spatially between  $9.5$  and  $10.2 \text{ ms}^{-1}$  (Fig. 1) from the north-east to the south-west. The annual geostrophic wind speed is about the same as the wind speed found at 153 m in the southern part of the Baltic Sea. But in the northern part, the wind speed at 153 m is more than  $1 \text{ ms}^{-1}$  higher than the geostrophic wind speed. The high wind speed area in the northern part of the Baltic Sea is probably

caused by low level jets, i.e. local wind maxima at relatively low levels [3], [4], [5]. Studies show that the height of the low level jet maximum may vary from less than 50 m and up to 1000 m. Research has shown that there are many possible causes for the low level wind maximum in the boundary layer. One of these is the warm air advection over a cooler surface. The Baltic Sea is surrounded by land surfaces, which means that advective effects will influence the wind and turbulence structure regardless of wind direction. The location of the Baltic Sea at fairly high latitudes causes the land surface temperature to be higher than the sea surface temperature during a large

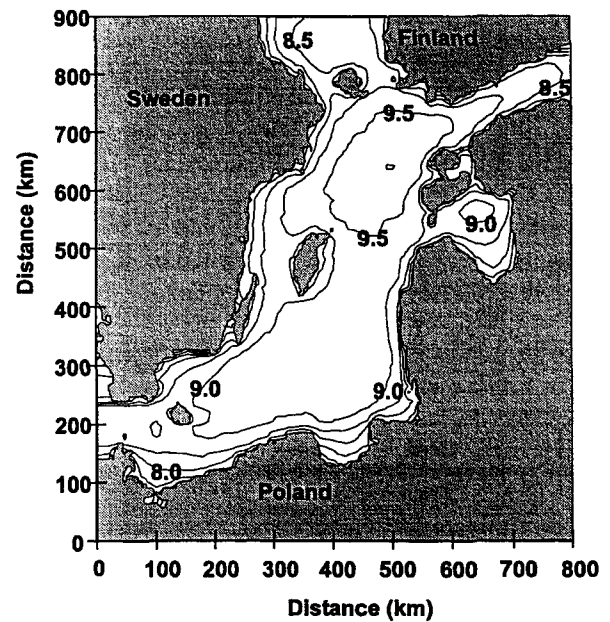


Fig 2. Simulated annual mean wind speed at 66 m.

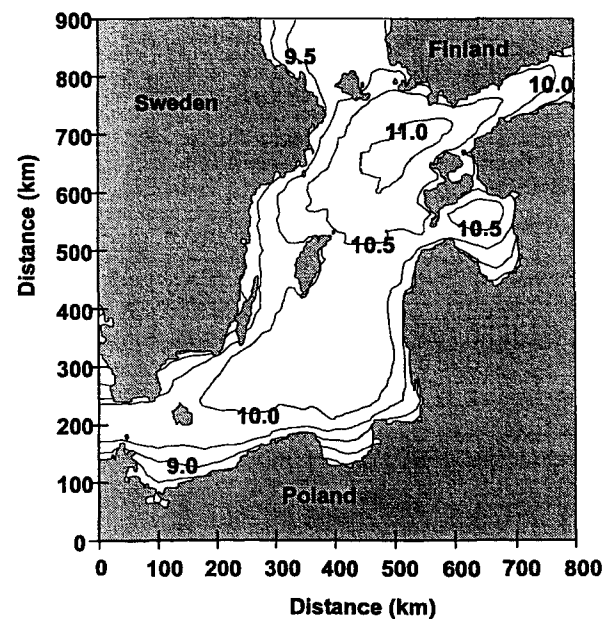


Fig 3. Simulated annual mean wind speed at 153 m

part of the year, which will give a stable internal boundary layer over the sea. At the top of this internal boundary layer a low level jet can develop as a result of frictional decoupling at the coast [4]. This produces an analogy in space to the well-known nocturnal jet [6]. Measurements show that the lowest 100 m of the marine boundary layer over the Baltic Sea is probably stably stratified during 2/3 of the year [4]. This indicates that low level jets could be a very often occurring phenomenon over the Baltic Sea. The fact that the annual simulated wind speed at higher levels in the Baltic Sea is supergeostrophic, implies that low level jets are frequent and with high speeds.

## 5. COMPARISON WITH MEASUREMENTS FROM LIGHTHOUSES

To obtain an estimate of the reliability of the climatological simulations, a comparison with measurements is necessary. For this purpose, an analysis of the wind data measured at Ölands södra grund and at Almagrundet has been made. Ölands södra grund is situated approximately 40 km away from the Swedish east coast and about 30 km south east of the southern tip of the island of Öland. The anemometer is sited on the helicopter platform at a height of 34 m above sea level. Measurements from the time periods 1961-70 and 1976-1989 were available, but data for the winter months in the second period are very incomplete. Almagrundet is situated 15 kilometres outside the Stockholm archipelago, which here extends about 20 km east of the Swedish mainland. The anemometer is also here sited on the helicopter platform and at a height of 31 m above sea level. Measurements from the time period 1976-78, 1982-95 were available. The anemometers placed at the lighthouse towers are disturbed by the air flow around the tower. Therefore, correction factors evaluated by SMHI (Swedish Meteorological and Hydrological Institute) based on wind tunnel and full scale measurements at the two lighthouses have been applied to the wind data.

Table 1 shows the observed wind speed at the two lighthouses together with the modelled climatological values for the months January, April, July and October. Also shown are the corresponding annual mean wind speeds. The agreement between observation and simulated wind speed is very good both at Ölands södra grund and at Almagrundet. The annual measured mean wind speed is  $8.2 \text{ ms}^{-1}$  at both Ölands södra grund and Almagrundet. The annual simulated wind speed at Ölands södra grund is only  $0.1 \text{ ms}^{-1}$  higher than the measured and at Almagrundet the simulated wind speed is  $0.1 \text{ ms}^{-1}$  lower than the measured.

## 6. COMPARISON WITH SHIP MEASUREMENTS

Figure 4 shows a comparison between the annual modelled wind field at 10 m and ship measurements [8]. The ship measurements are from voluntary observing ships in the Baltic Sea during the period 1992-1995 at 00, 06, 12 and 18 UTC. During this period about 20000 ship wind observations were gathered. Most of the ship observations were located in the south-east parts. The synoptic observations from these ships are fitted to a polynomial by

Table 1. Observed wind speed at Ölands södra grund and Almagrundet, together with the modelled climatological mean values at same height (about 30 m a.s.l.).

Almagrundet			Ölands södra grund	
Month	Measured	Model	Measured	Model
Jan	9.4	9.8	9.5	9.6
Apr	7.7	7.9	7.8	7.3
Jul	6.7	7.1	6.7	7.0
Oct	8.4	8.5	8.8	8.6
Year	8.2	8.3	8.2	8.1

using both wind speed and pressure observations [9]. By using both pressure and wind speed a better resolution is achieved, because more information is available. The ship observations have also been corrected for coastal influence. Figure 4 shows the difference between modelled wind speed at 10 m and the interpolated ship measurements at 10 m. As can be seen, the agreement is very good, with a difference less than  $0.5 \text{ ms}^{-1}$  in the main part of the Baltic Sea. The differences that occur might be explained by the fact that there are very few ship observations at places where the deviations are largest, that is, the Swedish east coast north of Gotland, the Gulf of Riga and the area between Åland and Finland. Another explanation could be the fact that the ship measurements cover only a 4 year period, 1992-1995, while the simulations are based on a period of 18 years for the geostrophic wind (1961-1970 and 1982-1989).

## 7. CONCLUSION

To conclude, it seems possible to use a meso-scale higher-order closure model to resolve the wind field over an area as large as the Baltic Sea down to horizontal scales of 5 - 10 km. The simulations presented in this paper and measurements support the opinion that the increased costs associated with offshore siting of wind turbines, can, at least partly be compensated by the increased energy content of the wind. The results can also be used for general siting purposes in the region. But when a particular area has been chosen for wind energy exploration purposes, on site measurements are recommended.

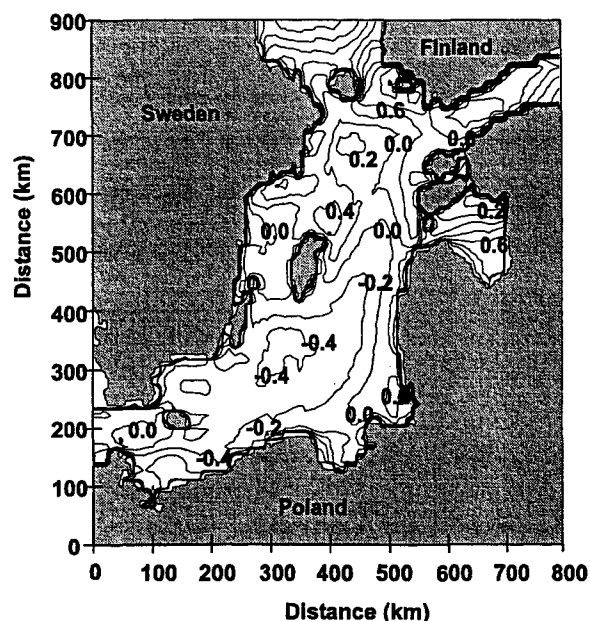


Fig 4. The difference between modelled wind speed at 10 m height and an interpolation of ship measurements.

## 8. REFERENCES

- [1] Enger L., 1990: Simulation of dispersion in a moderately complex terrain. Part A. The fluid dynamic model. *Atmos Environ.*, 24A, 2431-2446.
- [2] Bergström, H., 1986: A simplified boundary layer wind model for practical applications. *J. Climate Appl. Meteor.*, 25, 813-824.
- [3] Källstrand, B.: 1993, Effect of low level jets on wind energy potential in a coastal area. Rep. 93:1. Department of Meteorology, Uppsala University, Sweden, 54 pp.
- [4] Smedman, A., U. Högström, and H. Bergström, 1996a: Low level jets - a decisive factor for offshore wind energy siting in the Baltic Sea. *Submitted to Wind Engineering*.
- [5] Smedman, A., H. Bergström, and U. Högström, 1995: Spectra, variances and length scales in a marine stable boundary layer dominated by a low level jet. *Bound.- Layer Meteor.*, 76, 211-232.
- [6] Gerber, H., 1988: Evolution of a marine boundary-layer jet. *J. Atmos. Sci.*, 46, 1312-1326.
- [7] Blackadar, A. K., 1957: Boundary layer maxima and their significance for the growth of nocturnal inversions. *Bull. Amer. Meteor. Soc.*, 38, 283-290.
- [8] Højstrup, J., et. al. 1996: Wind resources in the Baltic Sea. Risø National Laboratory, Roskilde, Denmark.
- [9] Bumke, K. and L. Hasse, 1989: An analysis scheme for determination of true surface winds at sea from ship synoptic wind and pressure observations. *Bound.-Layer Meteor.*, 47, 295-308.

## Appendix 4

Computations of Aerodynamic Damping for  
Blade Vibrations in Stall

Anders Björck, Jan-Åke Dahlberg, Anders  
Östman, Hans Ganander





# COMPUTATIONS OF AERODYNAMIC DAMPING FOR BLADE VIBRATIONS IN STALL

Anders Björck\*, Jan-Åke Dahlberg\*, Anders Östman\*, Hans Ganander\*\*

\*FFA, The Aeronautical Research Institute of Sweden, P.O. Box 11021, SE-161 11 Bromma, Sweden

\*\*Teknikgruppen AB, P.O. Box 21, SE-191 21 Sollentuna

## Abstract

The aerodynamic damping of blade vibrations are calculated. The resulting aerodynamic damping is affected by 1.) the static aerofoil data used, 2.) dynamic stall modelling and 3.) mode shapes. A sensitivity study is carried out and it is found that all three parameters are important. It is shown that the description of the blade oscillation in terms of how the blade deflects is important. Specifically the aerodynamic damping of the lead-lag mode is found to be very sensitive to relatively small out-of plane blade deflections. This means that the orientation of the principal bending axes along the blade is important since this determines the relevant form of blade oscillations. It is thus important to have a correct blade structural description for calculations, but equally interesting is that the aerodynamic damping characteristics can be changed by changing the blade structure.

## 1. INTRODUCTION

The wind turbine industry is today faced with problems regarding stall induced edgewise vibrations. It is important to identify the causes for such problems and to develop good design tools.

For attached flow and flap-wise vibrations, the aerodynamic damping of oscillations is normally positive. I.e the air extracts energy from the rotor during each cycle of oscillation. For vibrations in the edge-wise direction, the damping is small or slightly negative. Still, the positive structural damping is large enough to prevent the blade from developing violent oscillations.

When the blade is stalled, the situation is different. The aerodynamic damping is then drastically reduced which can result in large vibrations.

The aerodynamic damping is dependent on the type of aerofoils used. The damping is also dependent on the structural behaviour of the rotor and the turbine since the angle of attack history is dependent on the blade motion. Further, unsteady profile aerodynamics (dynamic stall) modifies the static profile behaviour and affects the damping characteristics. Hence, several factors influence the aerodynamic damping.

The current study is performed in order to investigate the influence of various parameters on the aerodynamic damping of blade vibrations.

Parameters investigated are:

- Static aerofoil data
- Dynamic stall modelling
- Blade structure such as mode shapes

## 2. A MEASURE OF AERODYNAMIC DAMPING

Calculations are made with the blade rotating in homogenous inflow. The blade is also oscillating at its eigenfrequencies, one at the time, with constant amplitude. The blade oscillation is described by use of

mode shapes, which can contain displacement in the flap-wise as well as in the edge-wise direction. For one period of oscillation, the aerodynamic damping work,  $W_d$ , is calculated as

$$W_d = \sum_i \int_0^T (\mathbf{F}_i(t) \cdot \mathbf{r}_i(t)) dt \quad (1)$$

$\mathbf{F}_i$  is the aerodynamic force at blade node  $i$  and  $\mathbf{r}_i$  is the speed of blade displacement at node  $i$ . The displacement is described by the mode functions as:

$$\mathbf{r}_i = (x_i, y_i, z_i) = (\varphi_{ix} \cdot q, \varphi_{iy} \cdot q, z_i) \quad (2)$$

with  $q(t) = q_0 \sin(\omega_0 t)$

The aerodynamic work is normalised to obtain the logarithmic decrement:

$$\delta = \frac{W_d}{M_g \cdot \omega_0^2 \cdot q_0^2} \quad (3)$$

where  $M_g$  is the generalised mass and  $q_0$  is the oscillation amplitude of the specific mode at the eigen frequency  $\omega_0$ .

Blade-Element Momentum Theory with a dynamic inflow extension is used to calculate the inflow relative to the blade. Note that the blade is forced to oscillate at a prescribed motion. In reality, the forces acting on the blade will result in a different motion. Still, the method can be used to find the sensitivity to different parameters.

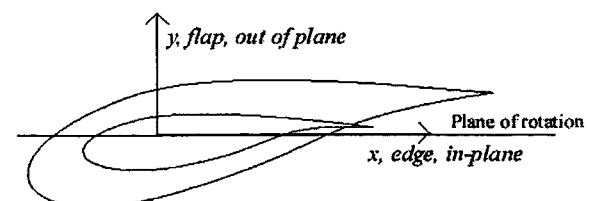


Figure 1. Coordinate system showing directions of oscillations.

### 3. BLADE USED IN THE STUDY

The LM 11 blade used on the DANWIN 180 kW turbine is used in the present study. The frequencies of oscillations have been set to 2.45 and 5.37 Hz for the first and second mode respectively. The rotational speed of the rotor has been prescribed to 42.3 RPM.

### 4. FIGURES OF CALCULATED DAMPING

The figures of aerodynamic damping shows the damping as the logarithmic decrement in %.

### 5. DIFFERENT AEROFOIL DATA

Different aerofoils will result in different damping characteristics. When performing calculations with tabulated aerofoil data it is always a bit of guesswork to define the lift- and drag coefficient curves, especially in the post stall region. In order to investigate how different static aerofoil data influence aerodynamic damping, three sets of aerofoil data, v1, v2 and v3, are used in the current study.

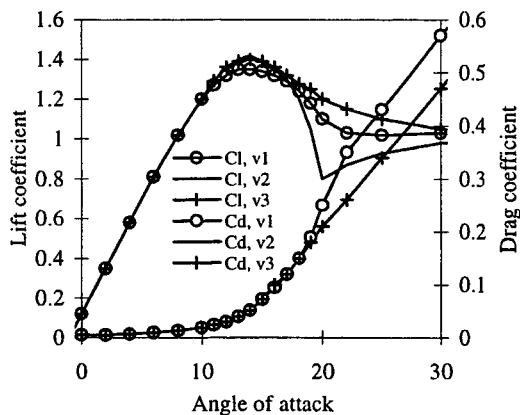


Figure 2a  $C_l(\alpha)$  and  $C_d(\alpha)$  for three different aerofoils

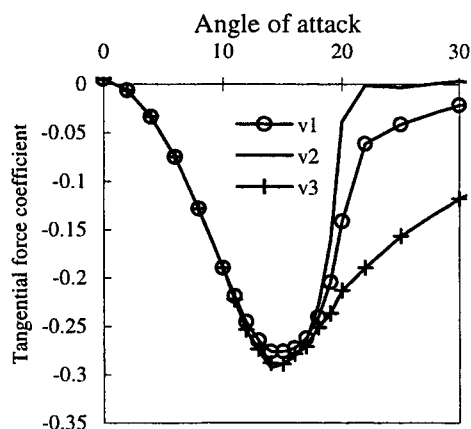


Figure 2b Tangential force coefficient,  $C_t$  as function of angle of attack for three different aerofoils.

For the flap-wise damping, the static post stall lift curve slope is somewhat indicative for the judgement of damping characteristics. Looking in figure 2a, it can be

seen that aerofoil v2 is the aerofoil with the most negative lift curve slope for angles of attack in the region  $\alpha=15-20^\circ$ . In figure 3 it can also be seen that the use of this aerofoil result in the lowest values of damping of the 1st mode.

However, for the damping of the 2nd mode the use of aerofoil v1 results in more negative damping than using aerofoil v2. It does not seem to exist any such obvious indicators as looking at the lift and drag coefficient curves in order to judge damping characteristics for edge-wise vibrations as exist for flap-wise vibrations. The slope of the tangential force curve might, however, reveal something (figure 2b).

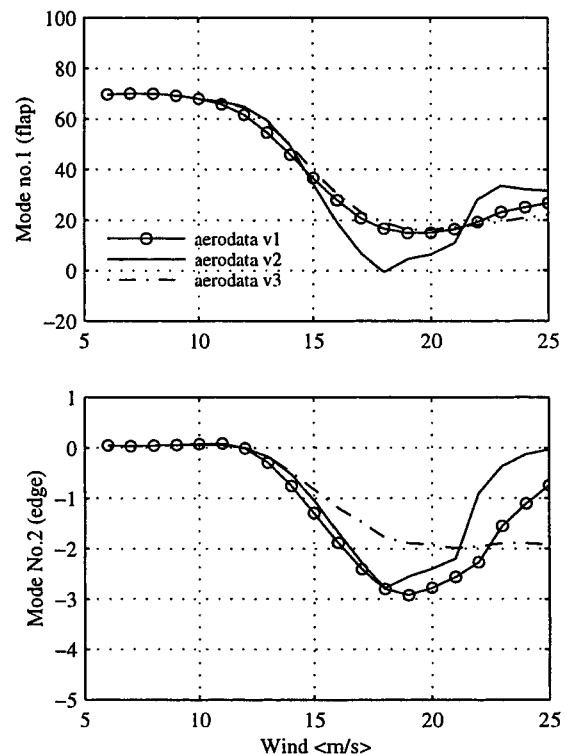


Figure 3. Damping calculated using three sets of aerofoil data

### 6. DYNAMIC STALL

It has long been recognised that the inclusion of unsteady aerodynamics (i.e dynamic stall) in aeroelastic codes for wind turbines is essential in order to obtain agreement between measured and predicted loads [1]. The way to include dynamic stall behaviour in aeroelastic codes is commonly to use a semi-empirical model.

Figure 4 shows calculated damping using two semi-empirical models for dynamic stall [2],[3]. It is seen that the inclusion of dynamic stall modelling, compared to using steady profile data, results in significant different values of damping in the stall region.

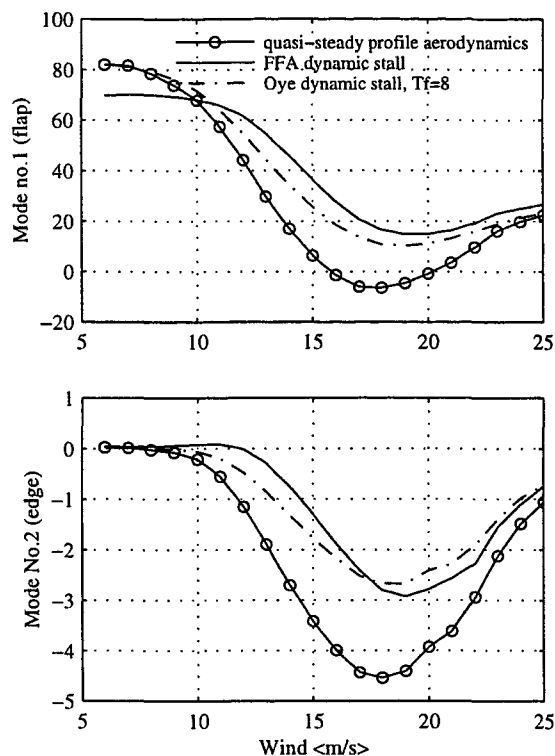


Figure 4. Damping calculated using different dynamic stall models

The usefulness of the semi-empirical models is, however, dependent on that physical mechanisms of dynamic stall are correctly enough described and/or that proper values for semi-empirical constants can be found.

A semi-empirical constant,  $T_f$ , is used in both the FFA and Oye dynamic stall models.  $T_f$  can be interpreted as a time-constant associated with the time-lag of the boundary layer separation process, but it can also be seen as a more general semi-empirical constant that should be tuned to give the best agreement between calculations and experiments. Tuning the dynamic stall model to best fit different 2-D wind tunnel experiments, however, results in different best choices for  $T_f$ . Such tunings can typically result in  $T_f$ -values in the range between 4 and 8. Figure 5 shows that such a variation of  $T_f$  results in substantial differences in calculated damping in the stall wind speed range. The reason why different values is needed could be that different values are needed for different airfoils. It is also possible that the model needs to be refined. Montgomerie has e.g. in [4] suggested that the time constant should be a function of the angle of attack.

There is, however, a lack of experiments with aerofoils used for large wind turbine blades and experiments for the conditions met at flap- and edge-wise oscillations. Until such experimental results are available as a base to tune and improve the dynamic stall models, a large uncertainty in the computation of aerodynamic damping will remain due to uncertainties associated with the dynamic stall modelling.

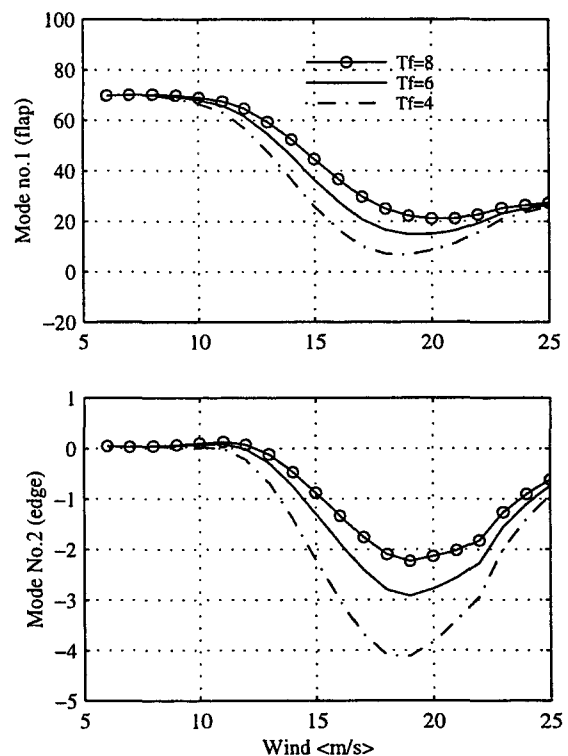


Figure 5. Damping calculated using different values of  $T_f$  ( $T_f$  corresponds to  $2 \cdot \tau_{aufac}$  used in [2])

## 7. MODE SHAPES

Mode shapes are commonly derived using simplifications in such a way that modes have deflections only in pure in- plane or out of plane motion. For this study, mode shapes have also been derived considering the structural twist of the blade. Each mode then includes deflections in both the in-plane and out of plane directions.

Figure 6 shows the calculated blade mode shapes for the 2nd mode<sup>1</sup>. The in-plane component for the mode calculated considering blade twist is very similar to the in-plane component calculated neglecting twist, but the mode now also contains out of plane deflection. Near the tip, the blade deflects with an angle of 14 degrees relative to the plane of rotation. The deflection is such that when the blade deflects in the direction of blade rotation it also deflects towards the wind.

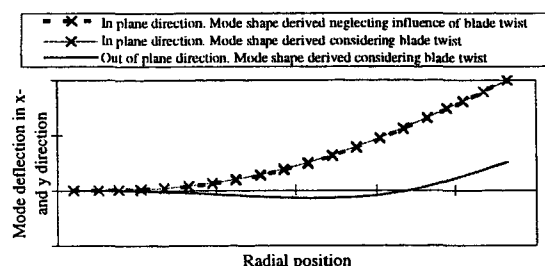


Figure 6 Mode shapes

<sup>1</sup> The 2nd mode in this context is the 2nd mode counting in frequencies. This mode is sometimes referred to as the 1st edge-wise mode using the simplifications mentioned above

Figure 7 shows the calculated damping using the mode shapes derived with and without considering the structural twist of the blade.

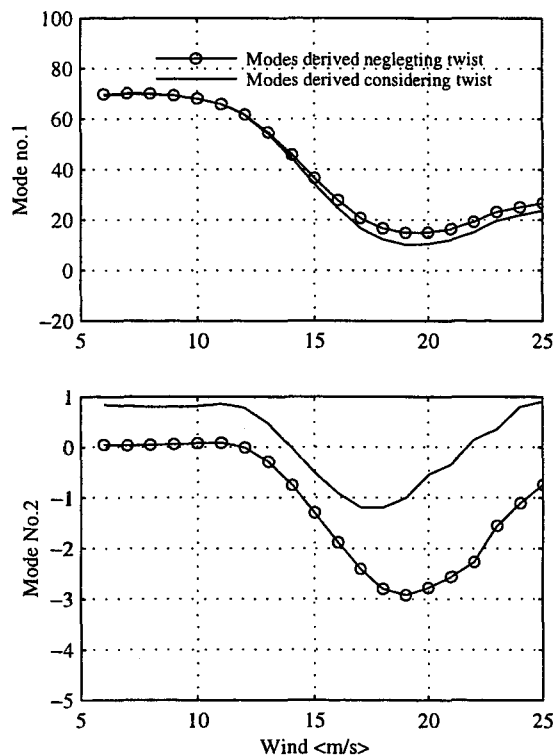


Figure 7. Damping calculated using different mode shapes

The damping for the 2nd mode is seen to be strongly affected by the inclusion of the out of plane deflection. The out of plane deflection results in a significant increase in damping for the 2nd mode. For the 1st mode the damping is reduced, but the margin to negative damping is still rather high. The derived mode shapes are based on "guesstimates" of the blade stiffness and mass distribution. Another guess results in different mode shapes and different calculated damping. The figure shows that the mode shape has a considerable influence on the aerodynamic damping and it therefore essential to have a good description of the blade.

In order to demonstrate the importance of the inclusion of out of plane motion for the damping of the edge-wise mode (2nd mode), calculations have been done with the modes "pitched". The ratio between in- and out of plane deflection is the same for the whole radius, hence the term "pitched" modes. (Positive pitch means that, for the second mode, the blade deflects slightly towards the wind at the same time as it deflects in the direction of the blade rotation.). The "aerodynamic pitch" of the blade is the same for all cases and the power(wind) curves are identical.

Results are shown in figure 8. It is seen that a positive pitch increases the damping for the 2nd mode and slightly decreases the damping for the 1st mode.

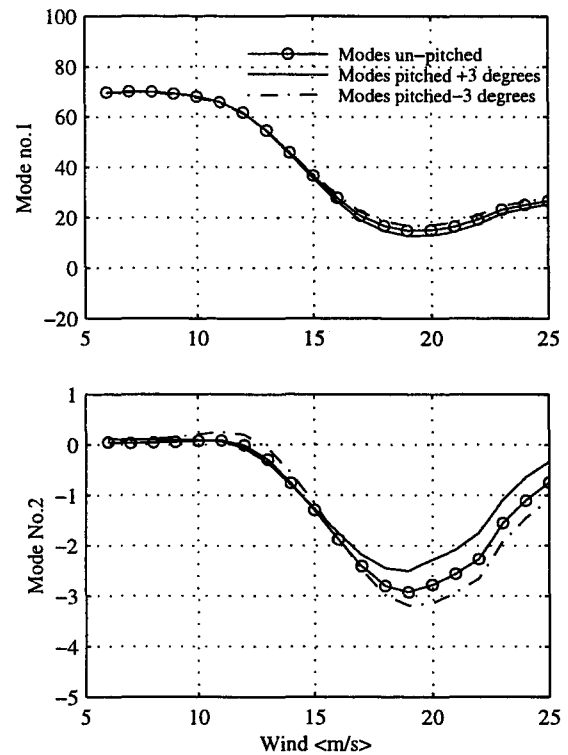


Figure 8. Damping calculated using different pitched modes

## 8. CONCLUSIONS

The aerodynamic damping has been calculated with varying dynamic stall modelling, aerofoil data and mode descriptions. It is found that the calculated damping to a large extent is influenced by all these three parameters.

### Aerofoil data

In the current study, three sets of aerofoil data have been used. The use of these different data sets as input results in different aerodynamic damping. The variation in damping is of the same order as the variation in calculated damping due to uncertainties in how to tune the dynamic stall models. However, the three sets of data used does not give the same average power, thrust and root bending moments as a function of the wind speed. If the static data can be tuned to obtain reliable power and root bending curves, then the remaining uncertainty in the computation of aerodynamic damping will be much less.

### Dynamic stall modelling

The inclusion of models for dynamic stall has considerably improved capabilities of proper computations of stall induced vibrations. However, uncertainties in how to tune the dynamic stall models still exist. Existing uncertainties in the selection of empirical constants result in large differences in calculated damping. In order to tune the models, appropriate wind tunnel tests and unsteady viscous calculations need to be carried out.

### Mode shapes

The damping is dependent on the structural behaviour of the blades since the angle of attack history is dependent on the blade motion. Specifically the aerodynamic damping of the lead-lag mode is found to be very sensitive to relatively small out-of plane blade movements. This means that the orientation of the principal bending axes along the blade, which determines the relevant form of blade oscillations is important. It is thus important to have a correct blade structural description for calculations, but equally interesting is that the aerodynamic damping characteristics can be changed by changing the blade structure.

### Future work

According to the present study the aerodynamic damping, and hence the development of stall induced vibrations is influenced by the mode shapes. The study is, however, carried out for the simplified case of a clamped rotating blade. The next step will be to study the tendency to vibrations for a more complete turbine. The importance of couplings between blade motions and motions of the rest of the turbine will be examined. The level of vibrations is dependent on the sum of aerodynamic and other types of damping. The blade structural damping is certainly important but couplings to the rest of the turbine will cause motions and possibly extract energy by these movements provided that there is damping in the system. Studies will also be carried out to identify how wind turbulence, yaw, tower blockage etc. influences the tendency to develop stall induced vibrations and large dynamic loads.

### **ACKNOWLEDGEMENTS**

The work presented in this paper has partly been funded by NUTEK, "National Swedish Board for Industrial and Technical Development" and partly by the European commission within the DGXII JOULE III program under contract JOR3-CT95-0047, Predictions of Dynamic Loads and Induced Vibrations in Stall, "STALLVIB".

### **REFERENCES**

- [1] Rasmussen, F. et al., "Response of Stall Regulated Wind Turbines - Stall Induced Vibrations" Risø-R-691(EN), ISBN 87-550-1094-8, June 1993.
- [2] Øye, S. "Dynamic Stall-Simulated as Time Lag of Separation", IEA 4th symposium on aerodynamics for wind turbines. Rome, January 1991, Edited by Ken MacAnulty, ETSU England.
- [3] Björck, A. "The FFA Dynamic Stall Model. The Beddoes-Leishman Dynamic Stall Model Modified for Lead-Lag Oscillations". IEA 10th Symposium on Aerodynamics of Wind Turbines i Edingburgh, 16-17 December 1996. Editor Maribo Pedersen, DTU Danmark
- [4] Montgomerie, B., "Dynamic Stall Model Called "Simple", Rep. No. ECN-C--95-060, Netherlands Energy Research Foundation ECN, June 1995.



## Appendix 5

Comparison of Load Measurements  
Between the Large Wind Turbines Aeolus II  
and Näsudden II

Christian Hinsch, Henry Seifert,  
Hans Ganander, Hjalmar Johansson





# COMPARISON OF LOAD MEASUREMENTS BETWEEN THE LARGE WIND TURBINES AEOLUS II AND NAESUDDEN II

C. Hinsch\*, H. Seifert\*, H. Ganander\*\*, H. Johansson\*\*

\* Deutsches Windenergie-Institut, Ebertstrasse 96, D-26382 Wilhelmshaven

\*\* Teknikgruppen AB, P.O. Box 21, S-191 21 Sollentuna

## ABSTRACT

This paper is an extract from an extensive report [1] which contains mainly the evaluation and comparison of load measurements and dynamic behaviour for two 3 MW sister wind turbines (AEOLUS II and NAESUDDEN II), which are identical except for the tower, the rotor speed and the control. It also presents results concerning various operational quantities like electrical power, rotor speed and blade pitch angle. Furthermore, the influence of turbulence intensity on loads, accelerations and operational quantities were investigated for AEOLUS II and are shortly presented within the report. The idea of the evaluation is to compare structural behaviour and dynamics of the two turbines at as similar conditions as possible in order to find out the importance of the differences between the two turbines.

## 1 INTRODUCTION

In the framework of the EU funded program "WEGA II Large Wind Turbine Scientific Evaluation Project" a sub-project CAN - Comparison of AEOLUS II (located in Germany) and NAESUDDEN II (located in Sweden) - was carried out in order to investigate the behaviour of two 3 MW sister wind turbines. The two turbines are identical except for the tower, the rotor speed and the control.

The AEOLUS II is a two-bladed, variable speed, pitch-controlled 3 MW rated power wind turbine with a hub height of 92 m and a rotor diameter of 80.5 m. The NAESUDDEN II is identical except for the hub height of 78 m and the operation with two fixed rotor speeds. Details about the turbines can be found in the WEGA-II Data Catalogue for Wind Turbines [2].

## 2. DATA ACQUISITION SYSTEMS AND EVALUATION SOFTWARE

### 2.1 The AEOLUS II

One blade of the AEOLUS II wind turbine is installed with strain gauges in six full bridges for the measurement of the loads (3 forces and 3 moments), identically to the NAESUDDEN II blades. All strain bridges are placed on the inner side of the blade root. Because of the short distance to the blade bearings, non-linearities occur which makes it necessary to perform a special calibration procedure. Taking into account all forces and moments as well as the rotor speed and the blade pitch angle, the edgewise and flapwise moments are calculated and transformed to the hub-fixed coordinate system.

To study the turbine behaviour in general and in special situations, six acceleration sensors were installed at the turbine's nacelle, measuring the accelerations twice in all three directions (see Fig. 1). By transforming the single

signals to the centre line between tower axis and rotor shaft, three translational and three rotational accelerations were calculated.

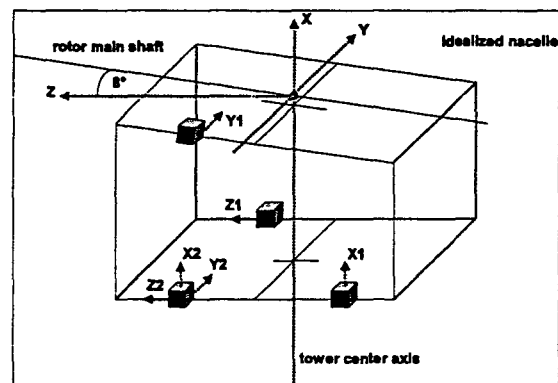


Fig. 1: Location of the accelerometers in the nacelle.

The operational quantities like rotor speed, blade pitch angle, rotor azimuth angle, nacelle azimuth angle and yaw status are measured at the turbine's nacelle and transferred to the ground station. The electrical power is measured by a power transducer at the ground station.

The wind speed is measured with calibrated cup anemometers at three heights (62m, 92m, 126m). The other meteorological quantities are described in [3] & [4].

DEWI's philosophy of evaluation software principles takes into account the recommendations given by ELSAM [5] and the IEA [6] and is based on the aim to save all relevant information, without generating hundreds of Megabytes of data. Therefore, a capture matrix was developed which allows to save a given amount of 10-minutes-time series in each matrix element. The matrix is mainly divided into wind speed and turbulence intensity classes of 2 m/s, resp. 5% intervals. Furthermore, some special matrix fields are reserved for special operational conditions like start/stop at low/high wind speed, high yaw misalignment, high vertical

wind shear and yawing. A maximum of ten 10-minutes time series of raw data are stored per matrix element. During the whole measurement period, time series were recorded for wind speeds up to 24 m/s and turbulence intensity levels higher than 20 %.

In addition to the time series of raw data (recorded with a sample rate of 20 Hz), a special file is written during the whole measurement campaign, containing ten minutes averages, standard deviation and extreme values of selected quantities. The software flow diagram for evaluation can be seen in [7].

## 2.2 The NAESUDDEN II

The measurement system consists of the distributed data acquisition system, the net work, the computer and the power backup device. When the turbine is running the sampling frequency is 20 Hz, otherwise the measurements are carried out with 1 Hz continuously. Measured data are stored on video8 tapes with capacity 2.5 Gbyte or 5 Gbyte. The data acquisition system is built up by four modules located in the rotor system, in the nacelle, at the tower top and in the measurement building. Connected to the computer there is a monitor which can be used for graphic presentation of signals, which also can be documented via the laser printer.

Two blades are equipped with strain gauges at the NAESUDDEN II, but only blade 1 is used for the comparison. An important part of using the continuous measurements is the overview plotting that is done routinely. On one hand they are used to check all signals, on the other hand they quickly give a picture of wind as well as turbine situations that are measured. Finally, they are complete and contain everything that has occurred, even very unforeseen situations, and can be used for evaluation of fatigue damage of all situations which have occurred.

## 3. CALIBRATION PROCEDURES

Because of non-linearities due to the short distance of the strain gauges to the pitch bearing and temperature effects a special procedure has been developed in order to calibrate the strain signals at the blade roots. The procedure takes into account rotational speed as well as forces and moments for deriving the resulting edgewise and flapwise bending moments [8].

## 4. RESULTS

### 4.1 Operational Statistics

The energy production of both turbines since starting operation (AEOLUS II: Dec. 1993, NAESUDDEN II: Mar. 1993) up to the 31<sup>st</sup> of August 1997 is given in Tab. 1, together with the distribution of operation modes. Both turbines had stand-still periods of around half a year due to gearbox repair in 1996 (AEOLUS II) and 1997 (NAESUDDEN II).

Tab. 1: Operational Statistics

	AEOLUS II	NAESUDDEN II
energy production	17.719 MWh	17.816 MWh
production	61.3 %	45.5 %
stand-by	15.7 %	19.2 %
fault / maintenance	21.4 / 1.6 %	33.4 %
start / stop	---	1.9 %

### 4.2 Main Loads

The mean loads of in-rotor-plane moment  $M_{in-plane}$  and out-of-rotor-plane moment  $M_{out-of-plane}$  as well as for the flapwise loading FlapM and edgewise loading EdgeM of the rotor blade are presented. The shown values of 10-min averages and standard deviation include also periods of yawing and all recorded turbulence intensity levels.

The bin-averaged curves of  $M_{in-plane}$  (Fig. 2) increase with increasing wind speed up to around 14 m/s, where the power reaches its rated value of 3 MW. At higher wind speeds, the blade pitch control reduces further increase, giving nearly constant power output and constant moment  $M_{in-plane}$ . The values of average  $M_{in-plane}$  for NAESUDDEN II are at rotor speeds of 21 rpm lower than for AEOLUS II; because of the higher rotor speed the driving mean loads are reduced at equal power output.

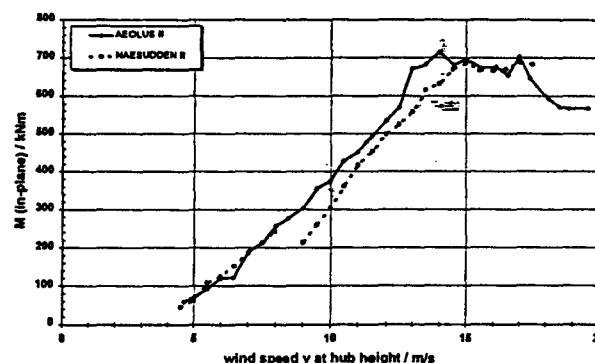


Fig. 2: Comparison of average  $M_{in-plane}$

The standard deviation of  $M_{in-plane}$  (Fig. 3) is mainly driven by the mass of the rotor blade (1175 kNm) with values between 750 and 800 kNm.

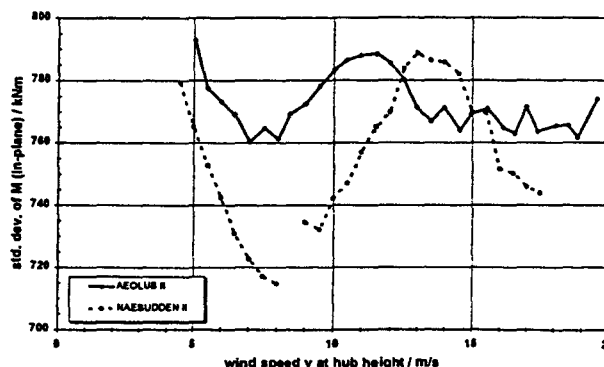


Fig. 3: Comparison of std. dev. of  $M_{in-plane}$

Due to constant rotor speed the variation of loads are lower for the NAE-SUDDEN II. The course of the curve at low wind speeds might be influenced by calibration problems and therefore needs to be more investigated.

For AEOLUS II, the bin-averaged curve of  $M_{out-of-plane}$  (Fig. 4) shows a similar course as the  $M_{in-plane}$  over the wind speed: Increasing values up to a wind speed of 14 m/s and then a drop of nearly 750 kNm up to 20 m/s. For NAE-SUDDEN II, the average  $M_{out-of-plane}$  has two levels for the two rotor speeds. At 14 rpm, the loads for NAE-SUDDEN II are remarkably lower than for AEOLUS II, which is due to lower rotor speed. At 21 rpm, the loads for NAE-SUDDEN II are higher caused by higher rotor speed compared to AEOLUS II.

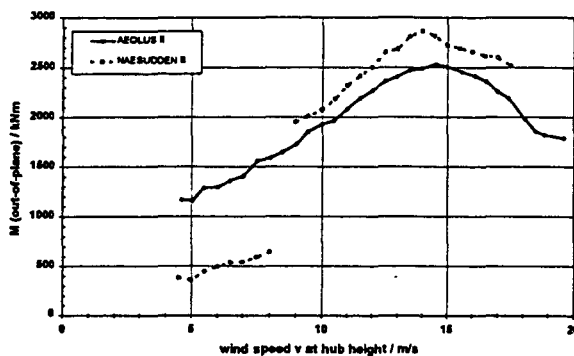


Fig. 4: Comparison of average  $M_{out-of-plane}$

For AEOLUS II, the standard deviation of  $M_{out-of-plane}$  (Fig. 5) increases slightly from cut-in wind speed up to 13 m/s and then more significantly, with the blade pitch mechanism in operation. For NAE-SUDDEN II, the constant rotor speed of 21 rpm also during blade pitch operation leads to lower load variations. At low wind speeds (up to 9 m/s), the variations in rotor speed are remarkably higher at AEOLUS II, thus leading to higher variations in  $M_{out-of-plane}$  in this wind speed range. At higher wind speeds, the variations in rotor speed as well as in blade pitch angle are higher at AEOLUS II. So it can be concluded that the control of AEOLUS II allows higher variations in operational parameters and leading therefore to higher variations in  $M_{out-of-plane}$ . Perhaps these differences are also influenced by the different tower concepts (soft for AEOLUS II, stiff for NAE-SUDDEN II).

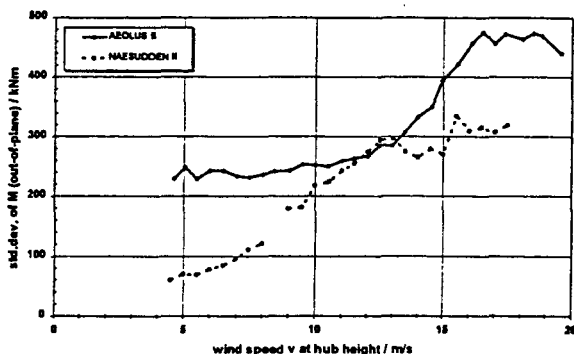


Fig. 5: Comparison of std. dev. of  $M_{out-of-plane}$

The course of the bin-averaged curves for average and standard deviation of the moments  $M_{b(edge)}$  and  $M_{b(flap)}$  do

not differ very much from the values for  $M_{in-plane}$  and  $M_{out-of-plane}$  respectively.

For the flapwise and edgewise bending moment of the rotor blade the 1-Hz-Equivalent Load  $L_{eq}$  and a fatigue spectra for a given wind speed distribution and assumed wind turbine duty cycles [5] can be determined.

Due to bad calibration conditions the calibration procedure for the blade root loads is not possible for low rotor speed (e.g. during start and stop procedures) and the resulting values for the moments can not be trusted in these cases. Therefore, start and stop cycles were not taken into account. No attention is paid to changes between 10-minutes periods nor to the changes of rotor speed in the case of NAE-SUDDEN II.

Besides the 3-dimensional way to describe the results in terms of matrix mean value, rms value and irregularity, the 1-dimensional quantity 1-Hz-Equivalent Load  $L_{eq}$  is very suitable to describe and compare fatigue phenomena [9], even if no structural dimensions are involved in  $L_{eq}$  and thus nothing about the damage level is said.

For AEOLUS II, the edgewise 1-Hz-Equivalent Load (Fig. 6) shows an increase with increasing wind speed and a remarkable peak at 5 m/s, eventually caused by resonance due to the low rotor speed of around 13 rpm ( $2p = 0.43$  Hz), which is very close to the natural frequency of the tower ( $0.42$  Hz), see the resonance diagram (Fig. 13). For NAE-SUDDEN II, the edgewise 1-Hz-Equivalent Load is lower at wind speeds up to 12 m/s, but then variations in wind speed causes higher equivalent load because of the fixed rotor speed not allowing these variations to be compensated by variations in rotor speed.

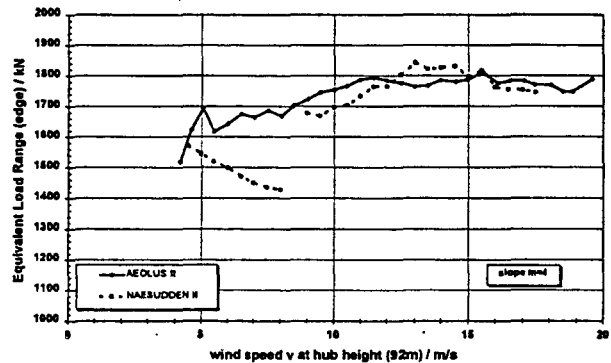


Fig. 6: Comparison of edgewise equivalent load

For calculation of the one-year fatigue spectrum a Rayleigh-distribution ( $V_m = 8.5$  m/s,  $t_f = 0.1-0.15$ , turbine availability 100%) were assumed. The resulting fatigue spectra (see Fig. 7) shows a typical vertical section representing nearly twice the amplitude caused by the mass of the blade for the operational number of around 7.500.000 cycles. At both turbines, the maximum range of 4300 kNm occurs in the wind speed class 16-18 m/s.

For AEOLUS II, the flapwise 1-Hz-Equivalent Load (Fig. 8) shows also a slight peak at 5 m/s, a slight increase with further increasing wind speed and a stronger increase above 13 m/s. For NAE-SUDDEN II, the increase is stronger at low wind speeds and slighter at higher wind speeds. Over the whole wind speed range, the equivalent load for NAE-SUDDEN II is lower than for AEOLUS II.

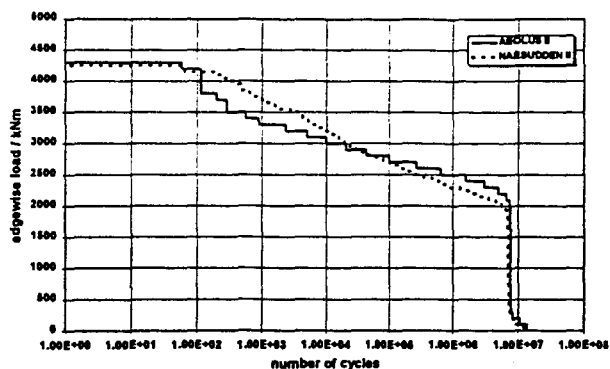


Fig. 7: Comparison of edgewise fatigue spectra

For AEOLUS II, the resulting fatigue spectra (Fig. 9) has a maximum of 4300 kNm for the wind speed class between 16 m/s and 18 m/s. The values for NAESUDDEN II are lower over the whole load range, having a maximum of 3700 kNm.

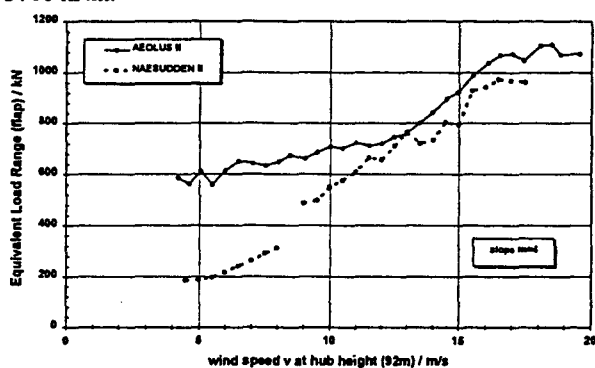


Fig. 8: Comparison of flapwise equivalent load

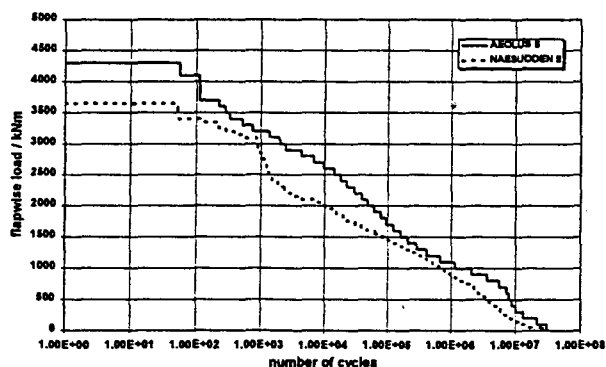


Fig. 9: Comparison of flapwise fatigue spectra

#### 4.3 Accelerations

The main intention of mounting the accelerometers on the nacelle was to determine more details about the dynamic behaviour and dynamic properties of the two turbines. The comparison of std. dev. of the acceleration within 10 minutes as a value for the dynamic response of the tower due to wind loading is presented.

All three translational accelerations ( $A_x$ ,  $A_y$ ,  $A_z$ ) and all three rotational accelerations ( $R_x$ ,  $R_y$ ,  $R_z$ ) at the nacelle (see also Fig. 1) show a very similar behaviour up to wind speeds around 8 m/s. Then, the first increase of deviation

takes place, the second increase starts at a wind speed of around 11 m/s. The highest translational acceleration is  $A_y$  (Fig. 10), representing the deviation of the tower in y-direction, which corresponds to the lateral direction of the rotor. The highest rotational direction is  $R_x$ , which corresponds to the torsional movement (yaw motion) of the tower around the tower axis.

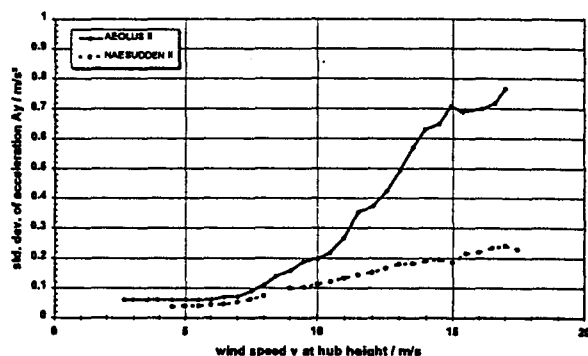


Fig. 10: Comparison of std. dev. of acceleration  $A_y$

Regarding the influence of the much more soft AEOLUS II tower compared to the stiff NAESUDDEN II tower, the std. dev. of accelerations within 10 minutes are larger by a factor of 4 at AEOLUS II for wind speeds exceeding 8 m/s. The picture is somewhat more clear when looking at the frequency content as shown in FFT diagrams [1]. The NAESUDDEN II is more dynamically excited at lower rotor speed than AEOLUS II. The opposite can be seen for the higher rotor speed. However, what is of interest is the corresponding loading of tower and nacelle. The relation of this loading  $F$  between the two turbines can roughly be estimated to be:  $F_{AEOLUS II} / F_{NAESUDDEN II} \leq 0.1$ . The main reason for this is the low stiffness constant of the AEOLUS II tower.

#### 4.4 Comparison of Special Situations

The std. dev. within 10-minutes describe more the variations of quantities with wind speed variations. The short term characteristics will be investigated by means of time series, FFT-Analyses and azimuthal binned curves.

The AEOLUS II is triggered at the low rotor speed in thrust direction ( $2p \approx$  natural frequency of the tower). The  $1p$  in electrical power indicates that there are some differences between the blades. This asymmetry causes odd  $p$ 's in other fixed system quantities (accelerations). A very peculiar out-of-plane behaviour at tower passage at high rotor speed occurs (Fig. 11).

At 20 rpm, a coupled mode (accelerations  $A_y$  and  $R_x$ ) with tower and yaw is seen to occur, the corresponding mode has higher frequencies for NAESUDDEN II due to the stiff tower. Also at 20 rpm, the odd  $5p$  (close to 1.flap of the blade) and  $7p$  (close to 1.edge of the blade) mode including  $A_z$ ,  $R_y$  and  $R_z$  is very clear. It is a kind of tilt and roll mode. The rotational acceleration is much more excited at 20 rpm than at 14 rpm.

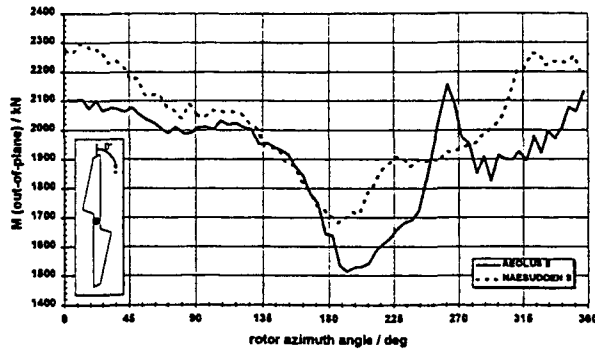


Fig. 11: Azimuthal binned curve of  $M_{out-of-plane}$  at high rotor speed

For NAESUDDEN II, the electrical power has obvious 2p at 14 rpm and 20 rpm. The 4p at 20 rpm is also coupled with the tower (acceleration  $A_z$ ). 9p is a very apparent frequency component at the lower rpm, due to differences between the blades. The rotational accelerations are lower at 20 rpm than at 14 rpm.

In comparison, the tower-yaw frequency, which can be seen in the accelerations  $A_y$  and  $R_x$ , is lower at AEOLUS II (1.46 Hz) than at NAESUDDEN II (2.07 Hz). The tower of the AEOLUS II is excited by 2p at the lower rotor speed, whereas the tower of the NAESUDDEN II is excited by 4p at the higher rpm (Fig. 12).

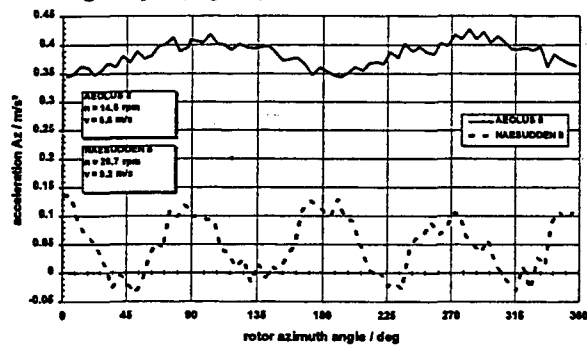


Fig. 12: Azimuthal binned curve of acceleration  $A_z$

As can be seen in the azimuthal binned curve of the out-of-plane moment (Fig. 11), the blade passage through the tower shadow is not less severe at the AEOLUS II, even if the distance between blade and tower is higher because of the slender construction.

Finally, it can be assumed that both turbines have blades which among themselves are not totally equal.

#### 4.5 Resonance Diagram

By means of a Fast-Fourier-Transformation Analysis the natural frequencies of the components *tower* and *rotor blade* were determined. The following figure shows the resonance diagram, containing the measured natural frequencies as well as the excitation frequencies caused by the rotor and the operational range.

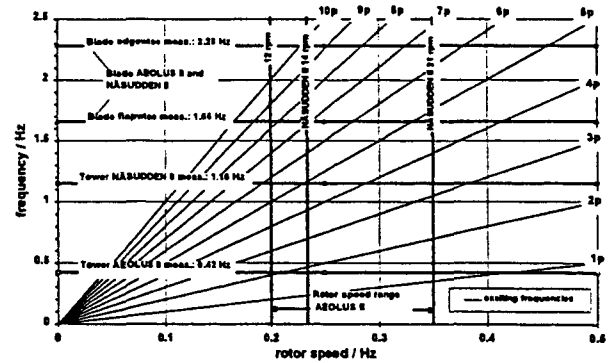


Fig. 13: Resonance Diagram

As can be seen, for AEOLUS II the natural frequency of the tower is very close to the common appearing 2p-exciting frequency in the low rotor speed range.

For NAESUDDEN II, the natural frequency of the tower is close to the 5p-exciting frequency of the turbine.

#### 5. CONCLUSIONS

The two 3 MW turbines AEOLUS II and NAESUDDEN II are similar except for two major differences: Rotor speed control and tower stiffness, and the question is to what extent divergences of loading and dynamics are influenced by these turbine inequalities.

Regarding the electrical power as an 10-minutes-average, there seems to be no significant differences between the two turbines, see also [3]. But details during shorter time periods reveals large differences in terms of amplitude frequency distribution. The AEOLUS II has a much more smooth behaviour, which of course reduces load variations in the rest of the turbine. On the other hand, which is very pronounced at low wind speeds, the variation of rotor speed causes out-of-plane moment variations during 10 minutes as an example. The sensitivity of the rotor speed on out-of-plane moment is quite obvious looking at the NAESUDDEN II turbine, when changing rotor speed.

Regarding the influence of the much more soft AEOLUS II tower compared to the stiff NAESUDDEN II tower, the standard deviations of accelerations within 10 minutes are larger by a factor of 4 at AEOLUS II for wind speeds exceeding 8 m/s. The picture is somewhat more clear when looking at the frequency content as shown in FFT diagrams. The NAESUDDEN II is more dynamically excited at lower rotor speed than AEOLUS II. The opposite can be seen for the higher rotor speed.

Another consequence of the different towers is that the distance between the tower and blade during the blade passage is larger at the AEOLUS II. However, this can not be seen in a reduction of the flap load variations.

Regarding evaluation of load variations in terms of fatigue, the determination of the total spectrum contains only ordinary situations and for this reason has a relatively limited importance for interpretation of fatigue. Furthermore, load spectrum itself, or the equivalent load, is independent on dimensions and the strains or stresses of the material.

However, the project has contributed to lots of measured data and knowledge about behaviour of the two turbines in

terms of mean values as well as dynamic response properties.

## 6. FUTURE WORK

The comprehensive measurements are a good basis for further investigations concerning the operational quantities, blade loads and accelerations at AEOLUS II and NAE-SUDDEN II.

Nevertheless, more should be done to refine the calibration procedure by installing also strain gauges on the second blade at AEOLUS II to get a more complete picture of the loading. The strain gauges then have to be located on the outside of the blades at a position which is not effected by load introductions. Especially, the start and stop operational modes should be modelled more adequate to take these situations into account for calculating a life-time fatigue spectra. Also the question of temperature dependency is not answered completely.

The influence of various further external meteorological parameters (e.g. wind shear, wind direction fluctuations, extremes in terms of wind conditions like gusts) on large wind turbines should be investigated and conclusions from the turbulence intensity investigations should be made in terms of finding a description of loading as a function of turbulence intensity (e.g. by applying a multivariate regression analysis or other mathematical procedures).

From the knowledge gathered by this project investigations should be carried out to improve the turbine control mechanism.

In addition more effort should be paid to investigate the influence of low cycle fatigue on the total fatigue load spectrum, especially when generating a spectrum from 10-minutes time series. Furthermore all turbine conditions should be taken into account and attention should be paid to the differences between 10-minutes situations.

## 7. REFERENCES

- [1] C.Hinsch, T.Kramkowski, H.Seifert, H. Ganander, H.Johansson, R.Lindström : CAN Final Report Part 3.3 Load Measurements AEOLUS II - NAE-SUDDEN II: DEWI, Teknikgruppen AB : 1997.
- [2] WEGA-II Large Wind Turbine Scientific Evaluation Project : Data Catalogue for Wind Turbines : Elsamprojekt A/S : 1997.
- [3] A.Albers, C.Hinsch, H.Klug, D.Westermann, G.Ronsten : CAN Final Report Part 3.1 Power Performance: DEWI, FFA : 1997.
- [4] A.Albers, C.Hinsch, H.Klug, D.Westermann : Power Performance and Operational Characteristics of the AEOLUS II : Appendix to CAN Final Report : DEWI: 1997.
- [5] WEGA-II Large Wind Turbine Scientific Evaluation Project : Guidelines and Recommendations : CEC DGXII Contract J0U2-CT93-0349 : Elsamprojekt A/S, ETA Plan: 1996.
- [6] IEA : Recommended Practices on Wind Turbine Testing : No. 3 : Fatigue Loads : 2nd Edition : 1990.
- [7] C.Hinsch, T.Kramkowski, H.Seifert : Operational Quantities, Blade Loads and Dynamic Behaviour of the AEOLUS II : DEWI : 1997.
- [8] J.A.Dahlberg, H.Johansson : Calibration Procedures for Improved Accuracy of Wind Turbine Blade Load Measurements : in Proceedings of the European Union Wind Energy Conference : Göteborg, 1996.
- [9] H.Söker (Editor) : Monitoring Fatigue Loads on Wind Turbines Using Cycle Counting Data Acquisition Systems : Final Report : J0U2-CT92-0175 : DEWI, FFA, CRES : 1995.

## Acknowledgement

The work presented in this paper has been co-funded by the European Commission within the DGXII Non-nuclear Energy Programme as a part of the WEGA II project (J0U2-CT93-0349). Part of the Swedish work is also funded by the utility company Vattenfall AB and The Swedish Board of Technical Development (NUTEK).

The authors would like to express their thanks to Mr. Bibricher, Mr. Roer and Mr. Wendt from the manufacturer MBB and Mr. Göransson from the Swedish manufacturer Kvaerner for assistance in the measurements.

DEWI also wants to thank the utility PreussenElektra Hannover, here especially Mr. Klemm, and Mr. Hoelscher with his colleagues from the Wilhelmshaven power station, for making their turbine AEOLUS II available for the measurements and assisting during the application of sensors, maintenance of the data acquisition systems and during special measurement campaigns in operating the turbine.

Teknikgruppen wants to thank the utility Vattenfall AB for their general support of this project and also many thanks to Mr. Andersson and Mr. Ohlsson at the NAE-SUDDEN II site for the engagement in running and maintaining the measurement system.

## Appendix 6

### Footprinting Wind Turbine Fatigue Loads

Holger Söker, Evangelos Morfiadokis,  
Theodore Kossivas, Anders Östman





# FOOTPRINTING WIND TURBINE FATIGUE LOADS

H. Söker\*, E. Morfiadakis\*\*, T. Kossivas\*\*, A. Östman\*\*\*

\* Deutsches Windenergie-Institut, DEWI, Ebertstrasse 96, D-26382 Wilhelmshaven, Germany

\*\* Centre for Renewable Energie Sources, CRES, 19th km Marathonos Ave., GR-190 09 Pikermi Attiki, Greece

\*\*\* The Aeronautical Research Institute of Sweden, FFA, P.O. Box 11021, S-161 11 Bromma, Sweden

## ABSTRACT

The effect of wind farm and complex terrain operation on wind turbine fatigue loading is of great interest but still not easily quantified. Within the EU Non Nuclear Energy R&D Programme the described project *Measuring Footprints of Wind Turbine Fatigue Loads Using Monitoring Methods* applies a monitoring method on three wind turbines of the same type operating under flat terrain / stand alone, wind farm and complex terrain conditions. Statistics - *footprints* - of the load quantities are established through on-line rainflow counting of the sampled data. These footprints are evaluated to identify relevant quantities that can serve as shape, intensity and validity parameters. The paper presents the project's objectives and technical approach as well as first measurements and evaluation results.

## 1 INTRODUCTION

Wind turbines have grown large in size and have strongly been modified in key components and employed technologies giving rise to a renewed necessity of load measurements. Cost effective, reliable load measurement and load prediction procedures maintaining reasonable safety levels are demanded by industry.

In acknowledgement of this demand and in the framework of the EU's Non Nuclear Energy R&D Programme a project consortium established by CRES, FFA, TACKE and DEWI set out to investigate wind turbine fatigue loads within the described project *Measuring Footprints of Wind Turbine Fatigue Loads Using Monitoring Methods*. The project employs the fatigue load monitoring method [1] for its appealing simplicity. As test turbines three TACKE 500 kW machines have been selected, each in their specific external conditions, i.e. stand alone, wind farm & complex terrain conditions.

The method delivers fatigue load statistics - *footprints* - through on-line rainflow counting (RFC) [2] of the sampled data. A footprint describes the fatigue loading of a wind turbine component in terms of occurrences of load cycles for a given measurement time interval, typically one day, 10 days or one month. Such load cycle frequency distributions are to be characterized by shape, intensity and validity parameters. Each footprint must be associated with a set of parameters related to the prevailing operational and external conditions during that time interval. The project work focusses on a proper choice of these governing parameters in a way to enable measurements to be scaled, extrapolated and rated for validity. Having accomplished this it will be possible to investigate the differences in loading of a wind turbine operating at different conditions (i.e. flat and complex terrain or wind farms).

The potential of the employed monitoring method to assess long periods of operation enables to estimate the relevance of low cycle fatigue which has been seen to become relevant with the use of modern fatigue resistant materials as a consequence of the turbines' growing sizes.

## 2. TECHNICAL APPROACH

The approach is to apply a common methodology on all test sites in order to create test data of comparable quality that can be evaluated. Missing information is to be complemented by employing FFA's vast data base of measurements at Alsvik and, moreover, by using their simulation capabilities.

CRES, TACKE and DEWI have jointly selected the wind turbine type TACKE TW 500 - this type of turbine is available in both countries - and the appropriate test sites in Greece and Germany. Since there exist two models of the TW 500 machine with slightly different technical data, both sets of characteristic values are given in table 1 along with those of the turbine type installed at Alsvik:

	TW500 model I	TW500 model II	Danwin 180kW
rated power	500 kW	500 kW	180 kW
diameter	36 m	37 m	23 m
rpm	29.6	30.9	42
blades	3, LM17	3, LM17	3
hub type	Y-type	spherical, extenders	Y-type, extenders
	upwind, stall	upwind, stall	upwind, stall

Tab. 1: Turbine characteristics

### 2.1 Site Descriptions

Toplou site on Crete is characterised by complex topography. On the greater area, the Public Power Corporation (PPC) operates a wind park consisting of seventeen 300 kW wind turbines and three 500 kW wind turbines, two of which are TACKE TW 500. All of them with the exception of one 300 kW machine are placed in a row with SW-NE orientation. The surrounding area is predominantly mountainous with many hills and ridges of various slopes covered with sparse and low lying vegetation of typical Mediterranean nature. The roughness length of the area is estimated as 0.10 m in terms of visual inspection.

In Germany two suitable model II turbines have been found assisted by TACKE: one in the commercially operated wind farm of the local utility of the city of Emden, SWE, and one privately owned stand alone turbine in the vicinity of Wilhelmshaven. Both sites feature flat terrain with meadows, single groups of trees and sparsely distributed buildings. The SWE wind farm consists of 10 wind turbines organized in two rows of 5 turbines in NW-SE orientation. Although the two test sites are some 70 km apart from each other, the meteorological conditions in the whole of Germany's coastal area are considered to be similar enough as to allow for long term comparison of measured load footprints.

FFA has performed measurements in the small wind farm at Alsvik during many years. The farm consists of four three bladed 180 kW Danwin turbines and the site features very flat terrain. The layout of the farm has been suited for wake studies [3].

## 2.2 Measuring Campaign

Extensive measurement programs are being carried out on the three TACKE TW500 wind turbines comprising meteorological, operational as well as load quantities.

All three test turbines have been equipped with strain gauge bridges for measuring blade root flapwise and edgewise bending moments, tower bending moments and tower torsion moments.

Wind speed measurements on the machine operating at Toplou site are performed using cup anemometers and vane resolvers at three different heights. In addition, for the description of the 3-dimensional character of the incoming wind flow, a fast responding sonic anemometer is used. Meteorological measurements include atmospheric temperature and pressure, while the operational wind turbine quantities include nacelle direction as well as active power and grid/brake status. All analogue signals from the sensors are sent to interface boxes housing power supply modules and transient protectors. After low-pass filtering and A/D conversion a PC is used to control automated data acquisition and data storage. Data are continuously recorded as time series on which off-line processing procedures are applied to obtain results equivalent to *real* monitoring data i.e. on-line rainflow counting of the fatigue load.

On the two test turbines in Germany wind speeds are measured using the wind turbine's nacelle anemometers with an appropriate calibration [4]. The nacelle wind vane signal can be used to determine duration of oblique inflow. Again operational wind turbine quantities include nacelle direction as well as active power and grid/brake status.

At the two German test turbines the data acquisition system (DAS) has been designed in pursuit of an improved load monitoring system featuring remote control and logging all data in one data logger network. The DAS performs *true* on-line data reduction into statistics using rainflow counting and time at level statistics avoiding time series recording.

In the current measurement campaign the time base for the individual monitoring periods has been chosen to be 1 day as a compromise between including low cycle fatigue relevant phenomena on one hand and on the other hand shortening the measurement campaign through the

possibility to compose a comprehensive fatigue load footprint from a pool of 1-day-footprints.

FFA has a large data base available from former measurement campaigns in the Alsvik wind farm. Measurements of blade and tower loads in one of the turbines, power from all turbines and meteorological data, wind speed and wind direction from 7 levels in two masts, have been archived. The location of the turbines enables investigation of wind farm operation effects for varying turbine distances.

In order to complement measurements FFA has, assisted by TACKE Windtechnik, further set up a simulation model in order to perform load calculations for the TACKE 500 kW wind turbine

## 3. SCIENTIFIC APPROACH

The principle of *footprints* refers to the archaic ability of men to *read* the traces left in the ground by other creatures and to interpret the information contained in them.

Transferring this principle to the task of describing a wind turbine's fatigue loading a *footprint* is to be understood as a suitable statistic representation of a wind turbine's load history under representative external conditions. The central aspect of the project work is to develop the skills and the experience in reading the information that is comprised in such a footprint.

### 3.1 Fatigue Loading Representation

The fatigue loading of the wind turbine components is described using RFC statistics in three representations:

- Equivalent Load Range, Leq:  
The information contained in the RFC statistics is used to calculate the 1-Hz-equivalent-load using the Palmgreen-Miner's rule [5].
- RFC Amplitude spectrum (1-dimensional):  
The information contained in the RFC statistics is transformed into a (cumulative) frequency distribution of load cycle amplitudes omitting the mean value at which the load cycle occurs.
- RFC Transition Matrix (2-dimensional):  
The transition or load cycle matrix contains the number of occurrences of a class of load cycles, information about their amplitude *and* their mean value.

### 3.2 Description of The External Conditions

In order to identify and quantify the effects of the external conditions on the machine fatigue loading, the following maximum set of parameters has been used to describe the character of the inflow to the turbine rotor (due to limitations in complexity of DAS not all of these parameters can be established for each of the test sites):

- Statistical descriptors for wind speed namely mean value ( $U$ ), standard deviation ( $\sigma_u$ ,  $\sigma_v$  and  $\sigma_w$ ), skewness ( $s$ ) and kurtosis ( $k$ ) of the wind speed distribution
- wind shear exponent ( $\alpha$ )
- wind velocity inclination ( $\epsilon$ )
- Turbulence length scale ( $L_u$ )
- Coherence decay factor for the longitudinal wind speed component between two points in the vertical direction.

### 3.2 Analysis

To establish the relative importance of these external conditions parameters statistical techniques have been used.

#### 3.2.1 Multivariate Regression Analysis

The equivalent load ranges for a body of  $N$  rainflow counts are expressed as a function of the independent inflow parameters given above:

$$y(x_i) = \sum_{k=1}^M a_k X_k(x_i) + E(x_i), \quad i = 1, N \quad (1)$$

where

- $y(x_i)$  = equivalent load range
- $a_k$  = coefficient of  $k^{\text{th}}$  independent variable
- $X_k(x_i)$  = value of  $k^{\text{th}}$  independent variable at  $x_i$
- $E(x_i)$  = associated error

In order to calculate the coefficients of this function the multivariate regression analysis as introduced in [7] and successfully applied in [6] has been adopted. The assessment of the regression findings is attained through the dependence coefficients  $S_k$  which represent the percent increase of the equivalent load range by an increase of one of the inflow parameters by one standard deviation:

$$S_k = a_k \frac{\sigma_{X_k}}{y_{\text{mean}}}, \quad \sigma_{X_k} = \sqrt{\frac{\sum_{i=1}^N (X_k(x_i) - \bar{X}_k)^2}{N-1}} \quad (2)$$

where

- $S_k$  = dependence coefficient
- $\bar{X}_k(x_i)$  = mean value of  $k^{\text{th}}$  independent variable
- $\sigma_{X_k}$  = std. dev. of  $k^{\text{th}}$  independent variable

#### 3.2.1 RFC Amplitude Spectrum Modelling

In an attempt to get insight into the statistical modelling of the fatigue process the RFC amplitude spectrum is considered. As a first step an appropriate distribution type to model the amplitude spectrum is chosen. Four two-parameters continuous distributions namely the Gamma, the Weibull, the inverse Gaussian and the lognormal distribution will be considered. For the estimation of the distributions' parameters a weighted maximum likelihood scheme will be employed in order to take into account the relative weight of different cycle amplitudes in the lifetime estimation. Furthermore, the parameters of the chosen distribution are modelled using the parameters describing the incoming flow and the system characteristics. This will be done via multiple regression method, not necessarily linear, depending on the form of correlation between the parameters of the chosen distribution and the external parameters.

#### 3.2.2 Rainflow Matrix Rating

If the rainflow matrix representation of a load quantity is directly obtained by on-line data reduction appropriate parameters describing the quality of the matrix have to be picked. In the framework of this project the following descriptive parameters have been adopted:

- matrix mean value  
equivalent to the center of gravity's position on the diagonal of the of the load cycle matrix.
- matrix rms value  
parameter rating the dispersion of the load cycle distribution
- matrix irregularity  
is defined by the number upwardly directed mean level crossings divided by the number of local maxima in a load sequence. This parameter rates the degree of *symmetry* of the load history with respect to its mean level (e.g. a load sequence that vibrates around the mean value will lead to an  $IR = 1$ ); In terms of RFC matrix shape  $IR$  says something about how the load cycle counts are distributed in the matrix with respect to the matrix mean value.  $IR=1$ : large numbers of counts are found around the matrix mean for varying amplitudes.
- matrix change parameter MCP[8]:  
MCP is a parameter sensitive to changes in the shape of the matrix. It is expected to become a constant when the matrix's shape stabilizes.

These parameters are calculated for each monitoring data set. Their relation to the inflow parameters is to be investigated during the measurement campaign. Special interest is also focussed on the MCP as it will serve as a measure for matrix validity.

#### 3.2.3 Normalised Load and Wind RFC Amplitude Spectra

There is a desire to find a general method by which the fatigue spectra, each obtained for different external conditions, can be standardized. Reversing the standardization will then enable to estimate the fatigue loading associated to any given set of parameters describing the changed external conditions.

Hans Bergström introduced and applied this approach on wind RFC spectra for different sites [9]. He normalized the range of each wind variation cycle with the standard deviation of the wind,  $\sigma_w$ , calculated for each one hour period. Encouraged by his promising results the same approach is adopted here to normalize measurements of blade root bending moments from the Alsvik data base as a test case. In order to assure validity as a scaling parameter the time period of one hour as a basis for standard deviation determination is maintained and start/stop events are excluded.

In case of the edgewise bending moment its variation is dominated by the sinusoidal effect of the gravitational bending moments, as the rotor rotates. In fact the sensitivity of the standard deviation in the edge moment to the external conditions is greatly diminished. In order to get around this problem the gravitational contribution to the edgewise bending moment has been excluded. After this is done, it's only the aerodynamical forces that has a contribution to the edgewise bending moment, and consequently, the calculated standard deviation will be affected by the stochastic nature of the wind instead of the deterministic gravitational force.

#### 4. FIRST MEASUREMENTS & EVALUATIONS

##### 4.1 Parameter Identification for Equivalent Load Range Representation

The parameter identification procedure was applied for all WT loading parameters. Figure 1 shows a sample sequence of 10-min time series records as used for this analysis.

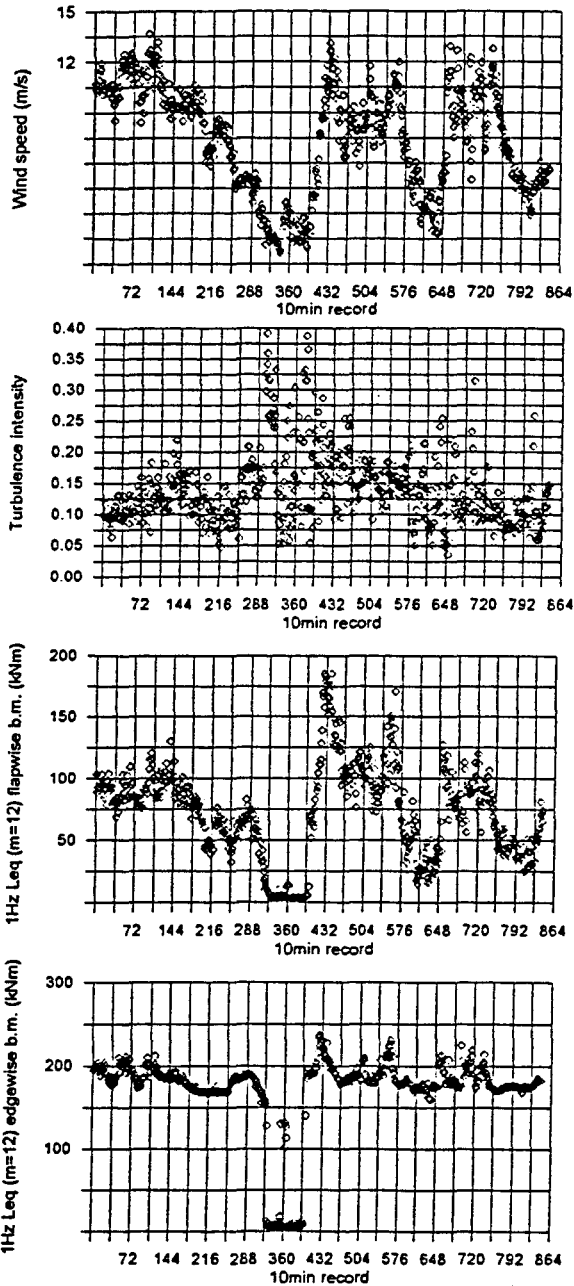


Figure 1. Measurement sample sequence of 10-min data sets

The results of the multivariate regression for the 1Hz flapwise equivalent load ( $m=12$ ,  $m$  being the slope of the chosen material S-N curve) are presented in figure 2. The chosen descriptive parameters are listed in table 2, where their basic statistics are included. It must be noted that the parameter increment, on which the dependence coefficients are estimated, equals to the standard deviation found in that table.

The following are the main conclusions:

- Fatigue is mainly governed by standard deviation of wind speed.
- The lateral and vertical turbulence ratios are imposing an additive effect on fatigue; these magnitudes are strongly connected to complex terrain characteristics.
- Mean wind speed appears as a strong parameter only in the high wind speed ranges.
- Wind inclination, wind shear, wind speed distribution magnitudes and length scale are imposing secondary effects.

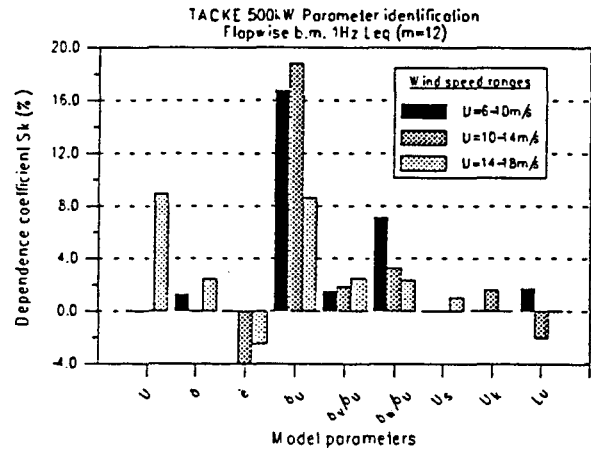


Fig 2: Dependence coefficients for 1Hz Leq of flap bending moment

Wind speed bin	U=6-10m/s		U=10-14m/s		U=14-18m/s	
Parameter	mean	SDV	mean	SDV	mean	SDV
Mean wind speed (U)	8,36	1,08	11,75	1,21	15,68	1,12
Wind shear exp. ( $\alpha$ )	0,072	0,061	0,094	0,038	0,085	0,036
Wind inclination ( $\epsilon$ )	-3,96	2,06	-1,75	1,51	-0,812	0,999
SDV wind speed ( $\sigma_U$ )	0,76	0,27	1,12	0,31	1,51	0,244
Lateral turb. ratio ( $\sigma_v/\sigma_u$ )	0,99	0,22	0,835	0,147	0,807	0,118
Vertical turb. ratio ( $\sigma_v/\sigma_u$ )	0,72	0,17	0,613	0,089	0,611	0,07
Wind sp. skewness ( $U_s$ )	-0,112	0,319	-0,325	0,277	-0,457	0,251
Wind sp. kurtosis ( $U_k$ )	0,062	0,54	-0,114	0,48	-0,098	0,49
Turb. length scale ( $L_0$ )	49,2	18,7	63,9	22,5	72,3	21,0

Table 2. Independent parameter variation.

##### 4.2 Matrix Rating

In the following an impression is given about the quality of data as it is acquired in the current measurement campaign. A complete data set consists of RFC matrices for all load quantities and the wind speed. Each day one such data set is read out from the DAS's memory. The idea is to continuously monitor the load quantities and to obtain snapshots of the actual status when reading out. Through subtraction of the data set of day N-1 from the data set of day N RFC matrices for each individual day may be obtained. Subsequently the matrix parameter as introduced above are calculated. Figures 3 - 5 depict the cumulative development of the flapwise blade root bending RFC matrix together with the matrix parameters.

M=112 kNm, IR = 0.349, RMS = 35,79 kNm, MCP=9474228

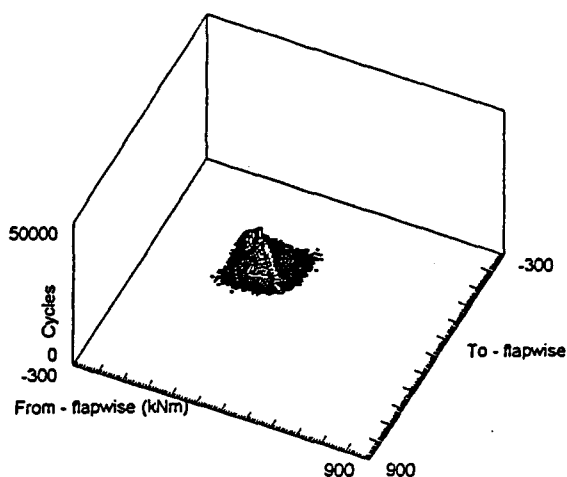


Figure 3: RFC matrix flap. bending moment, 3 days

M=121 kNm, IR = 0.297, RMS = 43.38 kNm, MCP=9799685

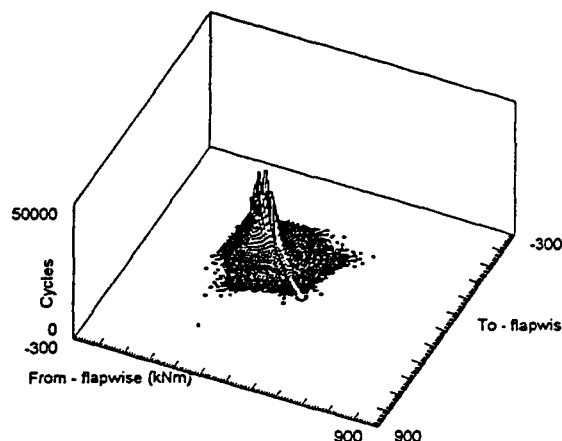


Figure 4: RFC matrix flap. bending moment, 11 days

M=102 kNm, IR = 0.235, RMS = 44.18 kNm, MCP = 5036108

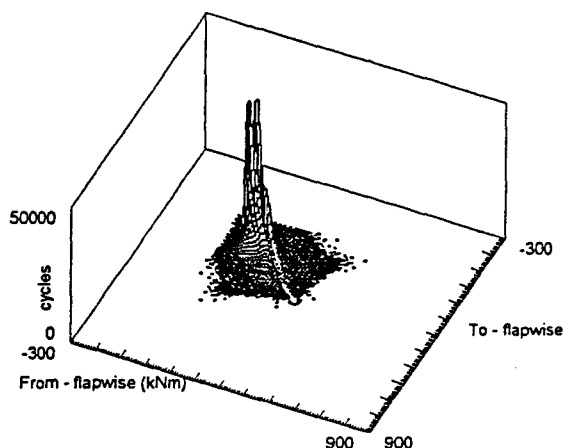


Figure 5: RFC matrix flap. bending moment, 21 days

It is expected that the RFC matrices stabilizes as time proceeds. Figure 6 shows developments of equivalent load and matrix rms for the flapwise blade bending moment and

matrix rms for the wind speed, each quantity normalized by its mean value. The observation time period is again 21 days and identical with that of the load RFC matrices in figures 3-5. As could be expected from the parameter identification exercise they behave in a similar way.

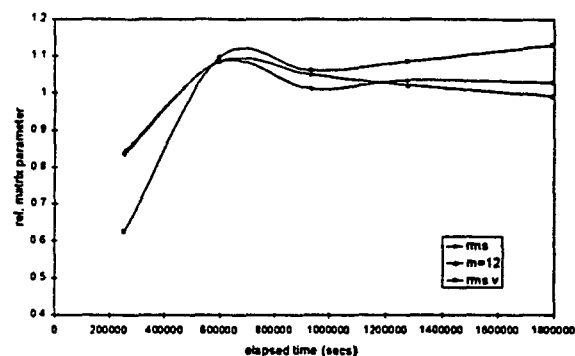


Figure 6: Relative RFC matrix parameter

However, the matrix change parameter MCP is not yet seen to stabilize. Once its value stay constant the matrix is believed to be stationary and thus representative.

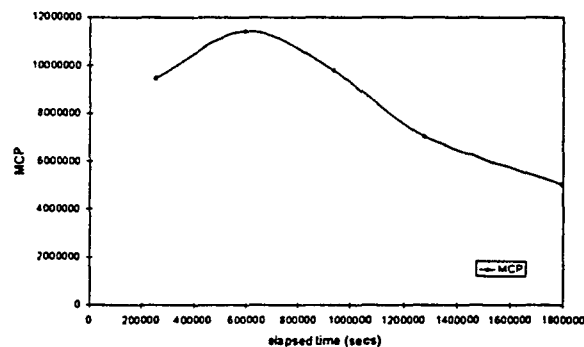


Figure 7: Matrix Change Parameter

#### 4.3 Normalized Load and Wind RFC Amplitude Spectra

Situations with and without wake operation have been studied. The qualitative effect of normalizing the load spectra is the same in both cases. This indicates that the load ranges scale on the load standard deviation in the same way, independently of the turbine operating in free or wake inflow. Figure 8 shows the flap load spectra for a period which includes wake effects making up for a complete measuring period of one day. Figure 9 depicts the spectra after normalisation. The standard deviation used for normalisation has been calculated for 1 hourly periods.

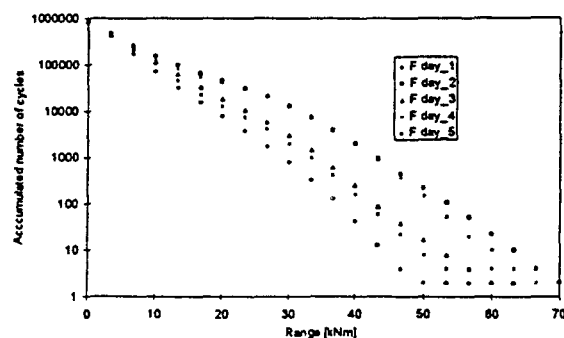


Fig 8: Flapwise load spectra. Each curve represents the

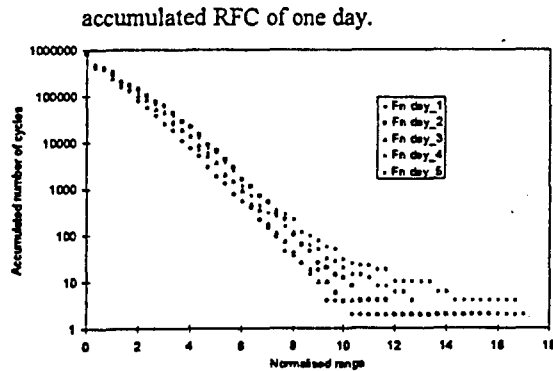


Fig 9: Normalised flapwise load spectra.

After the gravitational forces have been excluded from the edgewise moment, normalization of the edge moment works as good as normalization of the flap moment.

There is, however, a fairly large scatter in the normalised load spectra, indicating that there exist additional parameters having an effect on the spectra, not treated here. It is also possible that the amount of statistical data is to small, i.e. coincidence of the normalized spectra could be better if each curve had included sampled data for a longer period than one day.

The discrepancy is largest for the least frequent/high amplitude cycles, i.e. it is obvious that the standard deviation does not work well for the low cycle fatigue area.

#### 4.4 Low Cycle Fatigue Effects

An estimation of low cycle fatigue effects has been carried out by CRES and has been published in [10].

### 5. CONCLUSIONS

A statistical approach has been utilised for the parameter identification task. The parameters investigated describe the deterministic part of the wind, the main turbulent characteristics, the turbulence length scale as well as the wind speed distribution. The effect of the above parameters was captured and quantified.

Parameters describing the quality of RFC matrices have been adopted. The monitoring procedure has been started and the first data sets have been evaluated. The appropriateness of the chosen matrix parameter is indicated but as to the early stage of the measurements no conclusive statements can be made at this point.

Normalization of the RFC load spectra by the load standard deviation works well for the high cycle fatigue region. However, for cycles with low frequency and large amplitude there is a large scatter in the normalized spectra. Since the fatigue of the turbine is sensitive to these cycles, the method has to be further developed in order to be able to scale measured RFC spectra for changed standard deviations of the observed load quantity. Moreover, the standard deviation of the load quantity shall be mapped to the standard deviation of the wind speed in order to enable scaling of the load RFC with the wind standard deviation as a scaling parameter.

### 7. NOMENCLATURE

RFC = Rain Flow Counting

DAS = Data Acquisition System

### 6. REFERENCES

- [1] *Monitoring Fatigue Loads on Wind Turbines Using Cycle Counting Data Acquisition Systems*: final report for the Commission of the European Union, Directorate General XII for Science, Research and Development / Söker, Holger [ed.] ; Deutsches Windenergie-Institut <Wilhelmshaven> ; Flygtekniska Foersöksanstalten <Bromma> ; Centre for Renewable Energy Sources <Pikermi>. - Wilhelmshaven: DEWI, 1995. - (JOU-CT92-0175)
- [2] Matsuiski, M.; Endo, T.: *Fatigue of Metals Subjected to Varying Stress*: paper presented at the Kyushu district meeting of the Japan Society of Mechanical Engineers, March 1968.
- [3] Poppen, Maria; Dahlberg, Jan-Ake: *Fatigue Loads on Wind Turbine Blades in a Wind Farm* / Flygtekniska Foersöksanstalten <Bromma>. - Bromma: FFA, 1992. - (FFA-TN-1992-21)
- [4] Hinsch, Ch.; Westermann, D.: *Leistungskurvenvermessung mit Hilfe des Gondelanemometers*. DEWI-Magazin (1996) 8, p58-64
- [5] *European Wind Turbine Standards*: final report; vol.2 (Load spectra for wind turbine design) / Brüssel: EG, 1996. - getr. Zähl. - (JOU2-CT93-0387)
- [6] Mouzakis F., Morfiadakis E., Dellaportas P.: *Parameter Identification on Power Performance of Wind Turbines Operating at Complex Terrain*: 2<sup>nd</sup> EACWE, Genova, 1997.
- [7] Mouzakis F., Morfiadakis E., Fragoulis A.: *Complex Terrain Wind-WT Parameter Identification and Quantification*: Wind and - WT measurements, MOUNTURB final report (JOU2-CT93-0378), vol. II, 1996.
- [8] Reinke, Wilhelm: *Ein Beitrag zur Extrapolation von Wechselbelastungen aus zweiparametrischen Zählverfahren*. - Düsseldorf: VDI-Verl., 1988. - (VDI Fortschrittsberichte; 5, 151)
- [9] Bergström, H.; Ganander, H.; Johansson, H.: *Wind Description for Designing Weccs, Based on RFC Evaluated Wind Measurements*. In: Wind energy: technology and implementation; proceedings of the European Wind Energy Conference, EWEC '91, Amsterdam, The Netherlands, October 14-18, 1991. Amsterdam [u.a.]: Elsevier, 1991. - S. 762-766
- [10] Mouzakis F., Morfiadakis E.: *Identification of Low Cycle Effects on Wind Turbine Component Lifetime Estimation*. In: Proceedings of the BWEA'97 held at Edinburgh, July 16-18, 1997 [forthcoming]

### Acknowledgement

The work presented in this paper has been partially supported by the European Commission, DGXII Non Nuclear Energy Programme under contract nr. JOR3-CT96-0103.

The authors would like to express their thanks to Mr. Bädcker, private operator in Oldorf, Germany, Mr. Klug, Mr. Bruns and Mr. Frerichs from SW Emden as well as PPC in Greece.

Also the authors wish to thank TACKE Windtechnik and especially Mr. Siebers for their valuable contribution to the project work.

## Appendix 7

Tests and Design Evalution of a 20 kW  
Direct-Driven Permanent Magnet Gener-  
ator With a Frequency Converter

Anders Grauers, Ola Carlson, Erik Högberg,  
Per Lundmark, Magnus Johnsson, Sven  
Svenning





# TESTS AND DESIGN EVALUATION OF A 20 kW DIRECT-DRIVEN PERMANENT MAGNET GENERATOR WITH A FREQUENCY CONVERTER

A. Grauers\*, O. Carlson\*, E. Högberg\*, P. Lundmark\*, M. Johnsson\*\* and S. Svenning\*\*

\*Department of Electric Power Engineering, Chalmers University of Technology, S-412 96 Göteborg, Sweden

E-mail: ola.carlson@elkraft.chalmers.se. and anders.grauers@elkraft.chalmers.se

Phone: +46 31-772 16 37, Fax: +46 31-772 16 33

\*\*Pitch Wind AB, Fritslav. 34, 511 57 Kinna, Phone: +46 30216165

## ABSTRACT

This paper presents the tests and design evaluation of a 20 kW, direct-driven, permanent magnet generator with a frequency converter. The electrical system is designed for a gear-less wind turbine with a diameter of 14 m and a passive blade pitch system. The generator has an air gap diameter of 0.9 m, a stator length of 20 cm and a total weight of 610 kg. The main shaft and bearings are integrated into the generator design.

The results of the measurements and the theoretical evaluation show good system performance and high efficiency. It was also found that this direct-driven generator is more efficient than a conventional four-pole generator equipped with a gear.

## 1 INTRODUCTION

Despite the steady increase in the power rating of wind turbines up to the multi megawatt range, there is still an interesting market for small wind turbines up to about 20-30 kW. In developing countries these small wind turbines are applied in autonomous energy systems, while in the developed world an increasing interest can be noted for farms or individual homes.

The development of new permanent-magnet material and the reduction of the cost of power electronic components offer the opportunity to design cost-effective wind turbines with a direct-driven generator. However, the direct-driven synchronous generator needs damping, either with mechanical springs and dampers or, preferably, with an electrical damping, i.e., variable speed operation. By using direct-driven generators, which are optimized for low speed operation, the performance (efficiency, reliability) of the systems can be improved whilst the costs can be reduced. The assembly of the drive train is also simplified compared with a conventional drive train with gear and generator.

The tests and design evaluation of a 20 kW direct-driven generator with a frequency converter are reported in this paper. The direct-driven generator is connected to the grid via a frequency converter system. This electrical system allows a variable speed of the generator and turbine and it provides damping of the generator.

The generator, as well as the wind turbine, are designed and built by Pitch Wind AB. Laboratory tests of the drive train have been carried out at Chalmers University of Technology. The tests were performed within the whole speed and power range. On the basis of several years of design experience, the design of the generator is evaluated and performance is compared with

theoretical predictions. The evaluation focuses on generator voltage, resistance, inductance, losses and peak power.

## 2 THE WIND TURBINE

The wind turbine of Pitch Wind is equipped with a unique passive blade pitch control system. Figure 1 shows the wind turbine and Table 1 presents its data. Aerodynamic forces will automatically pitch the blades when the turbine reaches its nominal speed. With this system, together with a variable speed electrical system, it is possible to control the upper limit of the power in a very accurate way and no overshoot of the power will ever occur. This way of controlling the power is very seldom used. The passive blade pitch system also works as an emergency system which limits the maximum speed of the turbine in the event of loss of grid. The turbine blades are individually suspended in their own flap-regulation shaft joint, so that the turbine blades can freely move back and forth to permit flap action while in operation. Pitch Wind uses a tubular reinforced concrete tower. The tower is

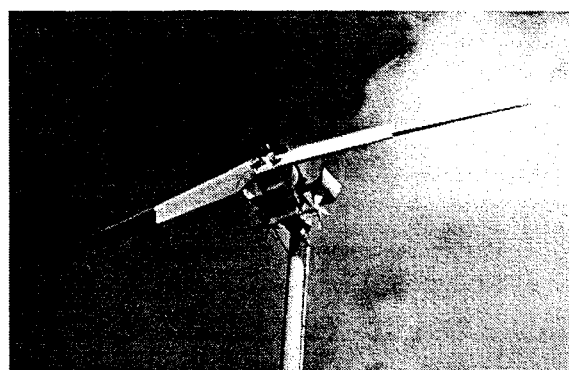


Figure 1. The Pitch Wind turbine.

Table 1: Main data of the wind turbine.

Rated power	20 kW
Turbine diameter	14 m
Number of blades	2
Hub height	30 m
Tower	Concrete

originally developed for high voltage line towers and it is made in large series. Because of the passive pitch control system the turbine needs no control computer, but there is a control computer integrated into the frequency converter.

The connection of the wind turbine to the grid can be made within the owner's local grid, i.e., on the owner's side of the electrical energy measurement equipment. At this point of connection, the grid is very weak and the risk for flicker disturbance is obvious. Since the wind turbine is equipped with a frequency converter for variable speed operation, there will be no power variations at rated power and only slow power variations below rated power. Consequently, this generator system will cause much less voltage flicker than a conventional generator system.

### 3 THE ELECTRIC SYSTEM

#### 3.1 The Generator

The generator is a permanent magnetized synchronous generator connected to the grid via a frequency converter. The generator is manufactured with NdFeB-magnets on the rotor. It has 66 poles and generates a three-phase armature voltage. The nominal speed is 75 rpm. The size and weight of the generator are as follows:

Active length of stator and rotor:	0.20 m
The internal diameter of the stator:	0.92 m
Air gap:	2.1 mm
Outer diameter:	1 m
Outer length:	0.4 m
Generator weight:	610 kg

A photo of the nacelle and the direct-driven generator is shown in Figure 2.

#### 3.2 The frequency Converter

The alternating current from the generator is converted into a dc current by a six-pulse diode rectifier. The diode rectifier is used because of its high efficiency, over 99 %, and its low cost. In order to smooth the dc current, an inductance (of 20 mH) is placed between the rectifier and the inverter. The dc-current is then converted to an alternating current of grid frequency by a three-phase thyristor inverter. The efficiency of this

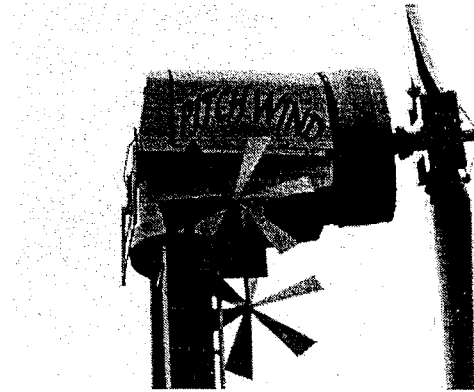


Figure 2. The nacelle and the direct-driven 20 kW generator.

type of inverter is high, more than 98 %, but the thyristor inverter will consume reactive power and produce current harmonics.

The power from the wind turbine is controlled by the control computer which is integrated into the thyristor inverter. The fifth harmonic in the grid current is filtered and the filter also produces reactive power to improve the power factor of the grid currents.

### 4 PERFORMANCES

The laboratory system and tests of the generator are reported in more detail in [1].

#### 4.1 Laboratory Set-up

Figure 3 shows the laboratory system. The generator is driven by a 40 kW dc machine. The nominal speed of the dc machine is 1500 rpm and therefore a gearbox of ratio 21:1 is mounted between the generator and the dc machine. The generator shaft speed and torque are measured, and thereby the input power. In addition the generator armature voltage, current and active power are measured by a three-phase power meter which measures the frequency of the voltage as well. The power to the grid is also measured with a second power meter.

During the tests the whole generator was hung on the generator shaft. Only a lever and a steel wire prevented the generator housing from rotating, see Figure 4. In this way, the shaft torque could easily be measured by a strain gauge, which measured the force in the wire.

#### 4.2 Results of Measurements

The impedance of the generator is very important, since it causes a voltage drop which limits the power of the generator. The armature resistance was measured to 0.54  $\Omega$ /phase. The inductance was estimated from the

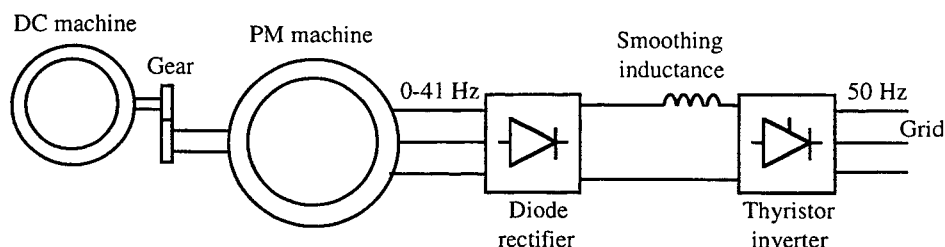


Figure 3: The laboratory system.

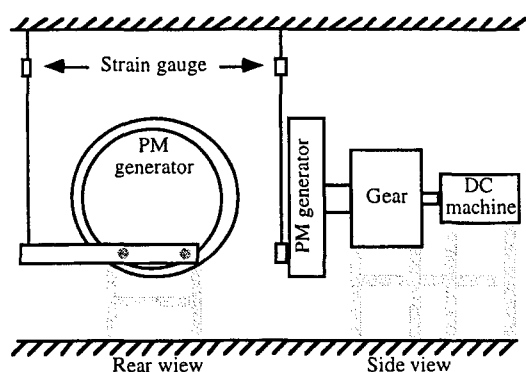


Figure 4. The laboratory set-up for measuring the generator shaft torque.

dc voltage-current characteristic to 7.0 mH/phase. Figure 5 shows the dc voltage and power as a function of the dc current at nominal speed. The power increases almost linearly with increasing current as the dc current increases from 0 to about 20 A. At high currents the voltage drop becomes so high, due to the armature impedance, that the power decreases. This drop limits the power. At 75 rpm the power maximum is 19.6 kW at a dc current of 74 A, for the generator prototype.

The maximum power of the direct-driven generator varies depending on which type of rectifier is used. If a transistor rectifier is used, the maximum power for this generator will be more than 50 % higher compared with the maximum power when a diode rectifier is used. The difference in maximum power is discussed more in [2]. The main reason for the higher power is the transistor rectifier's ability to provide the generator with reactive power to compensate for the internal reactive voltage drop in the generator. Of course, a transistor rectifier is more expensive than a diode rectifier.

The efficiency of the generator and frequency converter is only 86% at maximum power, but it is, which is more important, over 90% at part load. Moreover the efficiency is high at low power since the generator then operates at low speed. Figure 6 shows the efficiency as a function of output power for three different speeds.

The tested generator was the first prototype. To improve the performance, the series produced generator

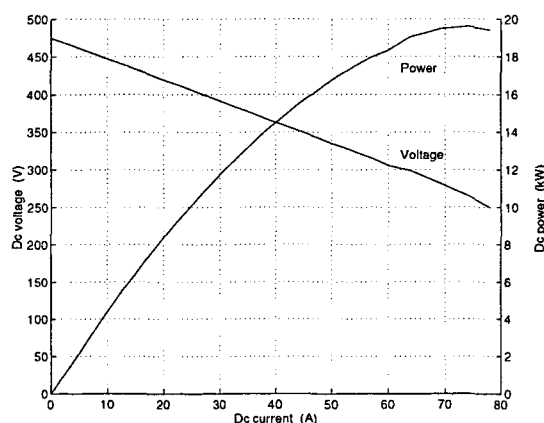


Figure 5. Dc voltage and power as a function of dc current at 75 rpm.

has been slightly changed. The air gap is reduced and the stator is longer, to improve the peak power of the generator. The generator will still be used for 20 kW rated power, however, copper losses will be reduced.

## 5 EFFICIENCY COMPARISON WITH A CONVENTIONAL DRIVE TRAIN

In this section, the energy efficiency of the direct-driven generator system is compared with that of a conventional fixed-speed direct grid-connected 4-pole induction generator with gear.

The direct-driven generator has much higher copper losses than a conventional four-pole generator, while the core losses are, instead, much lower. This difference makes the direct-driven generator less efficient than a conventional generator at rated load, but at part load it is, instead, more efficient. In Figure 7 the measured losses of the variable-speed direct-driven generator and its frequency converter are plotted. In the same diagram, the losses of the conventional induction machine and its gear are also shown. The Figure shows that the direct-driven generator system has lower losses than the conventional system below 13.5 kW input power.

To calculate the energy efficiency, the approximate power curve in Figure 8 is used. Since this wind energy converter is designed for low wind speed sites, a site with an average wind speed of 5 m/s has been considered to be typical.

The investigated wind energy converter, on a site with an average wind speed of 5 m/s, will stand still about 25 % of the time, because the wind speed is too low. It will operate 60 % of the time below 13.5 kW and only 15 % of the time above 13.5 kW. Because of this power distribution the direct-driven generator will lead to lower energy losses than the conventional system, since it has low losses at partial load. The annual energy efficiency, in Table 2, is calculated for both drive trains as described in [3]. Since the probability for different power depends on the average wind speed of the wind turbine site the energy efficiency also changes with site.

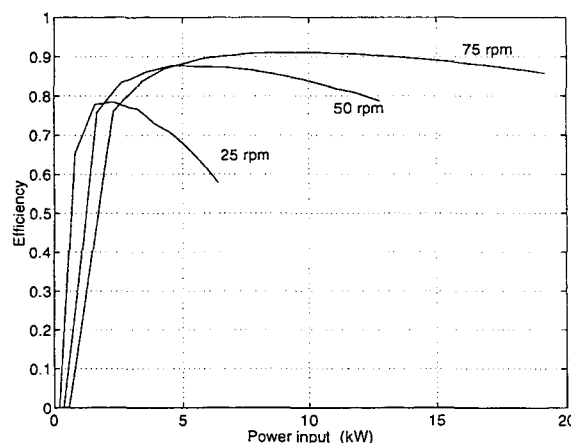


Figure 6. Efficiency of the generator and frequency converter.

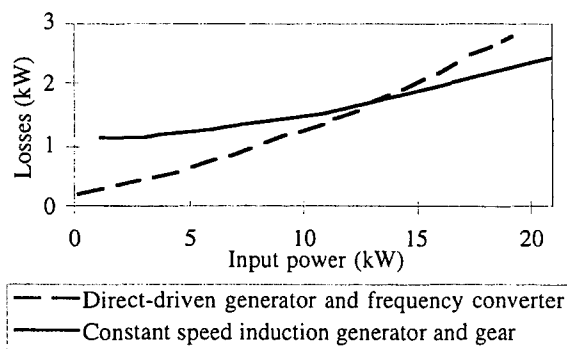


Figure 7. Losses of the generator systems as functions of input power from the wind turbine.

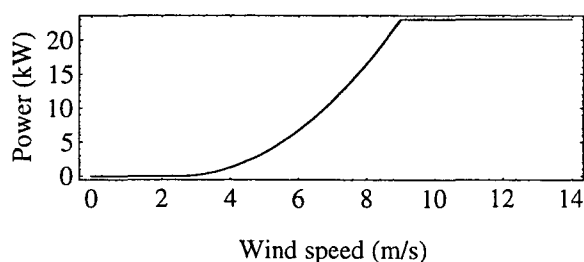


Figure 8. Approximate power curve for the 14 m wind turbine.

By using a direct-driven generator, instead of a conventional induction generator and gear, the drive train losses are reduced. The results in Table 2 show that this wind energy converter will produce approximately between 2 and 19 % more electricity since it is equipped with a direct-driven generator instead of a conventional drive train. The increased turbine efficiency caused by the use of variable turbine speed has not been included in these figures, since the same approximate power curve has been used for both drive trains. The different power curves for variable- and constant-speed turbines will make the difference between the systems even larger.

The energy efficiency of the induction generator system shown in Table 2 can be increased, since special designed low-loss induction generators can have lower losses than the standard induction machine assumed here. However, also the efficiency of the direct-driven generator system can be improved. If the direct-driven generator is designed for a forced-commutated rectifier it will on most wind turbine sites, almost certainly, have an energy efficiency which is higher also than that of a low-loss induction generator.

## 6 FURTHER DEVELOPMENT OF THE DRIVE TRAIN

The direct-driven generator used in the presented wind energy converter is very good. Still there is potential for further improvement. The size of the generator can be reduced significantly and the efficiency can be increased by designing the generator for a forced-commutated rectifier instead of a diode rectifier. A forced-commutated rectifier allows higher generator

Table 2. Approximate annual energy efficiency of the two drive trains at different sites.

	Average wind speed		
	4 m/s	5 m/s	6 m/s
Direct-driven gen. & frequency conv.	85.0 %	85.3 %	85.2 %
Induction generator & gear	71.5 %	80.0 %	83.3 %
Increased energy production for direct-driven gen.	+19 %	+6.6 %	+2.3 %

inductance and, therefore, the generator can be made with deeper slots for the windings. Deeper slots decrease copper losses and allow higher force densities in the air gap, leading to a smaller generator.

The thyristor inverter can be replaced by a transistor inverter which will reduce the grid current harmonics and improve the quality of the delivered power.

## 7 CONCLUSION

The results of the measurements and the theoretical evaluation show that the system with a permanent-magnet low-speed generator and a frequency converter has good system performance and high efficiency.

It has also been found that this direct-driven generator is more efficient than a conventional four-pole generator equipped with a gear.

## 8 ACKNOWLEDGEMENT

The authors would like to thank Mikael Alatalo for his valuable electrical design work with the generator. The financial support given by the Swedish National Board for Industrial and Technical Development and Elforsk is gratefully acknowledged. The authors would also like to thank Bo Lagerkvist for his valuable laboratory work.

## 9 REFERENCES

- [1] Högberg E. and Lundmark P. "Design and Test of an Electrical System for a Direct-Driven Permanent-Magnet Generator for a Wind Turbine" Göteborg, Sweden, Chalmers University of Technology, School of Electrical and Computer Engineering, M.Sc. Thesis No. 16E, October 1997.
- [2] Grauers, A. "Design of Direct-driven Permanent-magnet Generators for Wind Turbines". Göteborg, Sweden, Chalmers University of Technology, School of Electrical and Computer Engineering, Technical, Report No. 292, November 1996.
- [3] Grauers A. "Efficiency of three wind energy generator systems", IEEE Transactions on Energy Conversion, Vol. 11, No. 3, pp. 650-657, September 1996.

## Appendix 8

The Rating of the Voltage Source Inverter  
in a Hybrid Wind Park With High Power  
Quality

Jan Svensson



# THE RATING OF THE VOLTAGE SOURCE INVERTER IN A HYBRID WIND PARK WITH HIGH POWER QUALITY

Jan Svensson

Department of Electric Power Engineering, Chalmers University of Technology, S-412 96 Göteborg, Sweden

## ABSTRACT

A hybrid wind park consists of wind turbines which have different electrical systems: directly connected induction generators (IG) and variable-speed electrical systems. One of the variable-speed electrical systems has a voltage source inverter (VSI) connected to the grid, the others have grid-commutated inverters (GCI). The VSI can be used for reactive power compensation and active filtering, in addition to converting wind power. These additional features cause an increase of the VSI rating. The degree of over-rating depends on the wind park configuration. In a three-turbine wind park, consisting of an IG, a GCI and a VSI of equal rated active power, the rated current of the VSI becomes 1.33 pu for the rms-current comparison and 1.73 pu for the peak-to-peak current comparison. When a 5th-harmonic passive shunt filter is used to cancel the 5th harmonic current from the GCI and to produce the mean consumed reactive power of the wind park, the rated power of the VSI becomes 1.06 pu for the rms-current comparison and 1.2 pu for the peak-to-peak current comparison.

## 1. INTRODUCTION

The interest in the variable speed operation of wind turbines has increased in recent years because of the potential to improve the total wind turbine system performance. Usually, grid-commutated inverters (GCI), equipped with thyristors, are used on the grid side of the electrical system. The cost for these converters is rather low and the efficiency high. However, there are two problems associated with GCIs: low-frequency current harmonics are injected into the grid and the GCI consumes reactive power. Wind parks are often located in rural areas where the grid is often weak, i.e., the grid has a relatively low short-circuit power. A wind park connected to a weak grid will increase the voltage variations, and variable speed systems with GCI will also increase the voltage harmonic distortion. Today, these problems are solved by increasing the short-circuit power of the grid. Another solution is to equip all wind turbines with forced-commutated voltage source inverters (VSI), but the VSI costs more and has a lower efficiency than the GCI.

The benefits of all systems can be utilized by a hybrid wind park consisting of wind turbines which have different electrical systems: directly connected induction generators (IG) and variable-speed electrical systems. One of the variable-speed electrical systems has a VSI connected to the grid, the others have GCIs.

This paper deals with a hybrid configuration of a wind park, consisting of up to 3 turbines. The investigation is a continuation of [1], in which the focus was on reactive power compensation and the voltage level at the point of common connection (PCC). Here, the emphasis is on the rated current of the VSI when it converts active power and simultaneously operates as an active filter and a reactive power compensator. The rated active powers of the VSI, the IG and the GCI are assumed to be equal, and the total reactive power to the grid is set to zero to obtain a unity power factor. The required size of the VSI in different systems and operating modes is investigated.

## 2. THE SYSTEM CONFIGURATION

The hybrid wind park configuration is shown in Figure 1. The variable-speed systems use synchronous generators (SG) together with rectifiers. A 5th-harmonic passive shunt filter (PSF) is connected to the PCC.

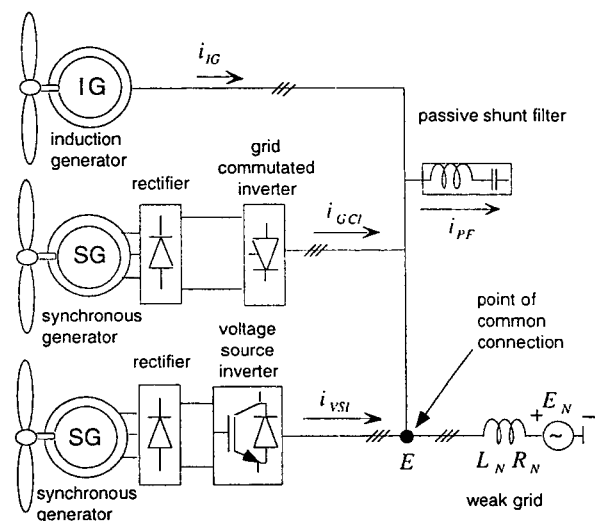


Figure 1: The hybrid wind park configuration.

For the variable-speed system with the GCI, two DC-link voltage control strategies can be used to control the SG. They are the constant flux mode (CF) and the optimal efficiency (OE) mode [1,2].

## 3. THE POWER QUALITY OF THE TURBINES

### A. Reactive Power

Since the reactive power consumed by the IG and the GCI cannot be controlled, the voltage level of the PCC will vary if the grid is weak. The two different control methods of the GCI will also affect the grid voltage differently. Figure 2 shows the reactive power of the IG and the GCI as a function of the active power. The units are in the process of consuming reactive power and delivering active power to the grid. For a typical 400 kW IG, the reactive power varies from approximately -0.26 pu to -0.46 pu. The reactive power of the GCI goes from 0 to -0.36 pu. The CF-mode has the largest reactive power span, from 0 to -0.46 pu. The reason for the different reactive power functions for the two types of GCI control methods is that the DC-link voltage is higher in the OE mode at intermediate wind speeds. The minimum advance angle of 20° is a trade-off between the DC-link voltage and safety margins of commutation failures.



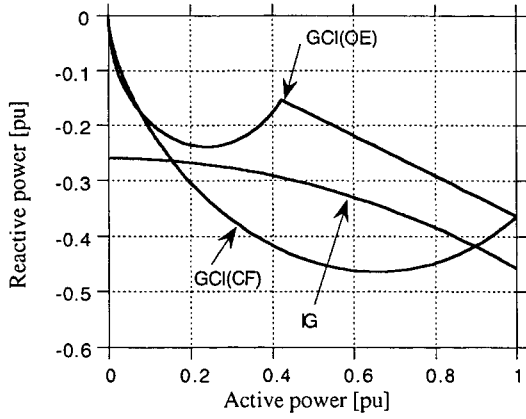


Figure 2: The reactive power (generator reference) as a function of the active power for the IG and the GCI. The GCI uses CF and OE modes.

The PSF produces a constant reactive power and is designed to deliver the mean reactive power consumed by the GCI and the IG, in the wind speed span from 0 to 1 pu. Due to the vector current controller of the VSI, the reactive power can be controlled independently of the active power.

#### B. Low-frequency Harmonics

The GCI produces low-frequency current harmonics with amplitudes dependent on the active power level. In the following analysis, the phase currents of the GCI will have a quasi square wave form due to a smoothing dc-link inductor [3]. Harmonics up to the 31st order are taken into consideration.

The vector-controlled VSI can act as an active shunt filter and cancel the current harmonics of the 5th, 7th 11th and 13th order. Furthermore, the VSI and its control system are assumed to operate ideally. Of course, active filters can cancel higher-order harmonics, but then the losses of the VSI increase.

#### 4. METHOD OF ANALYSIS

The required rated power of the VSI is analysed in various cases: when the VSI acts as an energy converter, a reactive power compensator, an active filter or as a combination of these acting modes.

The current rating of the VSI can be determined either by the rms-value or the peak-to-peak value of the current. For sinusoidal currents, the two methods result in the same converter rating. If the current from the VSI is distorted, the two methods will differ. Depending on the type of valves the VSI is equipped with, one of the two methods is more appropriate to use. The rms current of the VSI is a degree of total losses in the valves. Thus, the rms-current value of the VSI for non-sinusoidal currents can be compared with the rated sinusoidal current of a standard VSI. The peak-to-peak current value of the VSI should be used when the maximum current of the valves is the limiting factor. In this case, the peak-to-peak current of the VSI must be compared with the sinusoidal peak-to-peak current of a standard VSI. The most usual valves in medium-sized inverters are IGBTs. The IGBT does not have a maximum current limit, as the IGCT has [4], but the IGBT must be protected from overheating. Table 1 displays the maximum, minimum and the mean consumed reactive powers

for different wind park configurations together with the wind speed corresponding to the mean reactive power.

Table 1: The maximum, the minimum and the mean reactive power (generator reference) for different configurations. The wind speed varies between 0 and 1 pu.

Configuration	$Q_{\max}$ [pu]	$Q_{\min}$ [pu]	$Q_{\text{mean}}$ [pu]	wind speed [pu] corresponding to $Q_{\text{mean}}$
IG	-0.46	-0.26	-0.36	0.89
GCI(CF)	-0.46	0	-0.23	0.50
GCI(OE)	-0.36	0	-0.18	0.44
IG + GCI(CF)	-0.84	-0.26	-0.55	0.56
IG+GCI(OE)	-0.82	-0.26	-0.54	0.84

An example of the time variation of the currents is shown in Figures 3 and 4, when the wind park consists of a VSI, an IG and a GCI. The VSI operates as a reactive power compensator and an active filter in addition to active power generation. In Figure 3, the GCI current and the grid voltage for wind speeds of 0.7 pu and 1.0 are presented together with the grid voltage. The resulting VSI current and its fundamental component are shown in Figure 4. The peak-to-peak value of the VSI current at a wind speed of 1.0 pu becomes 1.73 pu, and the fundamental current component becomes 1.3 pu. Consequently, the active filter option requires a considerable increase of the rated current of the VSI.

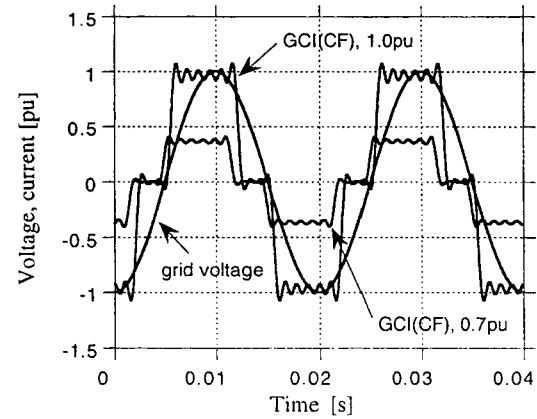


Figure 3: The GCI(CF) currents and the grid voltage for wind speeds 0.7 pu and 1.0 pu.

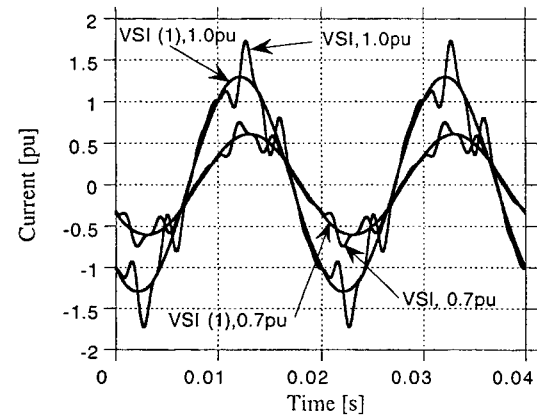


Figure 4: The VSI current and its fundamental component, VSI(1), for wind speeds 0.7 pu and 1.0 pu.

## 5. INVESTIGATED WIND PARK CONFIGURATIONS

Ten different wind park configurations were investigated as described in Table 2. Configurations A and F correspond to the active power production combined with the reactive effect compensation or active filtering. In configurations B to E, the VSI acts as an active filter and as a reactive power compensator. For the other variants (G to K), the VSI acts as an active power converter and the active filter and reactive power compensation modes alter.

Table 2: The different wind park configurations that have been simulated. The VSI compensates for the active power and/or reactive power and/or current harmonics.

Variant (and total active power)	VSI as active power converter	Reactive power compensated by the VSI	Orders of filtered harmonics
A (3 pu)	yes	IG, GCI	
B (1 pu)	no	GCI	5, 7, 11, 13
C (1 pu)	no	PSF, GCI	7, 11, 13
D (2 pu)	no	IG, GCI	5, 7, 11, 13
E (2 pu)	no	PSF, IG, GCI	7, 11, 13
F (1 pu)	yes		5, 7, 11, 13
G (2 pu)	yes	GCI	5, 7, 11, 13
H (2 pu)	yes	PSF, GCI	7, 11, 13
J (3 pu)	yes	IG, GCI	5, 7, 11, 13
K (3 pu)	yes	PSF, IG, GCI	7, 11, 13

## 6. RESULT EVALUATION

Table 3 presents the maximum rated current of the VSI for wind speeds from 0 to 1 pu for the wind park configurations described in Table 2.

Table 3: The maximum current of the VSI for the wind speed span 0 to 1 pu and for different system variants.

Variants	Maximum peak value [pu]		Maximum RMS value [pu]	
	CF-mode	OE-mode	CF-mode	OE-mode
A	1.30	1.30	1.30	1.30
B	0.74	0.73	0.52	0.47
C	0.47	0.47	0.28	0.27
D	1.13	1.12	0.88	0.87
E	0.56	0.56	0.34	0.35
F	1.10	1.10	1.04	1.04
G	1.38	1.38	1.10	1.10
H	1.17	1.18	1.03	1.04
J	1.73	1.73	1.33	1.33
K	1.20	1.20	1.06	1.06

### A. The RMS-Current Comparison

In this section, the rms-current comparisons of different wind park configurations are in focus. If the wind park consists only of a GCI and a VSI which acts as an active filter and reactive power compensator (B), the rated VSI size becomes 0.52 pu for the CF mode and 0.47 pu for the OE mode. The rms-current of the VSI as a function of the wind speed is shown in Figure 5. By introducing a PSF (C), the VSI size will be reduced to 0.28 pu and 0.27 pu for the CF-mode and the OE-mode, respectively. Furthermore, the OE mode of the GCI decreases the current of the VSI below the rated wind speed, as shown in Figure 5. The current reduction is important because the mean wind speed is lower than the rated wind speed of the wind power plants, and lower rms-currents result in a greater efficiency. If an IG is added to the wind park (D, E), the consumed reactive power is increased. It is obvious, according to Figure 6, that the use of the PSF is an advantage. The rated

current of the VSI is 0.87 pu without the PSF, and by using the PSF it decreases to 0.34 pu, a reduction of 61%.

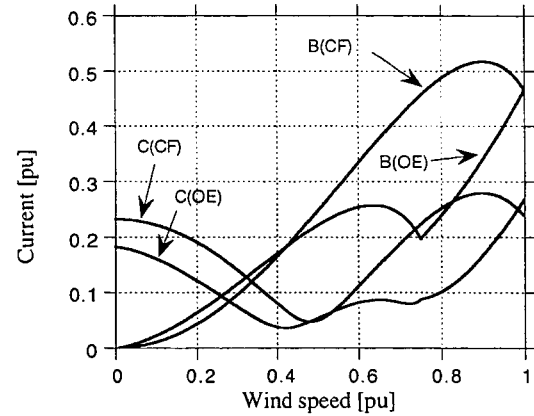


Figure 5: The rms-current of the VSI as a function of the wind speed. Wind park variants B and C are displayed.

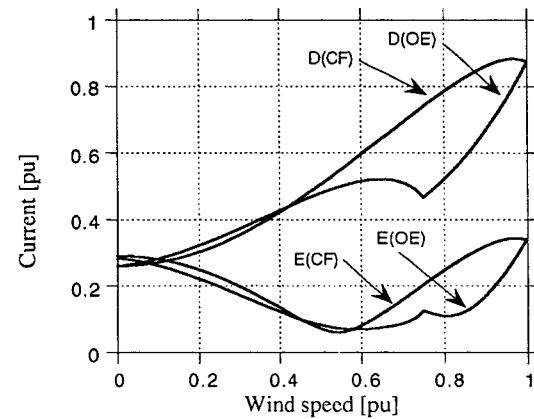


Figure 6: The rms current of the VSI as a function of the wind speed. Wind park variants D and E are displayed.

The complete wind park (variant K), consists of an IG, a GCI(OE), a PSF and a VSI. The VSI operates as an active power converter, an active filter and a reactive power compensator. The rated current of the VSI becomes 1.06 pu with and 1.33 pu without the PSF, according to Figure 7. When introducing the PSF, the VSI must consume reactive power at low wind speeds, because the IG and the GCI consume less reactive power than the reactive power produced by the PSF. The VSI current is thus higher at low wind speeds when the PSF is used. The crossing point for the VSI currents is at a low wind speed, approximately 0.1 pu in Figure 7. At low wind speeds the captured wind power is low, resulting in a minor current, and the losses become low or the turbines are shut off.

If a PSF is used, the IG does not influence the rated current of the VSI, as demonstrated in Figures 7 and 8. The addition of an IG increases the rated current of the VSI by 21% without the PSF but only by 3% with the PSF. Because of the almost constant reactive power demand of the IG, the current increase is low.

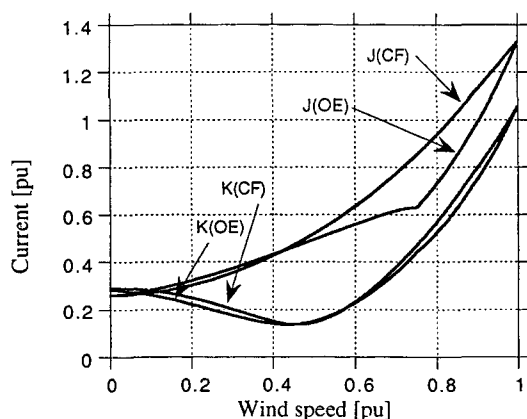


Figure 7: The rms current of the VSI as a function of the wind speed. Wind park variants J and K are displayed.

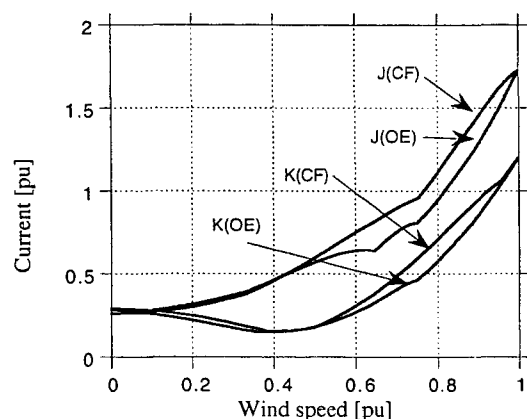


Figure 9: The peak-to-peak current of the VSI as a function of the wind speed. Wind park variants J and K are displayed.

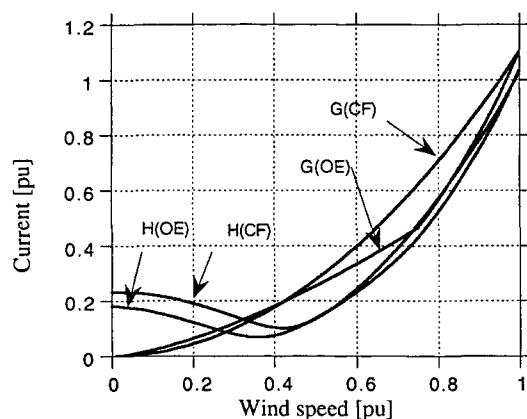


Figure 8: The rms-current of the VSI as a function of the wind speed. Wind park variants G and H are displayed.

### B. The Peak-to-peak Current Comparison

The results of the peak-to-peak current demand of the VSI in the different wind park configurations have almost the same characteristics as the rms-current demand. The peak-to-peak current is scaled up compared with the rms-current in the same wind park configuration. The result of the wind park variant K is shown in Figure 9. The VSI current increases by 13% when the peak-to-peak current method is used. The largest increase is 74% for the wind park variant C. As in the rms case, the OE mode of the GCI reduces the current above 0.5 pu wind speeds, and the use of a PSF results in a lower VSI.

## 6. CONCLUSION

In a hybrid wind park, the VSI can be used for reactive power compensation and active filtering in addition to converting wind power. These additional features cause an increase of the VSI rating. The degree of over-rating depends on the wind park configuration.

In a three-turbine wind park, consisting of an IG, a GCI and a VSI of equal rated active power, the rated current of the VSI becomes 1.33 pu for the rms-current comparison and 1.73 pu for the peak-to-peak current comparison. When a 5th-harmonic passive shunt filter is used to cancel the 5th harmonic current from the GCI and to produce the mean consumed reactive power of the wind park, the rated power of the VSI becomes 1.06 pu for the rms-current comparison and 1.2 pu for the peak-to-peak current comparison.

## 7. REFERENCES

- [1] Svensson, J., "Possibilities by Using a Self-commutated Voltage Source Inverter Connected to a Weak Grid in Wind Parks," 1996 European Union Wind Energy Conference and Exhibition, Göteborg, Sweden, 20-24 May 1996, pp. 492-495.
- [2] Grauers, A., "Synchronous Generator and Frequency Converter in Wind Turbine Applications: System Design and Efficiency," Chalmers University of Technology, School of Electrical and Computer Engineering, Göteborg, Sweden Technical Report No. 175L, May 1994.
- [3] Thorborg, K., *Power Electronics - in Theory and Practice*. Lund, Sweden: Studentlitteratur, 1993.
- [4] Gruening, H. E., Ödegård, B., "High Performance Low Cost MVA Inverters Realised with Integrated Gate Commutated Thyristors (IGCT)," 7th European Conference on Power Electronics and Applications (EPE'97), Trondheim, Norway, 8-10 September 1997. Proceedings, vol. 2, pp. 60-65.

## Appendix 9

Optimal Size of Wind Turbine Transformer

Åke Larsson



# Optimal Size of Wind Turbine Transformer

Åke Larsson M.Sc.

Department of Electric Power Engineering, Chalmers University of Technology, S-412 96 Göteborg, SWEDEN  
e-mail: ake.larsson@elkraft.chalmers.se, telephone: +46 31 772 1642, telefax: +46 31 772 1633

## ABSTRACT

During the past decade considerable efforts have been put into the efficiency of wind turbines. Almost every component in wind turbines has been the object of optimisation. Still, when it comes to grid connection the transformer is very often oversized.

In this paper the cost price of transformers is compared with the cost of transformer losses. The transformer losses are calculated from the wind probability curve and the power curve of the wind turbine. The temperature and thereby the lifetime of the transformer are calculated based on the IEC 354.

The results show that an optimal transformer kVA rating is 20% lower than the rated power of the wind turbine.

## 1 INTRODUCTION

During the past decade the efficiency of wind turbines has increased. Almost every component in wind turbines has been subjected to a technical and economic optimisation.

When it comes to connecting wind turbines to the grid, utility company or national regulations determine the transformer sizes. For example, in Sweden the recommended transformer size for a 500 kW wind turbine is 800 kVA [1]. It seems that other countries have similar recommendation. In papers from the UK, the Netherlands and the USA, where the generator and transformer data are given, the same pattern of over-sized transformer can be found [2][3][4]. It seems as if the rated power of the transformer is somewhere between 1.5 to 1.7 times the rated power of the generator.

Utility companies have a long experience of dimensioning transformers for transmission and distribution purposes. Since wind turbines have a power production unlike both transmission and distribution transformer loads, new dimension criteria must be derived. Hence, wind turbine transformers must, like all other components used in wind turbines, be chosen based on an optimal technical and economic basis. The technical optimum ought to be a transformer which can withstand the wind turbine load without forced ageing or at least having a lifetime greater or equal to the expected lifetime of the wind turbine. An economic optimum ought to be the lowest total price of the transformer, taking the cost of losses into account.

In this paper the cost price of transformers is compared to the cost of transformer losses. The losses for various transformers at a wind turbine site are calculated. The power production at the site is derived from the probability density of different wind speeds and the power curve of a wind turbine. In order to find the economic optimum of the transformer size, the cost of the losses are compared with the cost price of the transformer. Finally, to fulfil the technical optimum, the expected temperature and thereby the lifetime of the transformer is discussed in accordance with the International Standard IEC 354.

## 2 TRANSFORMER LOADS AND WIND TURBINE CHARACTERISTICS

When wind turbines are connected to the grid ordinary standard transformers are normally used. Transformers up to 2 500 kVA are called distribution transformers indicating their field of application. In a distribution network, the load normally consists of a base load and load peaks. The peak load appears during hours of high load demand on the grid. If a transformer feeds offices, the peak load will appear during working-hours. On the contrary, if a transformer feeds residential quarters peak loads will appear during the morning and during the evening.

### 2.1 Transformer Loads

When it comes to wind turbines the situation is quite different. Wind turbines do not have a load profile like ordinary distribution transformers. At a typical wind turbine site in Sweden, the wind speed is usually about half of the rated wind speed, see Fig. 1.

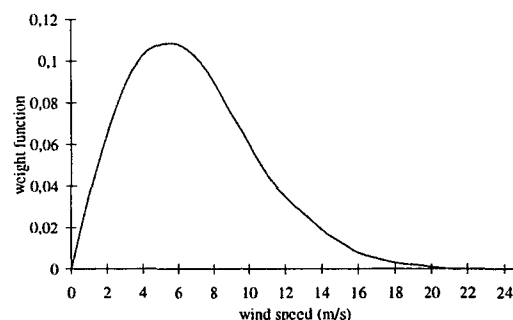


Fig. 1: The weighting function of wind speeds at the harbour in Falkenberg, Sweden.

In the figure, the weighting function of the wind speed at the harbour in Falkenberg, Sweden, is shown. Worth mentioning is that the wind speed at this location is typical for the west coast in Sweden. Normally, wind turbines produce rated power at wind speeds exceeding 12 m/s. As can be

seen in the Figure, only during a small fraction of time, less than 10% of the year, is the wind speed equal to or greater than 12 m/s. Hence, transformers used in wind turbines will only have a load equal to the rated power during less than 10% of the time annually. Most of the time the transformer will operate at only part load.

## 2.2 Wind Turbine Characteristics

Different types of turbines used in wind turbines have different power characteristics. The average value of the power output from a pitch regulated wind turbine is smooth and does not exceed the rated power of the generator.

Stall regulated wind turbines may, due to variations in the density of the air and imperfections in the aerodynamics, have a power output which sometimes is above the rated one. In the case of variations in the density, the cooling of the transformer will not be a problem. Over-production due to a high density of the air at a stall regulated wind turbine occurs at low temperatures. On these occasions, the transformer will also be better cooled by the ambient air.

As pertains to imperfections in the aerodynamics, the generator is protected from being overheated. The temperature of the generator in wind turbines is normally measured. Hence, in the case of over-temperature in the generator, the wind turbine is stopped. The generator is also normally more sensitive to over-temperatures than a transformer. This is due to a couple of hundred kilos of oil inside the transformer.

## 3 COST OF TRANSFORMER AND LOSSES

In order to choose a transformer based on economic criteria, the cost price of transformers must be compared with the cost of the losses.

### 3.1 Transformer Cost

The cost price of transformers is fairly linear. Fig. 2 shows the cost in ECU for different rated apparent power,  $S_n$ , for the same series of standard transformers manufactured by ABB.

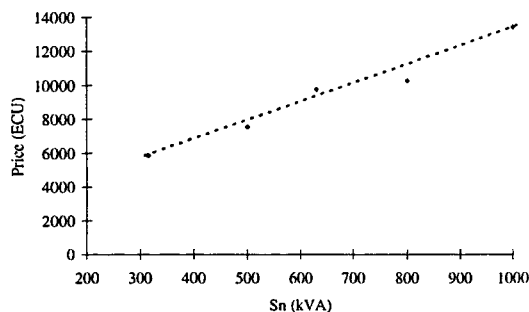


Fig. 2: Costs of different transformer sizes.

### 3.2 Transformer Losses

Transformer losses consist of two parts, iron losses and copper losses. The iron losses are also referred to as no-load losses and are due to the hysteresis loop in the iron core. The iron losses are proportional to the volume of the iron and constant for a given transformer provided that the voltage and frequency are constant. Since both the voltage and the frequency are fairly constant on a utility grid, the iron losses are also constant. Hence, a small transformer has smaller iron losses than a large one because of the amount of iron in the core. The iron losses are relatively small, considering that iron losses occur 8760 hours/year the total iron losses calculated over one year are considerable.

The copper losses are due to the current flow in the windings and are obtained by:

$$P_{cu} = 3RI^2 \Rightarrow P_{cu} = P_{cu, rated} \left( \frac{I}{I_{rated}} \right)^2 \quad (1)$$

where  $P_{cu, rated}$  and  $I_{rated}$  are the rated values given on the name plate of the transformer.  $P_{cu}$  are the copper losses for a given current  $I$ , and  $R$  is the resistance in the transformer windings. For a given apparent power, the current will be constant provided that the voltage is constant. As can be seen in Equation 1, if the current is constant a small transformer will have larger copper losses than a large one. Since the wind speed according to Fig. 2 is usually about half of the rated speed, the transformer benefits more from low losses at low power than it does from low losses at rated power.

Hence, the choice of transformer must be based on the balance between iron losses and copper losses, i.e., a small transformer in order to obtain low iron losses and a large transformer in order to obtain low copper losses. The total transformer losses as well as the iron and copper losses for different transformer sizes are plotted in Fig. 3.

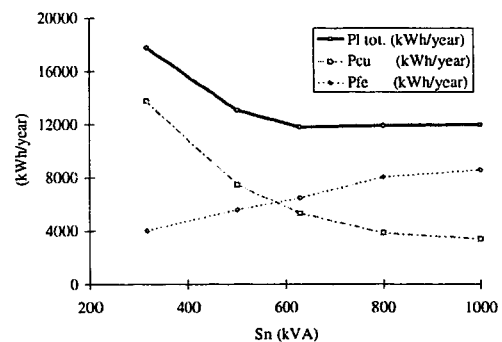


Fig. 3: Total, iron and copper losses, in the transformer.

The calculated losses in the figure are based on the power production of a 600 kW Vestas wind turbine placed on a site with a wind characteristic according to Fig. 1. The power production from the 600 kW wind turbine includes the active as well as the reactive power at different wind speeds.

As can be seen in Fig. 3, the iron losses,  $P_{Fe}$ , increase almost linearly with the transformer size. The copper losses,  $P_{Cu}$ , are decrease with the transformer size. The total losses,  $P_{Tot}$ , are kept at a minimum at a transformer size equal to the rated power of the wind turbine.

### 3.3 Cost Comparison of Price and Losses

As has been shown, a minimum of transformer losses is found at a transformer with a rated power equal to the rated power of the wind turbine. Following the Swedish recommendation, in the example with a 600 kW wind turbine, a transformer with a rated power of at least 800 kVA should be used. The increased cost price for an 800 kVA transformer compared with a 630 kVA transformer is 511 ECU. The 800 kVA transformer will also have increased losses of 638 kWh/year compared with the 630 kVA transformer. Consequently, the 800 kVA transformer will not be the most cost-efficient alternative.

In the case of a transformer with a rated power less than the rated power of the wind turbine, the losses will increase. However, the cost price of a smaller transformer is lower. A 500 kVA transformer costs 2 189 ECU less than a 630 kVA transformer. The 500 kVA transformer has 1 560 kWh/year higher losses than a 630 kVA transformer. In other words, a smaller transformer is less expensive but has higher losses compared with a transformer with a power equal to the rated power of the wind turbine.

In order to select the most cost-effective transformer an economic optimum must be found. The question is whether or not decreased losses will pay for the increased cost-price. One way is simply to calculate the annual cost of the transformer. The annual cost  $A$  of the transformer consists of the capital cost and the cost of the losses and can be expressed by:

$$A = CR + P_{Tot} E \quad (2)$$

where  $C$  is the cost price of the transformer,  $R$  is the fixed annual instalment,  $P_{Tot}$  are the total transformer losses and  $E$  is the electricity price. The fixed annual instalment is based on a 25 years of repayment at an interest rate of 5%. As can be seen in Eq. 2, the annual cost depend on both the rate and the electricity price.

The annual cost for different transformer sizes at different electricity prices are shown in Fig. 4.

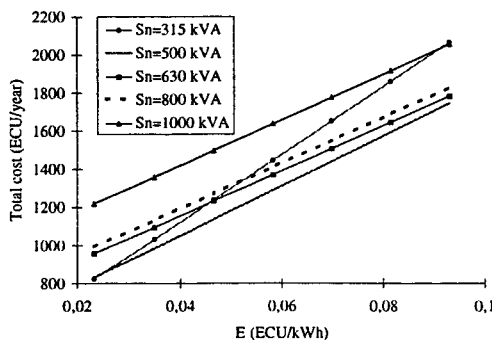


Fig. 4: The annual transformer cost in ECU at different electricity prices and at a rate of 5%.

As can be seen in the figure, although the 630 kVA transformer has the lowest losses the 500 kVA transformer is the most cost-efficient alternative. At least as long the electricity price is between 0.02 and 0.1 ECU/kWh. In the case of an electricity price below 0.02 ECU/kWh the 315 kVA transformer will be the most cost-efficient alternative. Worth mentioning is that the price for wind power generated electricity is approximately 0.046 ECU/kWh in Sweden today.

## 4 TRANSFORMER OVERLOAD AND LOSS-OF-LIFE CALCULATION

The remaining questions are whether or not it is possible to overload the transformer and if it possible to overload the transformer without jeopardising the expected lifetime.

### 4.1 Transformer Overload

At rated load and at an ambient temperature of 20°C the lifetime of a transformer is normally 30 years. Under these operating conditions the relative ageing is 1. According to the International Standard IEC 354 "Loading guide for oil-immersed power transformers" it is possible to overload a transformer. The IEC 354 stipulates that the normal cyclic loading not should exceed 1.5 times the nameplate rating on distribution transformers. The corresponding value for short-time emergency loading is 2.0 times.

Depending on the ambient temperature, transformers can withstand different degrees of overloading without high oil and hot-spot temperatures. Looking at the ambient temperatures present in Sweden and the rest of the northern part of Europe, a transformer will be able to withstand a loading of 1.2 times the rated power.

Tab. 1 shows hot-spot temperature and the relative ageing according to IEC 354 of a transformer at different ambient temperatures. The operating load is 1.2 times the rated power and the duration of the load peak is 24 hours. As pertains to high oil or hot-spot temperature the relative ageing will exceed 1. Note that the hot-spot temperature should not exceed 140°C and the oil temperature should not exceed 105°C [5]. In the IEC, only the hot-spot temperature is calculated. The hot-spot temperature has a quicker response due to load peaks compared with the oil temperature.

Tab. 1: Hot-spot temperature and relative ageing at a load of 1.2 times the rated power

Ambient temp. (°C)	20	0	-20
Hot-spot temp. (°C)	121	101	81
Rel. ageing (times)	15	1.5	0.15

As can be seen, a transformer can withstand a load of 1.2 times the rated power, even at an ambient temperature of 20°C but with a high relative ageing as a result. At lower temperatures the relative ageing declines quickly. At higher loads and an ambient temperature of 20°C the hot-spot temperature will increase quickly with loss-of-life as a



result. The relative ageing will be lower than what is shown in Tab. 1 if the transformer is placed outside and if the wind is blowing. As we all know very well, high power from wind turbines only occur during high wind speed conditions.

#### 4.2 Loss-of-life calculation

If a transformer is overloaded or if the ambient temperature is too high, the oil temperature will also be high. For transformers designed according to the IEC 76, the relative rate of thermal ageing is taken to be equal to unity for a hot-spot temperature of 98°C. The relative ageing is defined as:

$$V = \frac{\Theta_h}{\Theta_{98^\circ\text{C}}} \quad (4)$$

where  $\Theta_h$  is the ageing rate at the actual hot-spot temperature and  $\Theta_{98^\circ\text{C}}$  is the ageing rate at 98°C. The loss of life caused by month, days or hours of operation at a hot-spot temperature of 98°C is expressed in normal months, days or hours. If the load and the ambient temperature are constant during the period, the relative loss of life is equal to  $V \times t$ ,  $t$  being the period under consideration. The same applies if a constant operating condition and a variable ambient temperature are used. Generally, when operating conditions and ambient temperature change, the relative ageing rate varies with time. The relative ageing or loss-of-life over a certain period is equal to:

$$L = \frac{1}{t} \int_{t_1}^{t_2} V dt \text{ or } L = \frac{1}{N} \sum_{n=1}^N V \quad (5)$$

where  $n$  is the number of each interval and  $N$  is the total number of equal time intervals. For example, if a transformer has a relative ageing of 1.5 times during 1 hour and 0.9 times for 5 hours the relative ageing will be:

$$\frac{1 \times 1.5 + 5 \times 0.9}{6} = 1 \text{ times.}$$

In other words, in this example the transformer will not have any forced ageing.

As concerns transformers for wind turbine operation there are some factors which would make it possible to overload the transformer.

- during the time wind turbines work at part load (which is most of the time) the relative ageing will be much lower than 1.
- during the hours the wind turbines are at a standstill the relative ageing will be 0. Since the hours per year when wind turbines are at a stand still or produce below rated power are many times the hours with rated power, the total relative ageing will not exceed 1.
- during the time wind turbines produce rated power, the wind speed is at least 13-14 m/s. At these wind speeds, the transformer will be better cooled due to increased ventilation.
- during the cold winter season in Sweden 70% of the yearly amount of wind blows. At that time of the year, the ambient temperature is very often below 0°C.

- it is not reasonable to design the transformer for more than 25-30 years length of life.

## 5 CONCLUSIONS

The choice of transformer rating should be made based on cost price of transformer, cost of losses and length of life calculation.

The transformer should clearly not be larger than the rated power of the wind turbine.

A 20% smaller transformer will be more economic and it is not likely that it will have a length of life shorter than 30 years.

## 6 REFERENCES

- [1] Dimensioneringsrekommendationer för anslutning av mindre produktionskällor till distributionsnätet (DAMP), Svenska Elverksföreningen, 1994, (in Swedish).
- [2] Newton, S.C., Clark, N.R., "Power Quality Measurements on a 500 kW Variable Speed VAWT", *Wind Energy*, SED-Vol. 14, 1993, p. 149-154.
- [3] Looijesteijn, C.J., "Disturbances in Electrical Supply Networks Caused by a Wind Energy System Equipped with a Static Converter", *Proceeding of the BWEA 5*, Reading, Berkshire, U.K., 23-25 March 1983, p. 303-317.
- [4] McCrea A., Jenkins N., "Experience of a 300 kW Wind Turbine on an Extended 11 kV Network", *Proceeding of a BWEA/RAL Workshop*, Qxfordshire, U.K., June 1993, p. 1-12.
- [5] International Electrotechnical Commission, IEC 354, "Loading guide for oil-immersed power transformers", 1991.

## Appendix 10

Continuous Yaw-Control for Load Reduction

Tommy Ekelund



# CONTINUOUS YAW-CONTROL FOR LOAD REDUCTION

Thommy Ekelund

Address: Control Engineering Laboratory, Chalmers University of Technology, S-412 96 Göteborg, Sweden

## ABSTRACT

This work's objective is to investigate the potential of continuous yaw-control for active attenuation of structural dynamic load-oscillations. In two design examples various structural modes are studied. The tower lateral bending mode shows the best potential for active load reduction. The results also indicate the importance of considering the system's dependence on the angular speed and position of the rotor in the controller design.

## 1 INTRODUCTION

For maximum efficiency, the rotor should be directed towards the air flow. In medium to large sized wind-turbines alignment with the wind is predominantly achieved actively, with an electric or hydraulic yaw servo. However, the nacelle is mechanically parked most of the time. The servo is activated only when the mean relative wind-direction exceeds some predefined limits.

If the yaw parking mechanism is stiff, then large dynamic loads appear in its components and the tower. Therefore, it is often better to make it flexible, for instance, with mechanical suspension devices. An alternative is to use the yaw motor continuously, instead of parking the nacelle. The same dynamic behavior as with a spring and damper suspension can be obtained with feedback of the yaw angle. The disadvantage of this concept is the increased demands on the yaw servo. Continuous operation leads to increased wear, and the ratings of the motor, for example, the maximum torque and speed, may have to be improved. Furthermore, additional or improved measurements may be required.

However, continuous yaw control has more potential than merely substituting a spring and/or damper. It may also be possible to actively attenuate other structural dynamic oscillations, since the yaw motion is dynamically coupled with the tower and the blades.

The excitation of the structural dynamic modes comes from the wind turbulence and the periodic edgewise loads on the blades following from the revolution in a gravity field. The resultant periodic loads on the nacelle and tower are significantly smaller in case of three blades, due to the symmetry of the rotor. Therefore, the incentive for continuous yaw control is larger for turbines with two (or one) blades.

Very little seems to be done in this direction. There are some studies on yaw control for power regulation. However, here it is assumed that the rotor should be directed towards the wind. In [3] measurements are carried out on a Ø 5.35 m yaw controlled turbine in a 12×16 m wind tunnel. It is shown that feedback of the motor torque (hydraulic pressure) can improve the damping of the tower's lateral movements.

The intention of this study is to investigate the potential for active damping of structural dynamic loads by continuous

yaw control. For this purpose, we study a specific design case. As opposed to an earlier study, [2], the parameter values are based on a real plant, namely a Swedish 400 kW prototype machine [4]. Furthermore, the importance of the aerodynamic damping is also investigated. The work and the models presented here are reported in more detail in [1].

## 2 DYNAMIC MODELS

The analysis is based on a set of mathematical models of the plant. The equations of motion are derived with Lagrangian mechanics applied on two different models consisting of flexibly interconnected rigid bodies. The nonlinear equations are linearized, for analysis and design. If the rotor speed is assumed constant, the resulting system becomes periodically time-varying. In a dense matrix form the equations of motion can be stated as

$$\mathbf{M}(t)\ddot{\mathbf{q}}(t) + \mathbf{C}(t)\dot{\mathbf{q}}(t) + \mathbf{K}(t)\mathbf{q}(t) = \mathbf{G}(t)\mathbf{u}(t) + \mathbf{n}(t) \quad (1)$$

where  $\mathbf{q}(t)$  is a vector containing the degrees of freedom and  $\mathbf{u}(t)$  is the control input. The mass  $\mathbf{M}$ , damping  $\mathbf{C}$ , stiffness  $\mathbf{K}$  and input  $\mathbf{G}$  matrices all have a periodic dependence on time. The last term  $\mathbf{n}(t)$ , representing the excitation from the wind speed and the gravity forces, has stochastic as well as deterministic components. A natural state realization of the linearized system is

$$\dot{\mathbf{x}}(t) = \begin{bmatrix} -\mathbf{M}(t)^{-1}\mathbf{C}(t) & -\mathbf{M}(t)^{-1}\mathbf{K}(t) \\ \mathbf{I} & \mathbf{0} \end{bmatrix} \mathbf{x}(t) + \begin{bmatrix} \mathbf{M}(t)^{-1}\mathbf{G}(t) \\ \mathbf{0} \end{bmatrix} \mathbf{u}(t) + \mathbf{M}(t)^{-1}\mathbf{n}(t) \quad (2)$$

where  $\mathbf{x}(t) = [\dot{\mathbf{q}}(t)^T \mathbf{q}(t)^T]^T$

## 3 CONTROLLER DESIGN

In the following, the torque applied by the yaw motor is regarded as the control signal. This simplification is beneficial in this basic study, which merely aims at examining the potential of the concept.

The *primary* objective of the controller is to minimize structural dynamic loads, given a certain restriction on the

control torque. This constraint is considered since the achievable torque is limited. Furthermore, the control torque directly results in a torsion of the tower. The *secondary* objective is to keep the nacelle aligned with the wind direction. This is only important in a longer time scale, and has insignificant influence on the control signal variation during one single revolution.

The first and simplest method considered here is PD control of the yaw angle. The main reason for our interest in this configuration is that the dynamics are equivalent to a spring (P) and damper (D) in parallel, as in a mechanical suspension system. It also corresponds to the torsion in a flexible tower. Since both analogies are passive systems, it is referred to as passive control or passive system.

However, a controller based on a periodically time varying model ought to consider this dependence on time. Therefore, it is natural to use the LQ design method, which applies for such systems. As in time-invariant systems, the control law is obtained from a Riccati equation. The difference is the absence of a stationary solution in the same sense. Here we seek the stationary periodic solution, which is not derived as straightforwardly as its time-invariant correspondent.

The two main differences between the passive scheme and the LQ are that the latter is time varying and feeds back all variables in  $x$  (2). The PD controller, which is stationary, uses only information of the yaw motion. In practice it is not necessary to measure all state variables. One may use a state estimator. However, most likely, it is motivated to measure at least the motion that should be attenuated.

#### 4 TEETER ANGLE

The rationale for making a teetered hub is to reduce hub loads originating from the wind gradient; external loads result in teeter motion instead of internal loads. Nevertheless, there may be an interest in restraining the teeter motion. For example, there have been failures as a result of too excessive teeter motion [4].

Two main physical circumstances makes it possible to affect the teeter angle by the yaw motion. The first is the inertia of the rotor, with respect to the teeter axis. This coupling is strongest when the rotor is horizontal, that is, when the yaw- and teeter axes are parallel, and vanishes in vertical position. The second phenomenon is the gyroscopic torque, following from the rotation of the turbine being orthogonal to the applied yaw torque. The resultant gyroscopic torque is horizontal and perpendicular to the drive shaft.

Most of the LQ weight functions studied here are diagonal and time-invariant. The objective is chosen to keep the teeter and yaw motions as small as possible, and that the turbine should move in a reference plane orthogonal to the shaft.

The model we use here are of fourth order. The state variables are indicated in Figure 4.1, which shows an example of how the four elements of a control law vary during one turbine revolution. Note the difference between the periods of the yaw and teeter feedback. Since the yaw dynamics, due to symmetry, are periodic with 180° turbine

rotation, so is the feedback. Likewise, the teeter dynamics and the associated feedback gain are periodic with a full turn, due to the anti-symmetry of the rotor orientation after 180°. Therefore these gains change sign with a period of 180°, whereas the yaw feedback is strictly positive. This indicates that time-invariant feedback of the teeter angle is ineffective for teeter damping.

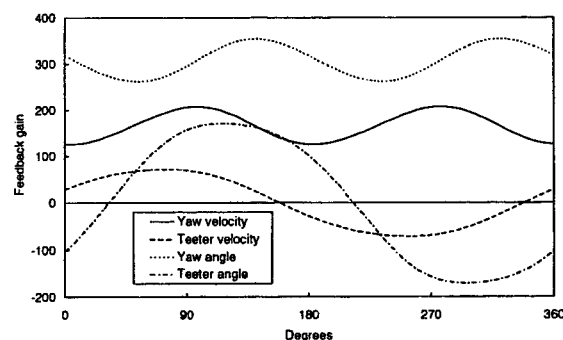


Figure 4.1 Periodic control law in case of no aerodynamic damping.

The improvement with the periodic feedback gain shown in Figure 4.1 is demonstrated in Figure 4.2. Compared with passive feedback, the improvement is striking. The passive concept only marginally changes the damping compared with a stiff yaw system, even though the parameters are chosen to increase the teeter damping. The improvement with LQ is achieved by means of larger yaw motion, which is altogether acceptable since this motion is not directly associated with any loads. The control torque is, in fact, significantly smaller with the periodic control law.

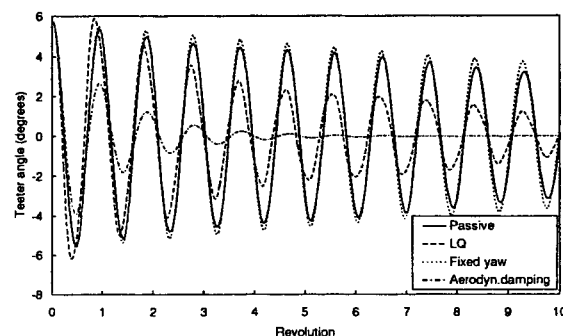


Figure 4.2 Impulse response of the teeter angle. Only the last curve, where the yaw is fixed has aerodynamic damping.

Although the control torque is important for the loads in the yaw mechanism and the tower torque, it is a poor measure of the actuator demands. A large torque can be achieved with a small motor, simply by using a large gear ratio. Therefore, it is more adequate to study the control power. Here, the power is limited to 1.5 kW.

Since there is a desire to minimize the control power, it ought to be included in the LQ cost function. However, this involves an essential difficulty. The power is the product of the yaw angular velocity and yaw torque. It has to be linearized, since the LQ methodology requires a linear expression. The problem is that the power has a saddle point in the operating point (the origin). Therefore, the partial derivatives with respect to speed as well as torque,

are zero. Hence, the linearized equation is identically zero, and consequently of no use.

The aerodynamic damping, which is a very important phenomenon, is not considered in the simulations discussed so far. Figure 4.2 shows that this damping is very significant for the teeter motion. Our results clearly demonstrate that the improvement achievable by yaw control is highly dependent on the amount of aerodynamic damping. Therefore, the potential for active attenuation depends on the blade characteristics as well as the mode of operation (for instance if the blades are stalled or feathered).

Next, we look at the response to a wind gradient. The applied wind speed corresponds to a constant wind speed that increases linearly with height. Here the LQ control law is modified, since the aerodynamic damping is included in the model. The the control law in Figure 4.1 result in a large yaw misalignment. This follows from the wind gradient creating a steady-state force, which strives to turn the nacelle aside. This error can be reduced. For instance, the weight on low control torque can be decreased a factor 100. This significantly increases the feedback gain of the yaw angle. Thus, the nacelle is kept in position by a large "spring constant". This is an inappropriate manner to compensate for a static torque-disturbance. The spring constant should be used for the dynamic response. What we need is merely a constant torque, balancing the above mentioned static side-turning aerodynamic force. Integral feedback of the yaw angle is the most obvious way to achieve this compensation.

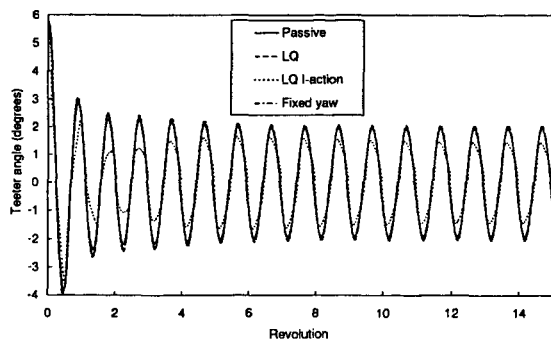


Figure 4.3 Teeter angle, impulse response with linear wind gradient. The passive controller has the same parameters as before.

Figure 4.3 shows that it is very difficult to reduce the teeter motion. Only the LQ controller including integral feedback manages to accomplish this to any noteworthy extent. However, the required effort, is very large, with exceptional demands on the controller bandwidth.

The above results show the problem in opposing the natural teeter motion originating from the wind gradient. It requires the gyroscopic torque to balance the flatwise force produced by the wind gradient. Furthermore, the gyroscopic torque works in the desired direction (parallel to the teeter axis) only during a small part of the revolution. On the other hand, we want the rotor to be self adjusting and level out load gradients. This is the reason for using a teetered hub in the first place. Therefore, the objective in the above example is slightly improper. Instead of forcing the rotor back to the plane perpendicular to the wind

direction, we ought to consider an alternative reference trajectory. One suggestion is to determine this trajectory from the mean periodic variation that follows from the external loads. In other words, we let the rotor self-adjust to some stable mean-path and then try to minimize the deviations from this path. Thus, one need to decide what should be regarded as natural steady-state motion versus transients. The former is determined not only by the wind field, it is also dependent on the yaw angle. Normally, the nacelle is directed straight towards the wind. However, it may be better to have a small misalignment so that, for instance, the plane of rotation is sideways perpendicular to the wind direction.

The conclusion from these results is that the potential for controlling the teeter angle is highly dependent on the aerodynamic damping. It is also evident that effective control for reduction of transient teeter-motion should consider the speed and angle of the rotor.

## 5 LATERAL BENDING

The interaction between the lateral bending of the tower and the yaw motion of the nacelle originates from the center of gravity, of the nacelle together with the turbine, not being placed on the yaw axis. As before, the LQ control law is derived with constant costs. It still seems pointless to use time varying cost functions. Furthermore, the integral of the yaw angle, rather than the angle and its velocity, is penalized. Figure 5.1, where state variables are listed, shows an example of the control law. The period of the gains being one half rotation follows from the symmetry of the two-bladed rotor. From the tower point of view, after a 180° turn the rotor is in an equivalent position. This symmetry also leads to gains that do not change sign, although there is a small exception in the feedback gain of the bending angle. Therefore, it is reasonable to assume that the damping can be improved by a constant control law.

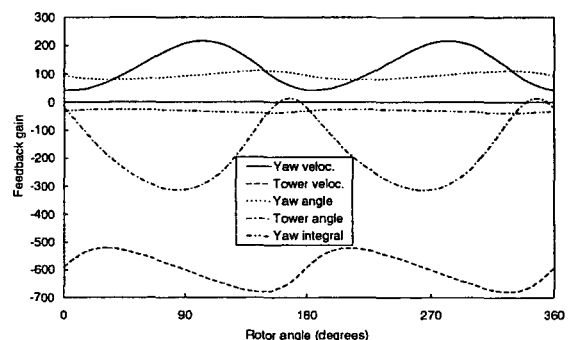


Figure 5.1 Control law with integral feedback of the yaw angle.

The impulse response in Figure 5.2 shows improved damping, both with a passive controller and the time varying control law in Figure 5.1. In all three simulations the aerodynamic damping is included in the model. However, the aerodynamic forces on the blades are much too small to have any significance on the heavy bodies in motion.

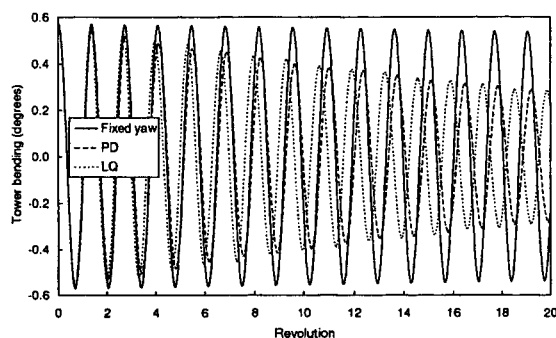


Figure 5.2 Impulse response with moderate control action.

Although the tower oscillation declines at equal rate with the two controllers, there is a distinct difference in phase. The passive system has approximately the same phase as the uncontrolled fixed-yaw system. This important difference represent two separate modes of oscillation, see Figure 5.3. The LQ controller uses the inertia of the nacelle and rotor in a dissimilar, more efficient, manner compared with the passive PD controller. The controller effort is less than 10 percent of the passive controller. The magnitude of the actuator power is, with the LQ feedback, comparable with the rated value of the present servo.

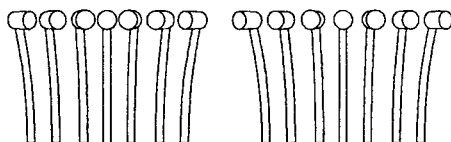


Figure 5.3 Illustration of the motion of tower and nacelle: left LQ, right PD.

A controller with less weight on the control effort attenuates the tower resonance faster. In the design of the LQ-controller above, the penalty on control torque was chosen by comparing the resulting control power with the rated value of the existing servo. The PD parameters are selected in order to accomplish the same tower damping as the LQ controller.

We can conclude that there is a potential for reducing the lateral tower-bending with continuous yaw control. Compared with the teeter motion, the aerodynamic damping is less important for the performance. It is also possible to improve the damping with a conventional PD controller. However, for effective attenuation, it is still preferable to feed back the rotational angle when deriving the control signal.

## 6 CONCLUSIONS

The main result of this study is, in general terms, improved understanding of the limitations and requirements associated with active damping of some structural resonances by continuous yaw control.

The lateral bending mode of the tower shows the best potential. This motion may even be reduced with a passive yaw system. However, the associated yaw torque is considerably smaller when the damping is achieved with

time-varying feedback and measurement of the bending motion.

The teeter angle is significantly more difficult to control. The reason is the aerodynamic damping, which makes the effort required to change the natural teeter motion very large.

None of the above results are conclusive, but it is reasonable to assume that the plant parameters have to change considerably to affect these basic results.

Considering the present results, the method of reducing structural dynamic loads by yaw control cannot be recommended as a standard solution. In some cases it may be advantageous, but it is not altogether clear which these are. Therefore, it is desirable to investigate how the system parameters affect the performance and the cost efficiency. One question arising from the results concerning the teeter motion is if there are any cases where the aerodynamic damping is sufficiently low to consider continuous yaw control. The aerodynamics are less important for the lateral tower-bending.

It is also of interest to explore the dependence on the mechanical system parameters. It is advisable in such studies to use the basic models applied here. The model order can presumably not be further reduced. However, the analysis can be clarified by normalization, which reduces the number of parameters.

The results are based on the assumption that the yaw torque is controlled. There is another interesting possibility for hydraulic yaw systems, namely to use a valve to regulate the hydraulic oil flow. This would be like controlling a viscous damping coefficient, or using time-varying derivative feedback. What makes this idea interesting is that no effort is put into the system. Thus, the ratings of the yaw motor can be lower.

## 7 REFERENCES

- [1] Ekelund T. (1997), *Modeling and Linear Quadratic Optimal Control of Wind Turbines*. Control Eng. Lab., Chalmers Univ. of Techn., S-412 96 Göteborg. Technical Report No. 306, ISBN 91-7197-458-x.
- [2] Ekelund T. (1996), *Yaw Control for Active Damping of Structural Dynamics*. Proc. Europ. Union Wind Energy Conference and Exhibition, Göteborg.
- [3] Ulén E. (1993), *Wind Tunnel Tests of a  $\varnothing$  5.35 m Yaw Controlled Turbine*. The Aeronautical Research Institute of Sweden, Report no: FFA TN 1993-20.
- [4] Vattenfall (1995), *Final report Evaluation of Lyse wind power station 1992-1995*. Vattenfall AB, 162 87 Vällingby, SWEDEN.

## Appendix 11

A New IEA Document for the Measurement  
of Noise Immission from Wind Turbines at  
Receptor Locations

Sten Ljungren





# A NEW IEA DOCUMENT FOR THE MEASUREMENT OF NOISE IMMISSION FROM WIND TURBINES AT RECEPTOR LOCATIONS

---

*Sten Ljunggren*

*Address: Dep. of Building Sciences, Kungl. Tekniska Högskolan, S-100 44 Stockholm, Sweden*

## ABSTRACT

A new IEA guide on acoustic noise was recently completed by an international expert group. In this guide [1], several practical and reliable methods for determining wind turbine noise immission at receptor locations are presented: three methods for equivalent continuous A-weighted sound pressure levels and one method for A-weighted percentiles. In the most ambitious method for equivalent sound levels, the noise is measured together with the wind speed at two locations: one at the microphone and the other at the turbine site. With this approach, the turbine levels can be corrected for background sound and the immission level can be determined at a certain target speed. Special importance is attached to the problem of correcting for background noise and to techniques for improving the signal-to-noise ratio. Thus, six methods are described which can be used in difficult situations.

## 1. INTRODUCTION

A starting point for the work of the IEA group has been the practice developed by local and national authorities for specifying limits for the noise from wind turbines. Such limits are usually expressed as an immission level, that is a level to be measured in a relevant noise sensitive area. Immission limits can, in principle, be verified by measurements in the same way as noise immission limits for other outdoor sources such as road traffic, aircraft, industries etc. However, a major problem when measuring noise immission from wind turbines is the presence of the wind. Another important factor is the fact that the immission levels specified by the authorities tend to be low. Thus, the background noise is often of the same order of magnitude as the sound level from the turbine, which makes reliable measurement results difficult to achieve.

An immission limit is usually specified for a certain wind speed at the turbine. However, that wind speed will never

occur during a measurement. For this reason, an interpolation scheme must be used.

In addition to the requirements on broadband sound, usually expressed as an equivalent sound level or an A-weighted percentile, the requirements often contain a penalty for audible tones. Such tones are defined in different ways in different countries. The presence of different methods is a severe drawback for an international industry, which prefers a single method.

Thus, a major part of the work of the IEA group has been devoted to these three issues.

## 2. MEASUREMENT OF EQUIVALENT SOUND LEVELS

According to the main method, the noise level is measured with a microphone at a height of 1.5 m above the ground together with the wind speed at the turbine

site and also close to the microphone. The instrument

configuration is illustrated in Figure 1.

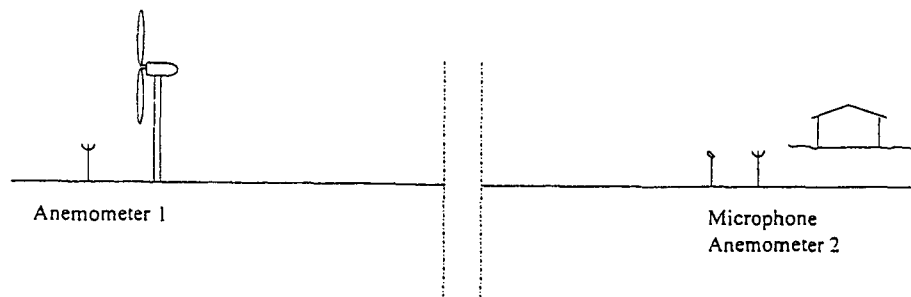


Figure 1. Illustration of instrument configuration for measurement of equivalent sound levels

The sound level is measured simultaneously with the wind speed at the two anemometer positions and averaged over the same time intervals (each interval 1 - 10 min, number of intervals  $\geq 10$ ). These measurements are carried with the turbine or turbines in operation. Before and/or after these measurements the background sound (with the turbine(s) parked) is measured and averaged over similar time intervals together with the wind speed at the microphone. It is now possible to plot the total sound level from the first measurement and the background sound alone as a function of the wind speed at the microphone, see Figure 2, and to determine the sound level from the turbine(s) alone.

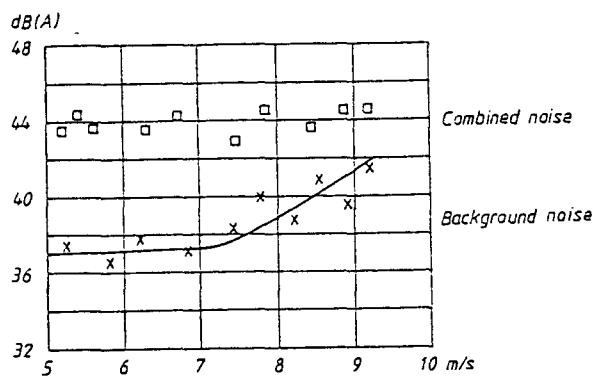


Figure 2. Plotting of combined sound level (sound from turbine(s) and background) and background sound level as a function of the wind speed at the microphone.

The level of the sound from the turbine(s) is finally plotted as a function of the wind speed at the turbine site, and the level at a target wind speed, often 8 m/s at 10 m height, is determined, see Figure 3.

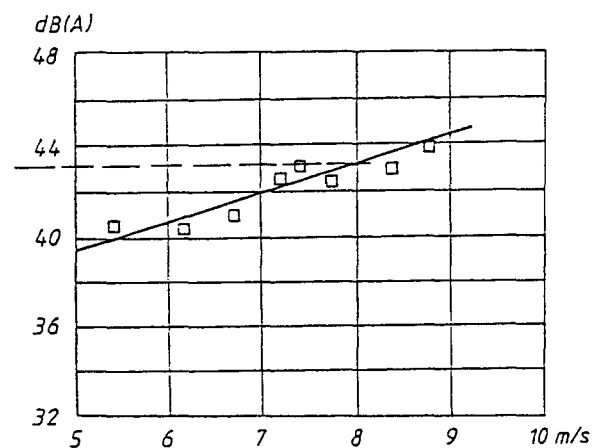


Figure 3. Determination of the turbine sound level at the target wind speed (here 8 m/s).

The measurement of the wind speed at the turbine site must be undertaken with caution. In the case of a single turbine, the speed should in the first place be obtained from an anemometer at hub height or from the electric output together with the power curve. If an anemometer is used, it should be placed according to Figure 4.

An anemometer at a height of 10 m and placed in front of the turbine tower can also be used.

In the case of a wind farm, the anemometer should be placed in a position which is relevant for the sound generation, see the two examples of Figure 5.

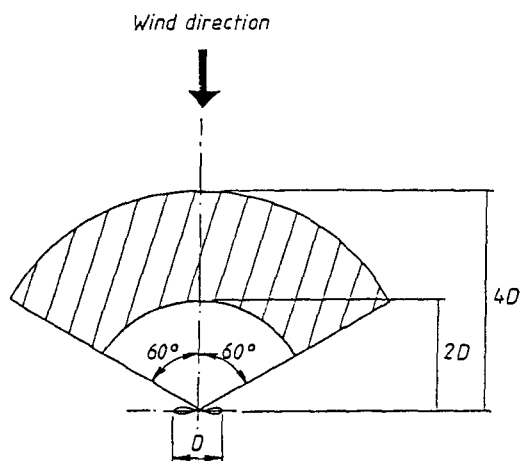


Figure 4. Recommended position of the turbine site anemometer for the case that the anemometer is positioned at hub height.  $D$  is diameter of wind turbine rotor.

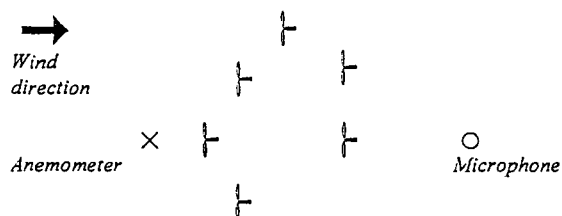
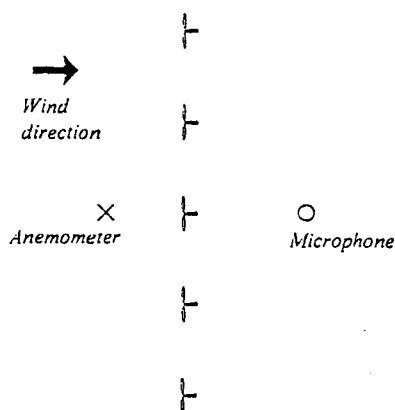


Figure 5. The upper part of the figure illustrates a case where the wind speed should preferably be measured at the closest turbine, while the lower part illustrates the case where the wind speed should be measured at an undisturbed position in the vicinity of the group of turbines.

Two methods, which are simplified with respect to the wind speed measurement, are also described in the document. The very limited use of these methods in practice is pointed out in the document.

### 3. MEASUREMENT OF A-WEIGHTED PERCENTILES

As an alternative to a measurement of an equivalent sound level, one or several A-weighted percentiles can be determined.

In this case, the sound from one or several wind turbine(s) is measured at receptor locations together with the wind speed, obtained from an anemometer positioned on a meteorological mast at the wind turbine or wind farm site. The background sound is also measured as a function of the wind speed obtained from the same anemometer. A procedure for obtaining a conservative estimate of the levels of the turbine(s) alone is described.

This method is used if the limits are expressed in percentiles and in particular where the noise immission limits are related to ambient sound measured previously at the receptor location. The technique is applicable for measurement of any A-weighted percentile. However, it should be noted that the percentiles  $L_{A10}$ ,  $L_{A90}$  and  $L_{A95}$  are the ones most often used in practice.

### 4. MEASUREMENT TECHNIQUES FOR CASES OF LOW SIGNAL-TO-NOISE RATIOS

Noise immission measurements around a wind turbine will often be influenced by background sound. If the equivalent sound level of the turbine together with the background is more than 3 dB over that of background alone, the level of the turbine can be determined directly. However, it is a common experience that the signal-to-noise ratio is lower. Then one or several of the following methods can be used:

- change of time of day for measurements from, for instance, day to night,
- repositioning of microphone to a position at the same distance and sound propagation conditions but with a lower background sound level,
- use of a secondary (and larger) wind screen,
- use of a large vertical measurement board, see Figure 6.

Two approximate methods are also described. One uses measurements at a lower wind speed together with a correction for the change in source strength. The other uses measurements at a reduced distance together with an appropriate correction.

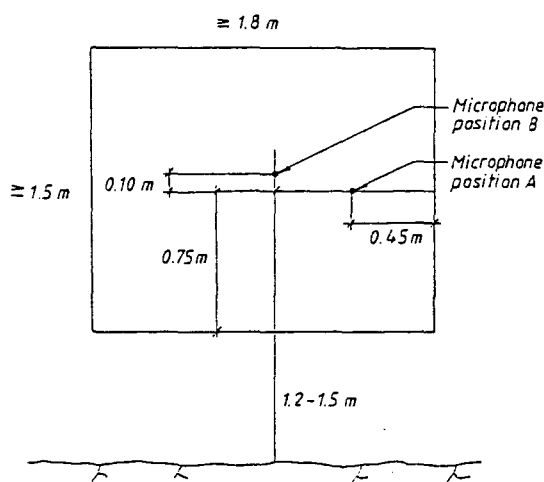


Figure 6. Position of the microphone on the large measurement board. Front view. Microphone position A is recommended when the board is used to reduce the influence from sources or reflecting surfaces shielded by the board. Microphone position B is recommended when the board is used to reduce the wind induced microphone noise.

## 5. EVALUATION OF TONES

Two methods are presented for the analysis of the tones. According to method I, at least five RMS spectra are obtained with a bandwidth of typically 2 - 5 Hz and an averaging time of 1 - 2 min. For method II at least 50

short term spectra are obtained with time weighting 'F' and an averaging time of 0.2 - 0.5 sec.

For both methods, the analysis of the tonality comprises four steps:

- identification of the lines in the spectra as either tones, masking noise or neither,
- calculation of masking level,
- calculation of tonal noise level,
- evaluation of tonality.

## 6. ACKNOWLEDGEMENTS

The IEA document [1] has been developed through a series of meetings with participants from different countries participating in the IEA R&D agreement. The members of the expert group have been:

Bent Andersen, Denmark

T. James Du Bois, USA

Nico van der Borg, Holland

Maurizio Fiorina, Italy

Helmut Klug, Germany

Mark Legerton, UK

Sten Ljunggren, Sweden

B. Maribo Pedersen, Denmark.

In addition, valuable information has been received from Jørgen Jakobsen, Denmark.

The work was partly founded by the EU commission under contract No JOR3-CT95-0065.

## 7. REFERENCES

- [1] S. Ljunggren (ed), Recommended Practices for Wind Turbine Testing. 4. Acoustics. Measurement of Noise Immission from Wind Turbines at Noise Receptor Locations (in print - the document will be available through the members of the IEA standing Committee).
- [2] O. Fégeant, Measurement of Noise Immission from Wind Turbines at Receptor Locations: Use of a Vertical Microphone Board to Improve the Signal-to-Noise Ratio. EWEC 97.

## Appendix 12

Measurements of Noise Immission from  
Wind Turbines at Receptor Locations: Use  
of a Vertical Microphone Board to Improve  
the Signal-to-Noise Ratio

Olivier Fégeant



# MEASUREMENTS OF NOISE IMMISSION FROM WIND TURBINES AT RECEPTOR LOCATIONS: USE OF A VERTICAL MICROPHONE BOARD TO IMPROVE THE SIGNAL-TO-NOISE RATIO

*O. Fégeant*

*Address: Dep. of Building Sciences, Kungl. Tekniska Högskolan, S-100 44 Stockholm, Sweden*

## ABSTRACT

The growing interest in wind energy has increased the need of accuracy in wind turbine noise immission measurements and thus, the need of new measurement techniques. This paper shows that mounting the microphone on a vertical board improves the signal-to-noise ratio over the whole frequency range compared to the free microphone technique. Indeed, the wind turbine is perceived two times noisier by the microphone due to the signal reflection by the board while, in addition, the wind noise is reduced. Furthermore, the board shielding effect allows the measurements to be carried in the presence of reflecting surfaces such as building facades.

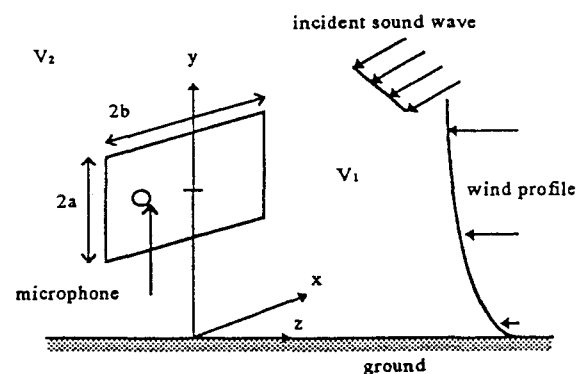
## 1 INTRODUCTION

Acoustical outdoor measurements are often made difficult by the action of the wind on the microphone system, the existence of ambient noise and the presence of scattering obstacles (building facades, etc.) around the measurement position as they contribute to lower the signal-to-noise ratio. Mounting the microphone on the surface of a rectangular vertical board is expected to be an efficient solution to improve it as the reflection by the rigid board adds 6 dB to the signal-to-noise ratio whereas the microphone is sheltered from the background sources located behind the plate. Furthermore, the wind velocity, viz. the pseudo-noise generation, is reduced at the microphone due to the blocking effect of the board on the flow.

Nevertheless, diffraction occurs at the plate boundaries, affecting not only the reflection of the incident noise but also the sheltering effect. This study was designed to evaluate the scattering effect of a board placed vertically above a ground as well as the wind noise generation.

## 2 DIFFRACTION EFFECTS

The board is oriented so that the microphone is mounted on the side facing the turbine, considered here as a point radiator. For any source located in the semi-infinite space  $V_1$  (Figure 1), the corresponding pressure at the microphone is the sum of the incident, the reflected and the diffracted fields.



*Fig 1. Description of the problem*



As the microphone is mounted on the rigid board, the reflected and incident pressure are equal, and this leads to a pressure doubling effect (+ 6 dB) while the diffraction effects are responsible for the deviation from pressure doubling.

### 2.1 Deviation from pressure doubling

The expression of the pressure at the microphone has been derived by writing the problem in its integral formulation and using the Kirchhoff's assumptions. The diffraction field appears then under the form of a sum of several integrals which might be evaluated asymptotically by the method of stationary phase as described by [1]. Thus, in the simplest case, i.e. at the centre of a square plate of half edge length  $a$ , the expression of the total field under normal incidence is given by:

$$\frac{p}{p_i} = 2 - \frac{2\sqrt{2}e^{i\frac{\pi}{4}}}{\sqrt{\pi}} \frac{e^{ika}}{\sqrt{ka}} + \frac{4i}{\pi\sqrt{2}} \frac{e^{ika\sqrt{2}}}{ka} \quad (1)$$

The first term at the right shows the pressure doubling due to the reflection, the second the diffraction by the edges and the third the one produced by the corners. It appears that diffraction depends only on the Helmholtz's number ( $ka$ ) and the bigger it is, the less the diffraction effects. Eqn.(1) also shows that the edges and the corners generate respectively cylindrical and spherical waves. Due to the simplicity of the solution obtained by the method of stationary phase, it is quite easy to obtain a presentation of the diffraction field over the board surface. Indeed, by computing eqn.(1) over the frequency range (100, 5000 Hz) sampled with a frequency resolution of 10 Hz, the standard deviation of the departure from pressure doubling may be calculated at each frequency and summed over all the frequencies. Figure 2 shows the result of such a simulation repeated for numerous board points. It appears that some positions minimise the diffraction effect and that, under normal incidence, the centre and the board axis of symmetry are maxima of diffraction. The position of the best minimum depends of course on the angle of incidence, the size of the board and the frequency range

of interest. For the sake of convenience, this point will be denoted  $M_{opt}$  in the rest of the article.

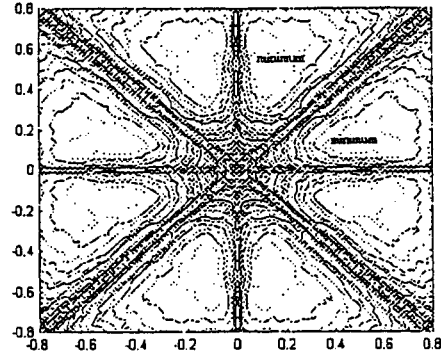


Fig 2. Standard deviation of departure from pressure doubling plotted over the board surface

### 2.2 Ground reflection

The ground induces reflection for both the acoustical waves launched by the turbine and by the diffracted field. Nevertheless, this latter is neglected due to its poor contribution and the scattering effects of the direct and reflected fields from the turbine may be assessed separately by considering two plane waves impinging on the board with different angles of incidence.

### 2.3 Sheltering effect

The microphone perceives only the diffracted fields of the sources located in the volume  $V_1$  and, thus, the shielding effect is also maximum at  $M_{opt}$  as the diffracted fields are equal on the two board sides. This effect is especially important when the measurement location allows reflections to occur from building facades situated behind the microphone. By considering a plane incident field impinging on one side of the board and its image by the board plane impinging on the other side, the shielding effect is defined as the difference between the sound pressure levels induced by both fields at the microphone. Figure 3 shows the result of a calculation made with an incident field composed of two non-correlated waves of incidences  $10^\circ$  and  $-10^\circ$  respectively impinging on a board of dimensions (1.8mx1.5m). It is observed that the sheltering is already 10 dB at about 150 Hz when the microphone is

positioned at  $M_{opt}(0.45, 0)$  while this effect, assessed at the centre is lower and more irregular.

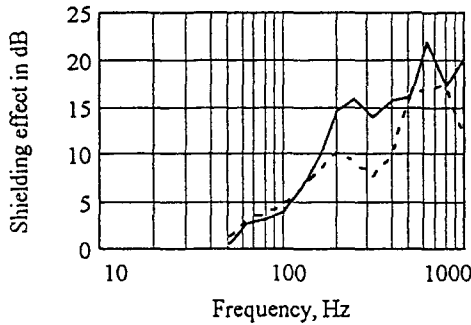


Fig 3. Shielding effect assessed at  $M_{opt}$  (—) and at the board centre (---)

### 3 WIND NOISE GENERATION

The wind noise arises from the action of the wind on the measurement system itself and is composed of a non-radiated aerodynamic noise due to the internal flow velocity fluctuations and of the near field aeroacoustical noise of the measurement system. According to previous studies [2][3][4], the first component is dominant in the wind and the second in a low turbulence rate oncoming flow.

#### 3.1 Flow description

As the flow passes the board, bands of vorticity are generated at the edges of the obstacle and, at some distance behind, they roll up and form the vortex street also called the wake [5]. In the windward, the flow velocity decreases as it approaches the board surface and even vanishes at the stagnation point which characterises a division of the stream. The pseudo-noise is then expected to be lower at this point compared to any other point of the board.

#### 3.2 Measurement description

Outdoor measurements have been carried out to provide an estimation of the attenuation given by the use of a board measurement system instead of a free microphone. They were performed in the neighbourhood of Stockholm in July 1996. The records were made with

two board sizes, (1.8m x 1.5m) and (0.9m x 0.75m) during the day and for wind velocities contained in the range (4m/s, 7m/s). The velocity is given at 1.5 m above the ground which is the board centre height. The pressure perceived by a microphone mounted on the board and sheltered by a 9.5 cm hemispherical windscreen is compared with the 'free microphone' value given by a microphone embedded in a 9.5 cm spherical windscreen. On the board, the microphone was located at the centre and at the point  $M_{opt}(0.45, 0)$ .

#### 3.4 Measurement results

It has been observed that the wind noise generation is strongly dependent on the board size, on the flow velocity and on the frequency of interest. Thus, it was straightforward to express it under the dimensionless form adopted by Strasberg [3]. And it has thus appeared that the measurements satisfy eqn.(2) with a standard deviation of 3 dB.

$$20\lg\left(\frac{p_{13}(f)}{\rho V^2}\right) = A + B \lg(St) \quad (2)$$

where  $p_{13}$  is the pressure in the third octave band  $f$  and  $\rho$  is the flow density.  $St$ , the Strouhal number, is defined by  $St = fD/V$  where  $D$  is a typical dimension of the board or of the windscreen and  $V$  is the flow mean velocity.  $A$  and  $B$  are two constants which vary with the measurement point. Finally, as expected, it has been observed that the gain is slightly better when the microphone is placed at the stagnation point.

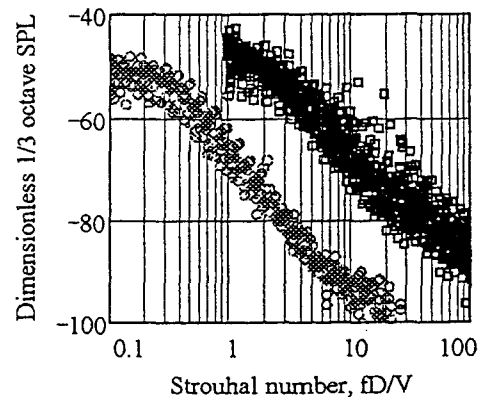


Fig 5. Outdoor dimensionless wind noise  
(o) Measurements with the free microphone  
(□) Measurements with the boards

Figure 6 shows the gain of signal-to-noise ratio obtained by using the board instead of the free microphone. It is seen that this gain is greater than 5 dB over the frequency range [20, 1000 Hz].

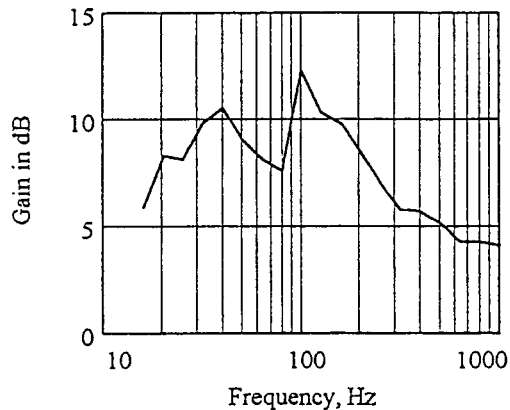


Fig 6. Gain of signal-to-noise ratio

#### 4 DISCUSSION AND CONCLUSIONS

Dimensionless laws giving the wind noise generation for both the board and the free microphone have been derived, allowing the results to be extrapolated to different board sizes or wind velocities. Nevertheless, these laws could have suffered from the influence of the short velocity range [4-7m/s]. It has been shown that the board should be placed normal to the wind direction in order to maximise its blocking effect. Then, a suitable microphone position on the board surface is the stagnation point, which may be located a bit over the board centre (about 10 cm) due to the logarithmic wind velocity profile. Both indoors and outdoors, it has been observed that the board measurement system might lead to a higher background level compared to the free microphone at middle and high frequency. It is difficult to conclude if it arises from the generation of pseudo-noise by the board, i.e. a high sensitivity to the flow turbulence, or if it is the consequence of the reflection of the background noise by the board. Anyway, the addition of 6 dB to the incident signal counteracts largely this negative effect and makes the board measurement system still interesting for improving the signal-to-noise ratio.

Concerning the diffraction effect, it has been seen that it might be reduced at suitable positions on the board surface. For those points, the sheltering for a board of (1.8mx1.5m) is greater than 10 dB above 150 Hz. Thus, this study shows that the use of a board is advantageous for outdoor measurements when one is dealing with low signal-to-noise ratios or with reflecting surfaces around the measurement location.

#### 5 ACKNOWLEDGEMENTS

This project was partly funded by Contract N° JOR3-CT95-0065 from the EU-commission and partly by Contract N° P1887-2 from the Swedish National Board for Industrial and Technical Development (NUTEK)

#### 6 REFERENCES

- [1] J.Stamnes, Waves in Focal Regions: Propagation, Diffraction and Focusing of Light, Sound and Water Waves. Adam Hilger, Bristol and Boston, 1986.
- [2] M.Strasberg, Dimensional analysis of windscreen noise. Journal of the Acoustical Society of America, 83(2) (1988) 544-48.
- [3] M.Strasberg, Nonacoustic noise interference in measurements of infrasonic ambient noise. Journal of the Acoustical Society of America, 66(5) (1979) 1487-93.
- [4] S. Morgan, R. Raspet, Investigation of the mechanisms of low-frequency wind noise generation outdoors. Journal of the Acoustical Society of America, 92(2) (1992) 1180-83.
- [5] A.Fage, F.Johansen, On the flow of air behind an inclined flat plate of infinite span. Proceeding of the Royal Society of London, A116 (1927) 170-97.

## Appendix 13

The Social Impacts of Wind Power

Karin Hammarlund



# THE SOCIAL IMPACTS OF WIND POWER

---

Karin Hammarlund  
Department of Human and Economic Geography  
School of Economics and Commercial Law,  
Gothenburg University  
S-411 80 Göteborg, Sweden

## ABSTRACT

This paper attempts to compress the multiplicity of perspectives often found under the denomination 'social aspects of wind power'. The main part of the research so far focus on opinion surveys. This paper outlines the main acceptance problems and sum up the acceptance situation in Sweden in comparison to Holland, Denmark, Germany and United Kingdom. Public acceptance is connected to public participation in the planning procedures as legally prescribed or in different ways enhanced. The study gives a general picture of how differences in planning practice and legal systems effects the acceptance of windpower. When the authorities give priority to other land use interests and treat wind power as a threat to recreational and environmental interests, it is obvious that policy concerning the use of a landscape contains alot of values and contradictions. I will try to provide you with some examples of this. The pros and cons of renewables will appear at different geographical and administrative levels. This result in a situation where immediate visual disadvantages will shade long term benefits of sustainable energy supply. We must begin to understand the social impacts of not accepting windpower. The benefits of renewables often require a global perspective in order to stress the fact that every energy system based on non renewable fules must come to an end. We do not need to argue about if it takes thirty, sixty or ninety years to complete these resources. Instead we now need a supreme effort to develop the best alternative energy system.

## 1 INTRODUCTION

Public relations are an important part of national programs for wind energy development. One aspect of public relations is to find out what people think about wind power relative to fossil fuels. Another aspect is to find out the public attitude towards a specific wind farm in the nearby environment. Public surveys concerning attitudes towards wind power have already been carried out, many in Britain, but also in the Netherlands, Denmark, Germany, Sweden and other countries.

Public acceptance of wind power can be looked on as a superfluous concern since the pros and cons are obvious. But are they obvious? Advocates of wind power do not understand why the effects of wind power on the landscape are more problematic than the effects of other constructions and development. So it seems that wind power can be harmless to some and a presumed disaster to others.

Opinion surveys in Europe show that acceptance of wind power development is more connected to the use of wind turbines than the aesthetic evaluation of them. Hence, one of the most important prerequisites for a positive experience of wind power is for the turbines to be in operation as much as possible. The visual impact of spinning turbines seem to be a central problem for planners but the practical solution for the public after siting.

I will discuss some of the social aspects of wind energy development and draw some general conclusions from different opinion surveys. Furthermore, I will discuss the use of public surveys. I will also discuss different ways of experiencing and making use of the landscape. This involves ideological contradictions manifested through legislation and planning procedures. Further, I will argue that the categorization of attitudes will help us to understand the makings of attitudes. Finally, I suggest that we look at the benefits of wind power, and understand the consequences of not accepting it as a renewable source of energy.

## 2. IDEOLOGICAL CONTRADICTIONS

### 2.1 The definition

Social stands for human society, its organization or quality of life [1]. Hence, the social aspects of windpower involve not only permit processing but also how it effects the quality of life of the people concerned. Competing perspectives on land use stem from the nature of land development plans and policies for conservation. It is therefore essential to clarify what values in a landscape we are trying to conserve and for whom.

### 2.2 The organization of society

The organization of society is held in place by different social institutions with a task in many cases to resist rapid change. This can be seen as a predicament when working with wind power development. Wind turbines result in a rapid visual change of the landscape in comparison to most constructions. It takes less than a day to erect a turbine extending 30, 60 or more meters up in the air. The effects are immediate.

In contrast, modern farming methods, and the large scale production systems they require, gradually alters the cultural landscape. Planners and the general public do not normally react to this type of gradual but extensive change. There is an explicit need to cultivate the land which prevents us from automatically questioning or discuss the aesthetic impacts of farming. There is however no explicit need for renewable energy yet.

### 2.3 The effects

In Sweden we have the unique "Allemansrätten" which gives the public recreational access to the countryside. In southern Sweden large grain fields prevent this access due to the fact that people can not just walk over the fields. This prevented access is not something that the public, living in this part of the country, thinks about. They usually do not stop to argue about long term visual, biological or other effects of modern farming methods.

There is no acute acceptance problem with the long term irreversible change of cultural landscapes caused by modern farming methods, pesticides or air pollution. Why then is there an acceptance problem with wind turbines,

even if the effects of wind power are quite reversible? The reason for this might be that it is easier to discuss something that is as immediately visual as one or many wind turbines. Also, the benefits of wind power to a public accustomed to a conventional energy system, based on fossil fuels (at what seems to be a rather low cost), are not yet apparent. Furthermore, nuclear power plants, strip-mining and waste-disposal often do not directly affect coastal areas of scenic beauty.

To protest against land use which has irreversible and wide spread long term effects requires an insight into these effects. Even specialists can fail to acquire such knowledge. To concentrate on the store of fossil fuels and how long they will last us might seem more beneficial than it is to recognize that every energy system based on non-renewable energy must come to an end.

These were a few examples of how we can look at or fail to recognize the environmental effects depending on:

- the visual evidence,
- the pace of change,
- the custom of use
- the accessibility of knowledge,
- and to a certain extent logical error.

## 2.4 The values

Environmental and cultural values are implicit in the landscape, but they become explicit through people. Consensus is difficult to achieve since we make use of the landscape in different ways. It is possible to group attitudes towards wind turbines according to what activity people are engaged in.

Farmers are dependent on rural survival and might look upon wind power as a contribution to their subsistence. Conservationists who wish to preserve existing rural landscapes and heritage might see wind turbines as a visual threat. Urban people who escape to their summer residence for recreation and recuperation might find the sound from wind turbines disturbing.

Local and regional planning authorities have a hard time stipulating the rules for what is to be seen as significant effects on the environment. The effects depend to a certain

extent on what we recognize as effects since nature can not speak for itself.

It is possible to diminish environmental effects through short term economic attractiveness. This is evident in today's energy system based on fossil fuels. In this context it may seem remarkable that renewables are not yet seen as economically attractive and advocates of wind power feel almost provoked when planning authorities and the general public speak about the environmental effects of wind power. Researches are trying to make the environmental costs (external costs) of fossil fuels explicit in order to promote the attractiveness of renewable alternatives.

It is easy to assume that wind turbines should stand a fair chance of being looked upon as environmentally acceptable. However, the benefits of wind energy often require a global perspective. The disadvantages of wind energy, on the other hand, are placed in a local setting where people experience visual and audible effects from wind turbines. The general attitude toward wind energy is however often found to be positive, and many wind enthusiasts would like to leave it at that.

I have chosen to study the makings of local opinion concerning wind turbines, in order to illuminate what other factors besides economic attractiveness makes it possible to view a wind turbine as something acceptable.



- M. Wolsink, The social impact of a large wind turbine, *Environmental Impact Assessment Review*, 32, 8 (4), pp. 301-312. 1988.
- M. Wolsink, Attitudes and expectancies about wind turbines and windfarms. *Wind Engineering*, 13 (4), pp. 196-206. 1989.
- K. Hammarlund, 'Havsaserad Vindkraft i Nogensund', Karlshamnsverkets Kraftgrupp/Sydskraft, 1990.
- K. Hammarlund, 'Varför satsar man på mindre och medelstor vindkraft i Sverige?', Intervjuundersökning kring privata satsningar på mindre och medelstor vindkraft. KVAB, 1992.
- AIM, Foreningen af Danske Vindmøllefabrikanter. Holdningsundersøgelse. Job nr. 6254, 1993.
- K. Hammarlund, 'Havsaserad Vindkraft i Nogensund', Karlshamnsverkets Kraftgrupp/Sydskraft, 1993.
- B. Young, Attitudes towards wind power A survey of opinion in Cornwall and Devon, ETSU/W/13/ 00354/ 038/REP, 1993.
- Wolsink, M., Sprengers, M., Keuper, a., Pendersen, T.H., Westra, C.A., Annoyance from wind turbine noise on sixteen sites in three countries. EWEC'93, Proceedings of an international conference held at Travemünde, Germany. pp. 273-276, Stephens & Associates, 1993.
- E. Esslemont, Cemnaes Windfarm, Sociological impact study: Final Report ETSU W/13/00300/REP, 1994.
- K. Bishop, A. Proctor, Love them or loathe them? Public attitudes towards wind farms in Wales. Report of research commissioned by BBC Wales, 1994.
- J. Jordal, Jørgensen, Samfundsmæssig værdi af vindkraft. Delrapport: Visuelle effekter og støj fra vindmøller - kvantificering og værdisætning. AKF, 1995.
- J. Munksgaard, A. Larsen, J. Jordal-Jørgensen, J. Rahlbæk Pedersen, Samfundsmæssig værdi af vindkraft. Delrapport 2: Miljømæssig vurdering af vindkraft. AKF, 1995.
- K. Hammarlund, Public Acceptance, Final Report: Evaluation of Lyse Wind Power Station 1992-1995, Vattenfall, 1995.
- [3] T. Hägerstrand, What about People in Regional Science, *Regional Science Association Papers*, Vol. XXIV, pp 7-21, 1970.
- [4] T. Hägerstrand, Landet som trädgård, in *Naturresurser och landskapsomvandling*, Rap. Bostadsdep. och FRN, pp 7-20, 1988.
- [5] A.H. Eagly, S. Chaiken, *The Psychology of Attitudes*, Harcourt Brace & Co, 1993.
- [6] S. Kaplan, R. Kaplan, *Cognition and Environment: Functioning in an Uncertain World*, Praeger N.Y., 1982.
- [7] J. Douglas Porteous, *Environmental Aesthetics: ideas, politics and planning*, Routledge, 1996.

## Appendix 14

Evaluation of the Nordic 1000 Prototype

Staffan Engström, Göran Dalén, Jan Norling



# EVALUATION OF THE NORDIC 1000 PROTOTYPE

Staffan Engström<sup>1)</sup>, Göran Dalén<sup>2)</sup>, Jan Norling<sup>3)</sup>, Anders Andersson<sup>4)</sup>, Göran Ronsten<sup>5)</sup>, Ulf Johansson<sup>6)</sup>, Natan Gothelf<sup>7)</sup>, Hans Ganander<sup>8)</sup>, Erik Rudolphi<sup>9)</sup>

1) Nordic Windpower AB, Box 968, S-191 29 Sollentuna, Sweden, Fax +46-8-754 99 17

2) Vattenfall AB, S--162 87 Stockholm, Sweden, Fax +46-8-739 55 62

3) Vattenfall Utveckling AB, S--810 70 Älvkarleby, Sweden, Fax +46-26-83670

4) Vattenfall AB, Box 88, S-620 20 Klintehamn, Sweden, Fax +46-498-489 164

5) FFA, Box 11 021, S-161 11 Bromma, Sweden, Fax +46-8-25 34 81

6) Vattenfall Utveckling AB, S-162 87 Stockholm, Sweden, Fax +46-8-739 60 76

7) Harmonizer Power Quality Consulting AB, Dalv. 57, S-141 71 Huddinge, Sweden, Fax +46-8-662 90 92

8) Teknikgruppen AB, Box 21, S-191 21 Sollentuna, Sweden, Fax +46-8-444 51 29

9) Ingemansson Technology AB, Box 47321, S-100 74 Stockholm, Sweden, Fax +46-18 26 78

## ABSTRACT

The Nordic 1000 is a 1000 kW two-bladed, horizontal axis, variable RPM stall controlled wind turbine. The project started in January 1993. The prototype was erected at Vattenfall's Wind Power Station at Näsudden on Gotland in April 1995. The commissioning has proceeded without any major problems. As of August 1997 Nordic 1000 has been operated grid-connected during 11800 hours and produced 2.8 GWh. The paper presents results from the evaluation, made to the same standard as the other CEC Joule 2 WEGA II projects.

Keywords: Wind Turbines, HAWT, Stall Regulation

## 1. THE NORDIC 1000 PROJECT

The Nordic 1000 project is one of the JOULE II/WEGA II projects. The main design work started in January 1993. The design is described in ref. (1). The prototype turbine was erected in April 1995 at Vattenfall's Wind Power Station at Näsudden on the island of Gotland in the Baltic. It has been operated since June 1995. Experiences from the commissioning process are described in ref. (2).

The evaluation has been managed by Vattenfall according to the same standard as the other WEGA II projects. For this purpose Vattenfall Utveckling AB has installed a data acquisition system. It consists of four PC-based computers that measure 50 channels at 32 Hz. All raw data are stored on CD-ROM. Each disc also holds 1 and 10 minute statistic files for all channels.

This report presents the main results of the evaluation.

## 2. OPERATIONAL STATISTICS

The operational statistics cover the whole period from the first grid connection in June 1995 to August 1997. This means that problems encountered during the commissioning have influenced the results presented in Table 1. The main cause for down-time and operational restrictions has been the frequency converter and its communication with the control system. Serial units will operate without frequency converters, see Table 2.

Table 1. Operational statistics from June 1995 to August 1997

	Availability (%)	Operation (%)	Net prod. (MWh)
Jun.-Dec. 95	-	58	462
Jan. 96	81	67	91
Feb.	59	46	82
Mar.	36	26	33
Apr.	32	26	44
May	83	66	118
Jun.	83	50	63
Jul.	83	66	120
Aug.	80	61	71
Sep.	65	63	94
Oct.	75	62	155
Nov.	94	84	215
Dec.	92	82	178
Jan. 97	76	70	141
Feb.	61	59	227
Mar.	79	67	217
Apr.	74	68	169
May	31	28	62
Jun.	96	76	96
Jul.	90	75	100
Aug.	79	58	51
Total	72 <sup>1)</sup>	61	2789

1) Based on the period January 1996 to August 1997

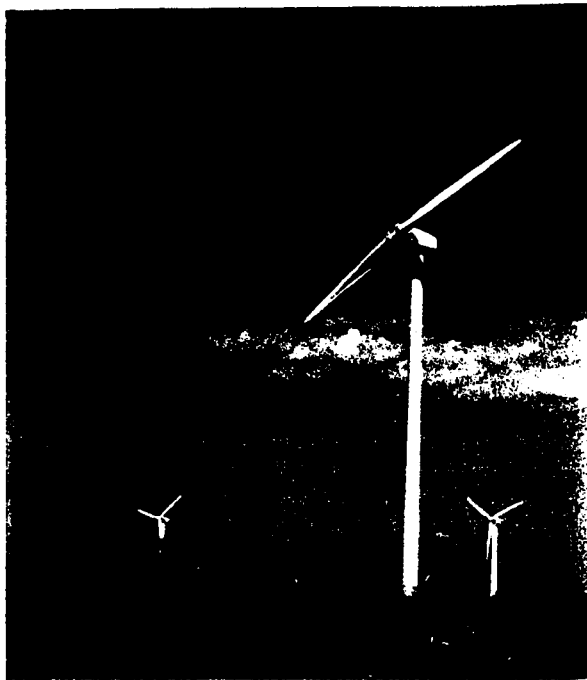


Figure 4. The Nordic 1000 prototype at Näsudden.

### 3. POWER PERFORMANCE

The power performance evaluation of the Nordic 1000 prototype has been based on wind data from an existing 145 m meteorological mast and a purpose built 58 m mast. The latter was erected when it became obvious that the wind speed measurements of the old mast did not fulfil today's standards of accuracy.

The wind turbine configuration evaluated has a pitch angle of  $2.2^\circ$ , two stall strips per blade and 9.5 m of vortex generators on each blade. The objective of the stall strips is to improve the stall behaviour. The vortex generators serve to increase the performance at wind speeds below rated.

The power performance was evaluated according to the recommendations of the IEC and is reported in ref. (3). The measured power versus wind speed curve appears in Fig. 2.

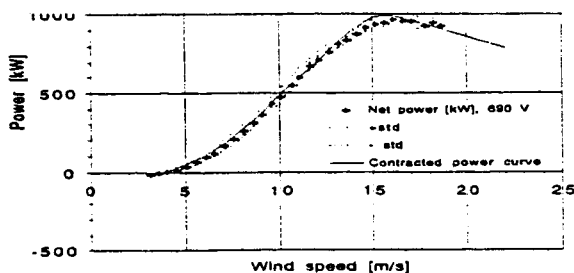


Figure 2. Power versus wind speed for Nordic 1000 during 970402-970615.

### 4. POWER CONTROL QUALITY

In order to evaluate the power control quality of the Nordic 1000 an analysis has been carried out, including time histories, amplitude spectra and histograms covering the power control behaviour.

In general the analysis reveals a behaviour which fulfils expectations. Above rated wind speed the power is effectively limited to rated power, with a maximum for instantaneous power excursions of around 25% of rated.

The frequency analysis reveals a spectrum with expected although low peaks due to the wind shear at  $2P$  (twice per rotor revolution) and, to some extent at  $4P$ ,  $6P$  and  $8P$ . In Fig. 3 an example of an amplitude spectrum is shown.

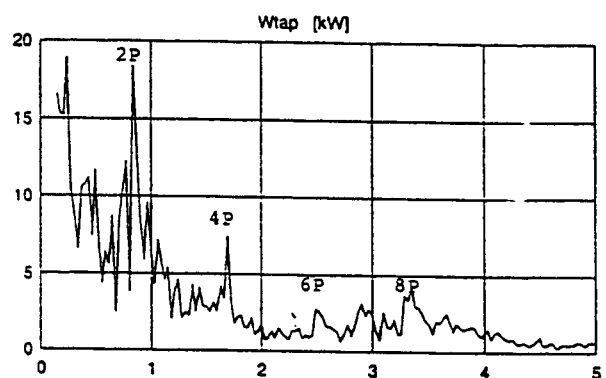


Figure 3. Example of an amplitude spectrum for active power at 15.8 - 19.1 m/s wind speed.

### 5. YAW QUALITY

The yaw error has been evaluated during roughly one month of operation. In general the analysis reveals a yawing behaviour that fulfils expectations. Below rated wind speed there is a maximum of the 10 minute mean yaw error of 2 degrees. Above rated wind speed the error increases to around 4 degrees. See Fig. 4.

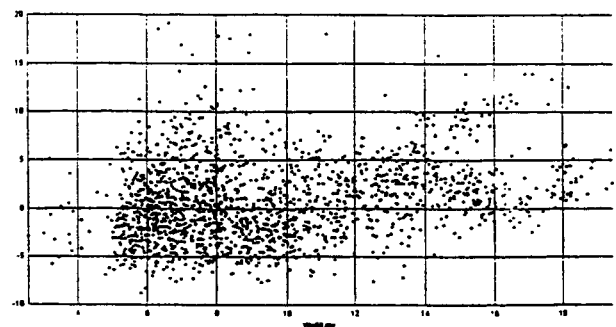


Figure 4. Yaw error as a function of wind speed measurements on top of the meteorological mast. 600 s mean values, 970402-970501.

It can be noted that the mean values of the yaw error as calculated from the meteorological mast measurements and from the observations on top of the nacelle differ only 4 degrees at all wind speeds. However, the standard deviation of the yaw error based on mast observations is considerably higher, which is a consequence of the distance between the wind turbine and the mast. Thus, one may draw the conclusion that the standard deviation observed on the nacelle is more representative than that based on the mast measurements. They are 3 and 5 degrees respectively at low wind speeds and 3 and 4 degrees at high wind speeds.

## 6. RESONANCES

In the Campbell diagram, see Fig. 5, a comparison between multiples of rotor speed excitations and some of the main component frequencies is shown. Note that the first and the second tower eigenfrequencies (Tower 1 and Tower 2) are well below  $2p$  and above  $6p$ , as intended.

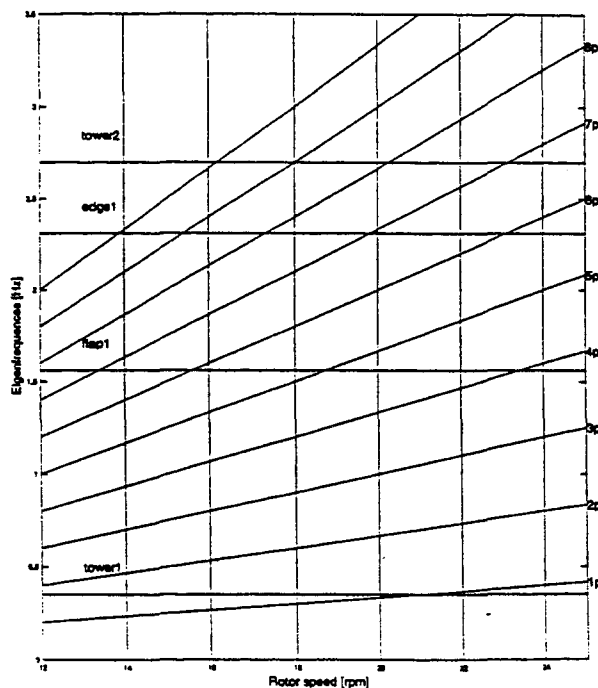


Figure 5. Comparison of multiples of rotor speed excitations and component frequencies.

## 7. MAIN LOADS

Loads during normal operation are illustrated in Fig. 6 which depict the average values of mean, max. and min. for some important parameters during consecutive 10 rotor revolutions on April 2 - 4 1997. Note that the data points form quite distinctive patterns.

In general the analysis reveals loads that are low and well within foreseen values. The dynamic behaviour of the turbine is benign. No unforeseen amplifications of motions or loads have been found.

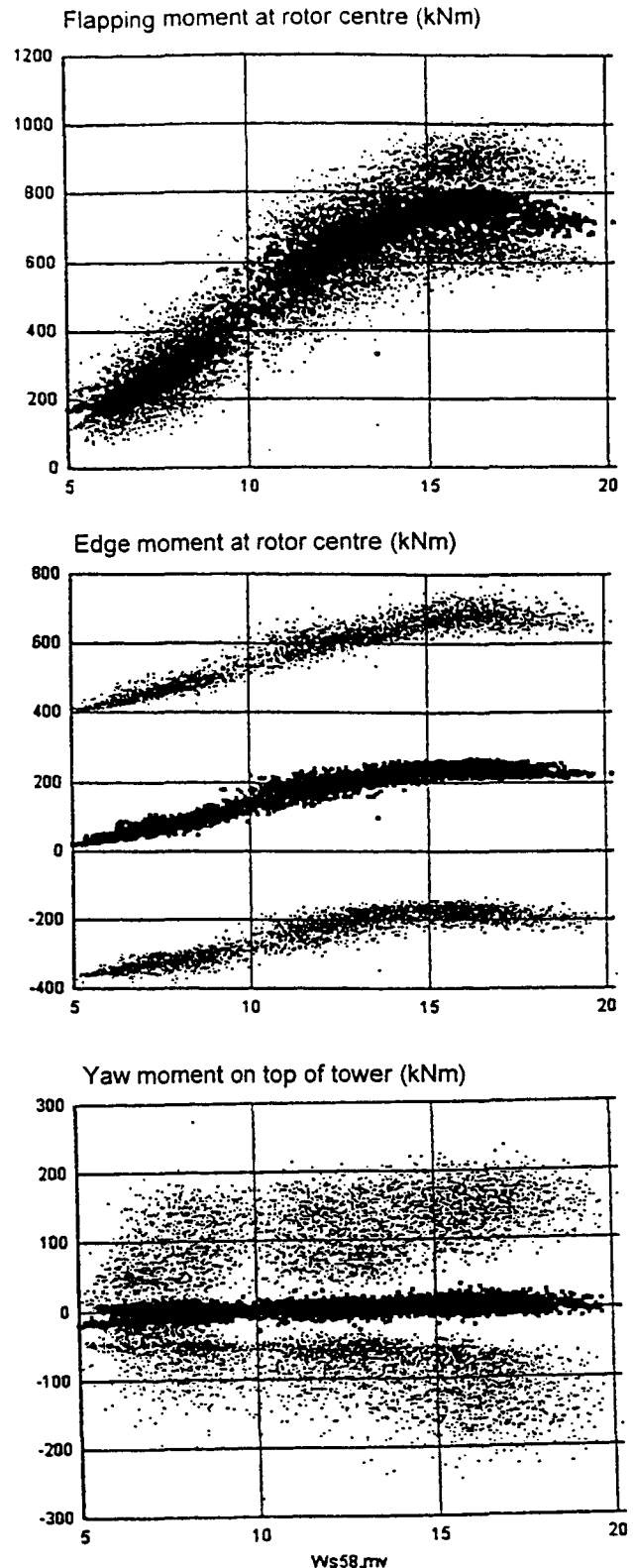
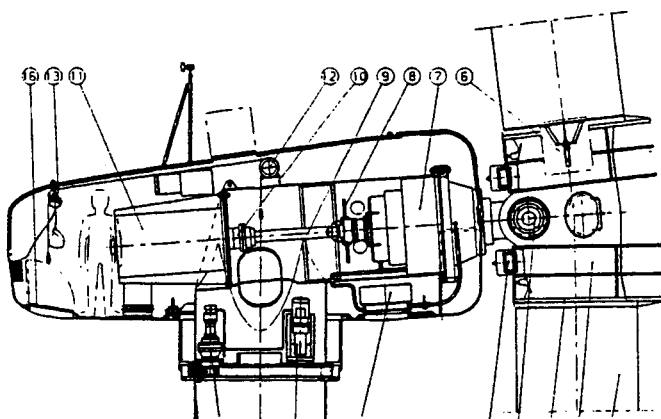


Figure 6. Mean, max. and min loads as a function of wind speed. Values calculated as averages during consecutive 10 revolutions of the turbine. Date 970402 11:00 - 970404 01:45.

**Table 2. Main data Nordic 1000**

	<i>Prototype</i>	<i>Serial version</i>
Type of design		soft
Control principle		stall
Hub		teeter
Orientation		upwind
<b>Turbine</b>		
Turbine diam. (m)		53.0
Rot. speed (r/min)	12-25	17/25
Tip speed (m/s)	33-69	46/69
Airfoil	LM2, NACA 63.4xx, FFA-W3	
<b>Machinery</b>		
Gear-box	2-stage planetary with integral turbine shaft bearings	
Ratio	1:51.7	1:60.6
Electrical system	Induction with frequency converter	Induction 2-speed
Power (kW)	1000	1000/250
<b>Tower</b>		
Type	steel-shell	
Diam. top/base (m)	1.9/2.6	
<b>Weights</b>		
Machinery and turbine (ton)	42	
Total excl. foundation (ton)	93	
<b>Electrical production</b>		
(Mean wind speed 7 m/s, MWh/yr.)	2100	2400



**Fig. 7. Nacelle and machinery of Nordic 1000.** 1. Blade. 2. Hub. 3. Platform. 4. Teeter bearing. 5. Teeter stop. 6. Hydraulic cylinder for blade-tip. 7. Planetary gear-box. 8. Brake disc. 9. Secondary shaft. 10. Safe-set coupling. 11. Generator. 12. Hoist. 13. Rescue equipment. 14. Oil cooler. 15. Nacelle. 16. Hatch. 17. Yaw bearing. 18. Yaw drive. 19. Hydraulic unit.

## 8. GRID INTERFERENCE

During the initial measurements of grid interference unacceptable high values of the 13th and 11th harmonics were noticed, probably due to a resonance. During these measurements four out of the six filters of the frequency conversion system were connected. The last two filters had been installed for fine-tuning of the system. After connection of the last two filters and minor adjustments, the resonance was reduced resulting in levels of harmonics below 3.5% in total harmonic distortion at the 690 V busbar.

## 9. NOISE

The noise level of the turbine has been measured according to the IEA recommendations No 4. Acoustics. The apparent A-weighted sound power level was determined to 104 dB(A) re 1 pW. Prominent tones probably originate from the second stage of the planetary gear-box. With these totally eliminated, the total noise level of the turbine would be reduced by 4 dB(A). The manufacturer is working on a solution to reduce the level of the tones.

## 10. CONCLUSIONS


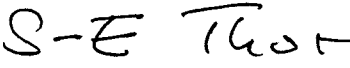
- The design, construction and commissioning of the Nordic 1000 prototype has proceeded without any major problems.
- The evaluation has been completed with a general conclusion that the technology works as intended.
- In general loads are low and well within foreseen values. The dynamic behaviour of the turbine is benign. No unforeseen amplifications of motions or loads have been found.
- Major modifications foreseen on the serial version are reduced noise emission and the use of a two-speed generator directly connected to the grid, resulting in lower cost and higher energy production.

## 11. REFERENCES

- (1) B. Bergkvist, S. Engström and G. Dalén: Commissioning/Design Experience with the Nordic 400 and 1000 kW Prototypes. 5th European Wind Energy Association Conference and Exhibition. 10-14 October 1994, Thessaloniki, Greece.
- (2) B. Bergkvist, S. Engström and G. Dalén: Evaluation and Commissioning of Nordic 400 and 1000 Prototypes. 1996 European Union Wind Energy Conference. 20-24 May 1996, Göteborg, Sweden.
- (3) G. Ronsten: Power Performance of the 1 MW Wind Turbine Nordic 1000. FFA TN 1997-31.
- (4) E. Rudolphi: NWP 1000 Prototype. Measurements of Noise Emission from a Wind Turbine according to IEA recommendations 4. Acoustics. Ingemansson Technology 1997-05-16.





Utgivare  Flygtekniska Försöksanstalten Box 11021 161 11 BROMMA	Beteckning  FFA 1997-48											
	Datum November 1997	Sekretess Öppen	Ex nr									
	Dnr 342/97-23	Antal sidor 28 + App 1 t.o.m. App. 14 + docsida										
Uppdragsgivare  NUTEK 117 86 STOCKHOLM	Projektnr  VE-0180	Beställning  P2939-2 Vindkonsortiet Dnr 4F6-97-04489										
Rapportens titel   <b>Vindkraftskonsortiet</b> <b>FFA MIUU CTH</b>  <b>Sammanställning av föredrag vid EWEC'97 i Dublin</b>												
Författare  Anders Östman												
Granskad av	Godkänd av   Sven-Erik Thor Chef, Vindenergi											
<b>Sammanfattning</b>  Den Europeiska vindenergiföreningen, EWEA, arrangerar vart tredje år en konferens och utställning, European Wind Energy Conference EWEC. I år, 1997, arrangerades EWEC'97 i Dublin. Vart tredje år arrangerar dessutom Europeiska Unionen EUWEC, sin vindenergikonferens. Konferenserna är förskjutna ett och ett halvt år inbördes. Det innebär att det i Europa arrangeras vindkonferenser var 18:e månad.  I föreliggande rapport redovisas erfarenheter från EWEC'97.												
Nyckelord Vindkraftskonsortiet, EWEC'97, Vindkraft												
Distribution  <table border="0" style="width:100%"> <tr> <td style="width:33%">NUTEK</td> <td style="width:33%">VKK Styrelse</td> <td style="width:33%">FFA</td> </tr> <tr> <td>Antal ex/ex nr</td> <td></td> <td></td> </tr> <tr> <td>1-7</td> <td>8-18</td> <td>19-70</td> </tr> </table>				NUTEK	VKK Styrelse	FFA	Antal ex/ex nr			1-7	8-18	19-70
NUTEK	VKK Styrelse	FFA										
Antal ex/ex nr												
1-7	8-18	19-70										